THE EFFECT OF OPERATING CONDITIONS ON EMISSIONS FROM A TWO-STAGE LUMP COAL COMBUSTOR

by

Jennifer Mackend

Thesis submitted to the Graduate Faculty of the
Virginia Polytechnic Institute and State University
in partial fulfillment of the requirements for the degree of

MASTER OF SCIENCE

in

Mechanical Engineering

APPROVED:

D. R. Jaasma, Chairman

C. H. Long

T. E. Diller

April, 1982

Blacksburg, Virginia

ACKNOWLEDGMENTS

The author would like to thank Professor D. R. Jaasma for his guidance during this research project and Professors C. H. Long and T. E. Diller for their advice and for serving on her graduate committee. Mr. Riding of the Bridger Coal Company is thanked for providing the coal used in this study. Mr. Rice of the Westmoreland Coal Company is also thanked for providing analyses on the coal. The fellowship provided by the Department of Health, Education, and Welfare was greatly appreciated. Special thanks are extended to the author's fiancé, Dan Waslo, for his assistance and encouragement during her graduate study.

TABLE OF CONTENTS

TABLE OF CONTENTS
(Continued)

LIST OF FIGURES

LIST OF FIGURES
(Continued)

LIST OF FIGURES
(Continued)

LIST OF TABLES

NOMENCLATURE

a	molar ratio of water to atomic hydrogen in the coal
A	area, m^2
b	molar ratio of carbon to atomic hydrogen in the coal
B	rotameter reading
CD	discharge coefficient
d	diameter, m
E	activation energy, J/mol K
$\dot{E}$	energy release rate which would occur if combustion were complete, kW
EF	emission factor, g/kg
HV	heating value, kJ/kg
k	reaction rate constant, units depend on reaction order
$\dot{L}$	energy loss rate, kW
$\dot{m}$	mass flow or burning rate, kg/s
mf	mass fraction
M	total mass, kg
MW	molecular weight kg/kgmol
P	pressure, kPa
ΔP	pressure drop across orifice, kPa
Q	volumetric flow rate, m^3/s
r	radius, m
R	universal gas constant, J/mol K
Re	Reynolds number
RWD	ratio of wet to dry basis mole fractions

NOMENCLATURE
(Continued)

S	swirl number
t	time, s
T	temperature, K
V	velocity, m/s
X	mole fraction
[X]	concentration, mol/cm^3
y	distance, m
α	pre-exponential factor for Arrhenius reaction rate constant
β	temperature exponent for Arrhenius rate constant
η	combustion efficiency
μ	viscosity, Pa s
ν	stoichiometric coefficient
ρ	molar density kg mol/m^3
ϕ	relative humidity

Subscripts

A	ambient
air	dilution air
c	coal
C	carbon
cc	carbon in coal
comb	combustor
cs	carbon in smoke

NOMENCLATURE
(Continued)

dry	dry basis
est	estimate
f	forward reaction
i	index for reactions, species, or position
j	index for area
k	index for reactions or species
m	meter conditions
o	distance between tangential inlets and center of combustion
or	orifice
r	reverse reaction
R	room
s	stack
sm	smoke sample
sr	water saturation at air temperature
SO_x	SO_x sample
ss	smoke in the stack
t	tangential inlets

Superscripts

'	reactant
''	product

1. INTRODUCTION

Combustion process emissions are the largest contributor to man-made air pollution (1). Therefore there is significant interest in reducing these emissions, which include both gaseous and particulate species. There are three sources of pollutant species: fuel contaminants (such as sulfur), species resulting from incomplete combustion (such as carbon monoxide), and species formed during combustion (such as oxides of nitrogen) (2). There are also three techniques for reducing emissions: precombustion fuel treatment, combustion control techniques, and stack gas cleanup (2). Combustion control techniques such as combustion design modification and operating condition adjustments have been successful in many applications and are preferred methods for reducing emissions (1).

Residential coal stoves are an increasing source of air pollution. Macumber (3) gives a review of the history of coal stove use and the recent increased concern about emissions from these combustors.

The research presented here is concerned with the effect of various design parameters and operating conditions on emissions from coal burned in a two-stage test combustor. The parameters that were considered include primary air mass flow rate, secondary air mass flow rate, secondary air temperature, secondary air inlet velocity, and secondary air swirl. Each parameter was varied independently to attempt to isolate its effect on emissions. Information from the various tests, indicating the operating conditions which produce the lowest emissions, can be used in designing future coal stoves.

In addition, probe sampling was conducted in the combustor's secondary combustion zone to determine the carbon monoxide concentrations. A chemical kinetic model of carbon monoxide oxidation was formulated and compared to the measured carbon monoxide concentrations.

2. LITERATURE REVIEW

2.1 Staged Combustion and Emissions Reduction

Research on coal stove designs in the United States essentially stopped in the early 1950's when oil and gas became more available and convenient. Only recently has residential coal use increased. The renewed interest in coal has lead to increased concern about coal stove emissions. Research on coal stoves, which is just beginning to get underway again, focuses on emissions control and staged combustion.

Emissions from coal stoves include carbon monoxide (CO), oxides of nitrogen (NO_x), sulfur oxides (SO_x), smoke, and volatiles. Similar pollutants are emitted from other coal-fired units such as industrial furnaces, utility furnaces, and from combustion of other fuels. While research concerning emissions reduction from domestic coal stoves has been dormant in the United States, research has still continued on emissions reduction from large coal furnaces and gas and oil burners. This information may be relevant to emissions reduction from coal stoves.

Staged combustion has been used successfully in the past to decrease emissions and to increase overall efficiency in coal stoves and other units. It involves the fuel-rich burning of fuel in a primary zone followed by mixing with a secondary air stream. The secondary air then reacts with the products from the primary combustion zone. The resulting air-fuel ratio usually creates overall fuel-lean conditions. Secondary combustion is utilized in contemporary combustors also.

Staged combustion has been used with both natural draft and forced air coal combustors, although most residential coal stoves have in the past used natural draft. Landry and Sherman (4) reviewed several coal stove designs while developing a "smokeless" stove for bituminous coal in 1948. The designs they reviewed all utilized air staging and natural draft, and many used downdraft or crossfeed air. Their final design was a two-stage, cross-fire air, natural draft stove. More recently, Engdahl (5) compared Landry and Sherman's design to a similar "Parkray" British smokeless heater which used forced air. Engdahl proposed that the forced air permitted "more flexibility in design and operation" and "might enable additional improvements of the emission characteristics" of Landry and Sherman's stove.

NO_x emissions reduction by combustor design changes has been studied extensively (4-11) for various types of combustors and various fuels. There are two components of NO_x emissions -- thermal NO_x formed from the nitrogen in air and fuel NO_x formed from the nitrogen in the fuel. High NO_x is generally caused by high temperatures and high oxygen concentrations in combustion zones (2). Fenimore (6) suggests that thermal NO_x production is more dependent on high temperatures than fuel NO_x is. Thermal NO_x is formed from N_2, which requires a high temperature to dissociate. In contrast, the nitrogen in the fuel is in other forms and can convert to NO_x at lower temperatures. Formation of NO_x from either source depends on the locally available oxygen supply.

Hangebrauck, et al. (7) found that NO_x emissions are lower for hand-fired coal combustors than other types such as pulverized and

mechanical stokers. The NO_x emission factor from a hand-fired unit was 1.6 g/kg while the NO_x emission factors from various stoker and pulverized coal units ranged from 4.1 to 5.5 g/kg. Although Hangebrauck, et al. found low NO_x emissions from the hand-fired combustors, the effect of operating conditions on the emissions was not studied. Further study of NO_x emissions from hand-fired units is warranted to confirm the previous findings.

Many methods have been used to reduce NO_x emissions. In large boilers methods of NO_x control include the following (2):

1. Low excess air.
2. Burner improvements for air and mixing control.
3. Staged combustion.
4. Improved windbox air distribution.
5. Flue gas recirculation into the combustion air.
6. Reduced air preheat.
7. Water injection into the combustion air.

Some of these methods can readily be applied to residential coal stoves. The effects of these parameters on NO_x emissions have been studied for various burners and fuels and are described below.

Martin and Dederick (8) burned gaseous fuel (simulating gas from a coal gasification process) in a premixed, turbulent jet, two-stage combustor and studied the NO_x yield produced by chemically-bound nitrogen in the form of NH_3. They varied the primary zone equilvalence ratio from 0.8 to 1.5 and found a decrease in NO_x yield with increasing primary zone equivalence ratio.

Gibbs, et al. (9) studied the effect of air staging on fuel NO_x emissions in a fluidized coal test combustor. They found that 0, 10, and 25% secondary air produced 470, 400, and 320 ppm of NO_x respectively for secondary air temperatures of 25°C. At 200°C, 10 and 25% secondary air produced 420 and 337 ppm of NO_x respectively. Thus, staged operation significantly reduced the NO_x emissions.

The effect of air preheat on NO_x emissions varies in different combustion systems. Gibbs, et al. (9) found that preheating secondary air in the fluidized bed combustor had little effect on the NO_x emissions. At temperatures of 25, 200, and 350°C, the NO_x emissions were 400, 420, and 420 ppm respectively with 10% secondary air. With 25% secondary air, temperatures of 25 and 200°C yielded NO_x emissions of 320 and 337 ppm respectively. Breen (2) discussed air preheat in large utility boilers and found that by reducing the air preheat the peak temperature was reduced, which in turn helped lower the NO_x emissions. However, a fuel consumption penalty was associated with the reduced air preheat. Sadakata, et al. (10) tested a single stage combustor that burned city-gas and determined that preheating combustion air up to 300°C increased NO_x emissions by a factor of 3. They also found that both thermal and fuel NO_x emissions were not significantly increased by preheating primary air to 300°C in a two-stage combustor. Since the ratio of primary air to stoichiometric air was less than 0.8, the oxygen deficiency could have prevented an increase in NO_x. Sadakata, et al. also reported that other species which might be intermediates in the NH_3

to NO conversion were reduced by 50% when the primary air was heated to 300°C. This may have also affected the changes in NO_x emissions.

Turbulence is also a factor in combustor design and emissions control. A useful parameter for discussing turbulence is the swirl number, S:

$$S = \frac{\text{angular momentum flux}}{\text{characteristic distance} \cdot \text{axial momentum flux}}$$

Assuming perfect mixing and conservation of momentum, the swirl number can be written in terms of combustor geometry as follows (11):

$$S_{geom} = \frac{r_o \pi r_t}{A_t} \left[\frac{\text{tangential flow}}{\text{total flow}}\right]^2 \qquad (1)$$

where

r_t = radius of the exits

r_o = radius of the tangential inlets from the center of the combustor

A_t = area of the tangential inlets

Although this swirl number was derived for a cylindrical combustor, swirl numbers can also be determined for other combustor geometries. Other researchers define the swirl number slightly differently although the swirl number is always an indication of the tangential momentum of the flow.

Several researchers have examined the effect of swirl on NO_x emissions. Beér, et al. (12) tested a high-nitrogen #6 fuel oil in a two-stage atmospheric combustor at 0.95 overall equivalence ratio. Two different swirl conditions, corresponding to swirl numbers of 2.7 and

0.53, were investigated. They found that at lower primary zone equivalence ratios (0.98 to 1.3) higher NO_x emissions were produced from the high swirl number test. At higher primary equivalence ratios (1.3 to 2.0) both the high and low swirl tests produced similar NO_x emissions. Baldwin and Long (13) studied the effect of swirl on NO_x emissions from a gas fired combustor. For swirl numbers ranging from 0.50 to 9.45, large variations in NO_x emissions (10 to 65 ppm) were seen at excess air values of 40 to 60%. At excess air values of 10 to 30%, the NO_x emissions varied from 50 to 70 ppm. An optimum swirl number of 4.00 produced the lowest NO_x emissions at the higher excess air values. Wendt (14) determined that low swirl corresponds to low NO_x emissions and high swirl corresponds to high NO_x emissions for staged pulverized coal combustion. In addition, he found a greater difference in NO_x emissions between the high and low swirl tests at low primary zone equivalence ratios than at high equivalence ratios. Wendt and Beér, et al. found similar trends over comparable ranges of equivalence ratios but Baldwin and Long studied a different equivalence ratio range. These investigations show that the effect of swirl on NO_x emissions is highly dependent on the equivalence ratio.

Although a significant amount of research has been done on NO_x emissions reduction by changes in combustor design and operating conditions, much less research has concentrated on SO_x emissions reduction by similar methods since the SO_x emissions are mainly a function of the sulfur content of the fuel (15). Some work has been done on the effect of staged combustion on SO_3 enhancement but the enhancement phenomenon

is believed to be transient and its effect is not that important (16). Reducing excess air also reduces conversion of SO_2 to SO_3 (2). SO_x emissions are often reduced in stack gas cleanup processes but this method is not practical for residential stoves.

Particulate emissions are also often reduced by stack gas cleanup processes. This is particularly true for coal-fired boilers (2). Fly ash can be reduced by lowering the amount of excess air (and the velocity of the flue gas). For example, a 10% reduction in excess air decreases the fly-ash emissions in the stack by up to 40% when a high-efficiency (90-99%) precipitator is used (2). However, since residential stove stack gases have considerably lower velocities than large boiler stack gases, fly ash is not a significant problem. Particulates from residential coal stoves consist mostly of condensed hydrocarbons and soot (solid carbon). The type of coal used also can affect particulate emissions. High volatile coals tend to emit more smoke than low volatile coals (17).

CO emissions are also of concern in combustion systems. Fenimore and Moore (18) studied CO emissions from ethylene-air flames and found that in single-stage combustion of lean mixtures the CO steadily decayed to the final equilibrium value. In two-stage combustion, the CO was partially quenched for lean primary mixtures, but in rich primary mixtures (primary equivalence ratio = 1.5), the CO was not quenched. Typically, staged coal combustors have rich primary flames with high CO concentrations in the primary products. CO is converted to CO_2 in the secondary combustion zone where the overall equivalence ratio is lean.

Gibbs, et al. (9) found that two-stage combustion produced lower CO emissions than single-stage combustion in a fluidized bed combustor.

Macumber (3) discusses some work that has been done on reducing emissions from coal stoves. Although emission reduction techniques have not been studied extensively for residential coal stoves, they have been studied for other coal units and other fuels. These techniques include utilizing staged combustion and changing air preheat, excess air, and turbulence in the combustor. The methods used to reduce emissions of NO_x, and SO_x, CO, and smoke from other combustion systems can be applied to residential coal stoves.

2.2 CO Oxidation Modeling

CO oxidation in post-flame gases has been modeled in various ways ranging from global one-step mechanisms to detailed mechanisms with tens of reactions. These various CO oxidation mechanisms were reviewed to determine which one would best model the CO concentrations in the experimental test combustor. Although little work has been done on modeling CO oxidation in particulate-laden product gases from coal-fired combustors, CO oxidation in products from gaseous, hydrocarbon-air flames has been studied extensively.

Howard, et al. (19) developed a global CO burnout law based on their own and others' work. Their rate of CO oxidation for a wide range of operating conditions is given by

$$\frac{-d[CO]}{dt} = k\,[CO]\,[O_2]^{\frac{1}{2}}\,[H_2O]^{\frac{1}{2}}\,\exp(-E/RT) \qquad (2)$$

where bracketed terms are concentrations of gaseous species (mol/cm^3), T is temperature, and k, E, and R are constants. This global mechanism was based on data where the temperatures ranged from 840 to 2360 K, the pressures ranged from 0.04 to 1 atmosphere, the equivalence ratios ranged from 0.04 to 3.0 and the fuels ranged from various hydrocarbons to CO and H_2O mixtures. The hydrocarbon concentration is not needed in this one-step burnout law. Bowman (20) also discussed various CO burnout laws but suggested that they might have to be coupled to some kinetics model to account for changing gas compositions in the reactor flow field. Therefore, global mechanisms may not have many advantages over detailed mechanisms.

Quasi-global mechanisms, which include both global reactions and detailed reaction mechanisms, have also been presented. Bowman (20) and Westbrook and Dryer (21) discussed mechanisms in which the fuel and oxidizer react to form CO and H_2. The CO and H_2 oxidation was then modeled via more extensive mechanisms which involve elementary reactions.

In general, CO oxidation in premixed flames is slower than CO formation (20). Researchers (18-28) agree that in the presence of H_2O, the reaction of primary significance in CO oxidation is

$$CO + OH \rightarrow CO_2 + H$$

Other reactions that include radical species such as H, O, and OH and molecular species such as H_2, O_2, and H_2O must also be considered since they directly affect the OH concentration. In some cases reactions

involving radicals can be considered locally equilibrated, and solution methods can be simplified with these assumptions.

Recently the effect of the radical species HO_2 and H_2O_2 on CO oxidation have been investigated. Various researchers (20-22, 25, 28) suggest that HO_2 is important in either the reaction

$$CO + HO_2 \rightarrow CO_2 + OH$$

or as a method of reducing the amount of OH available to react with CO.

Dryer and Westbrook (28) compared experimental results to two different CO oxidation models which used elementary reactions in detailed reaction mechanisms. One model included reactions with HO_2 and H_2O_2 and the other did not. They found that the experimental results more closely matched the model which included the HO_2 and H_2O_2 species. These two species helped slow the rate of change of temperature and CO and CO_2 concentrations in the first model. Without the presence of HO_2 and H_2O_2 in the second model, the temperature and species concentrations changed much too rapidly to reflect the actual conditions found by the experimental work. The mechanism that Dryer and Westbrook presented, which was chosen as the chemical kinetic model used in this investigation, was a detailed CO oxidation mechanism that was part of a larger hydrocarbon oxidation mechanism.

Detailed reaction mechanisms are available for carbon monoxide, hydrogen, methane, ethane, and methanol oxidation (28). Other fuels and species are more difficult to model, so global or simplified reaction schemes are formulated instead. Other phenomena, such as turbulence,

heat transfer, etc., can be included in the models but they add more complexity.

In summary, detailed reaction mechanisms seem to be preferred over global mechanisms although solution methods may be more difficult. OH radicals are particularly significant in the oxidation of CO but other radicals such as HO_2 and H_2O_2 have also been shown to be important. By including these two species in chemical kinetic models of CO oxidation, the calculated and measured CO concentrations are found to be in close agreement.

3. EXPERIMENTAL APPARATUS

3.1 Test Combustor and Air Supply

The test combustor used in this investigation is shown in Figure 1. The combustor is a type 304 stainless steel cylinder with an outside diameter of 32.4 cm, a wall thickness of 4.57 mm, and a length of 1.37 m. The vertical cylinder is supported by four legs and three sets of secondary air inlets are provided along the axis. There are seven probe holes on the right side of the combustor while the left side of the combustor has one probe hole directly opposite the top probe hole on the right side. Three inside wall temperature thermocouples, detailed in Figure 2, are located between each of the two secondary air inlets at each level on the left side.

The lid of the combustor contains two primary air inlets and the mechanism for supporting the coal bed. Three threaded rods pass through the lid and support a grate on which the coal bed rests. The grate consists of a tubular stainless steel frame which supports an Inconel mesh. The mesh wire has a diameter of 1.3 mm and there are three holes per cm. The rods allow axial variations in the grate position. A cable attached to the lid and passing over a pulley above the combustor facilitates raising and lowering the lid for fuel loading. There is no provision for stirring the coals or removing the ash once the lid is shut and the combustor is in operation.

The combustion products exit into a 15 cm diameter exhaust duct through the bottom of the combustor. The exhaust system is shown in Figure 3. The orifice plate, which has an orifice diameter of 4.2 cm,

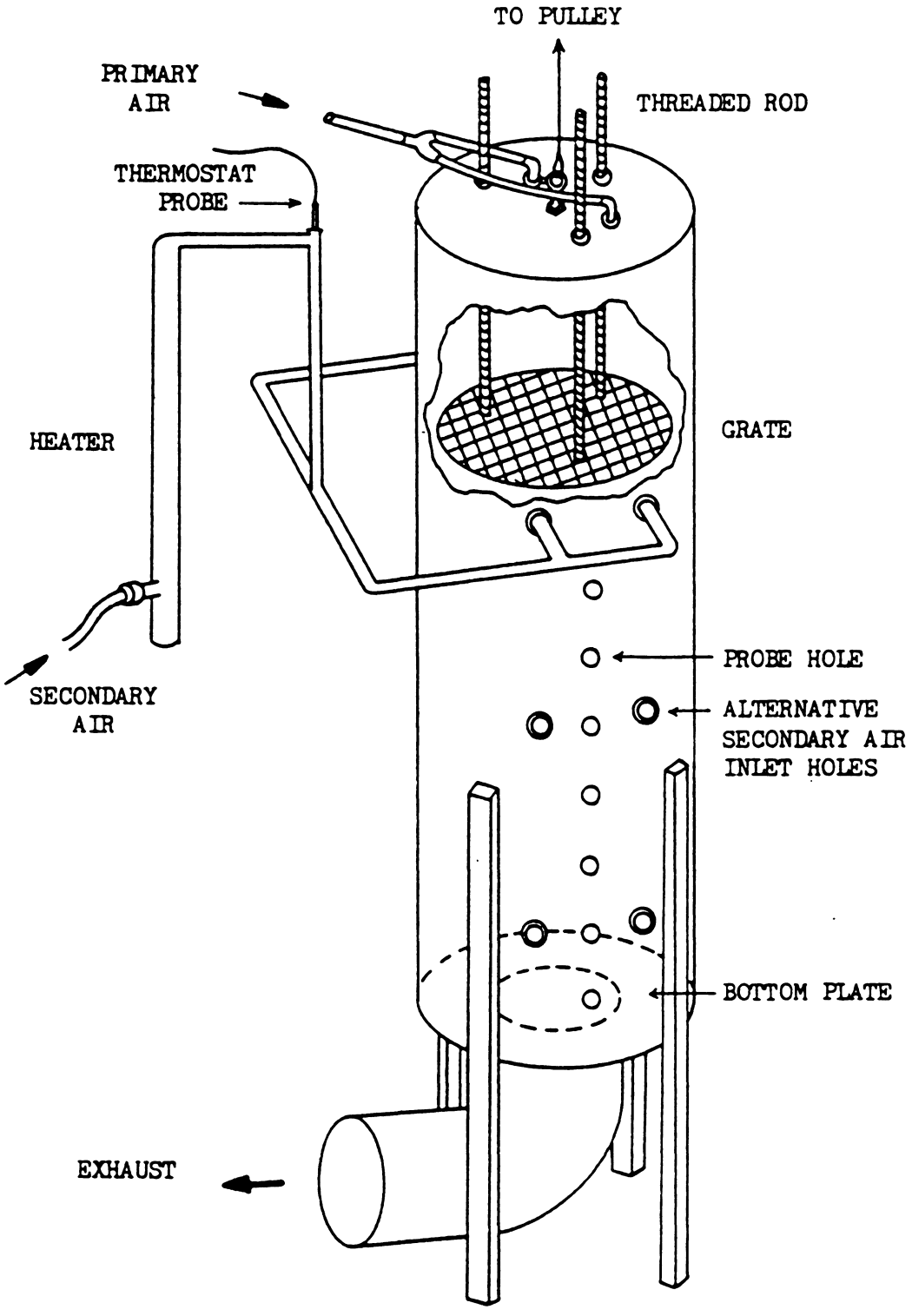

Figure 1. Test Combustor.

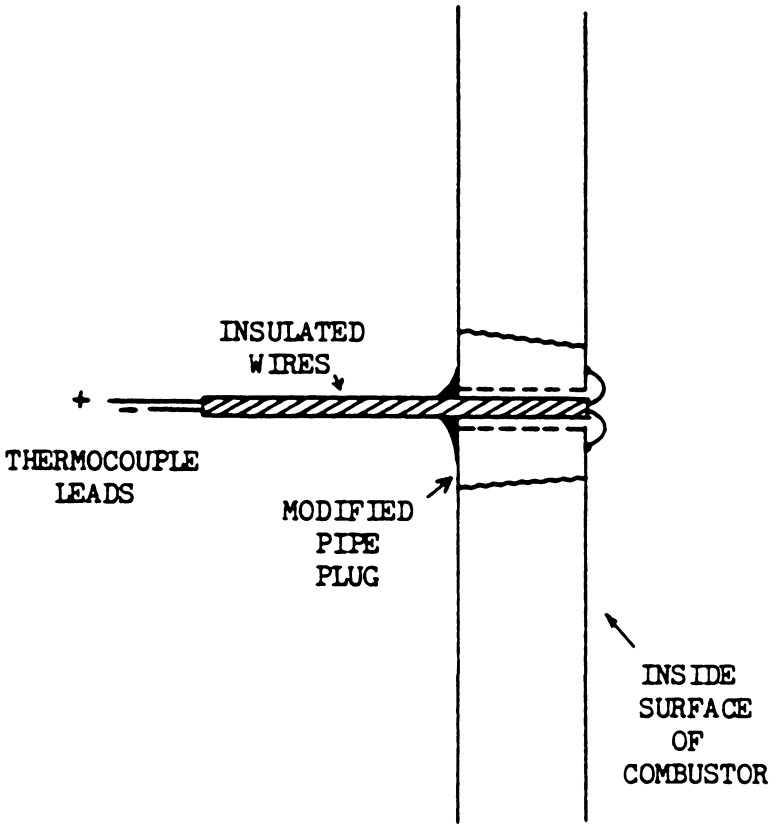

Figure 2. Detail of Surface Temperature Thermocouple.

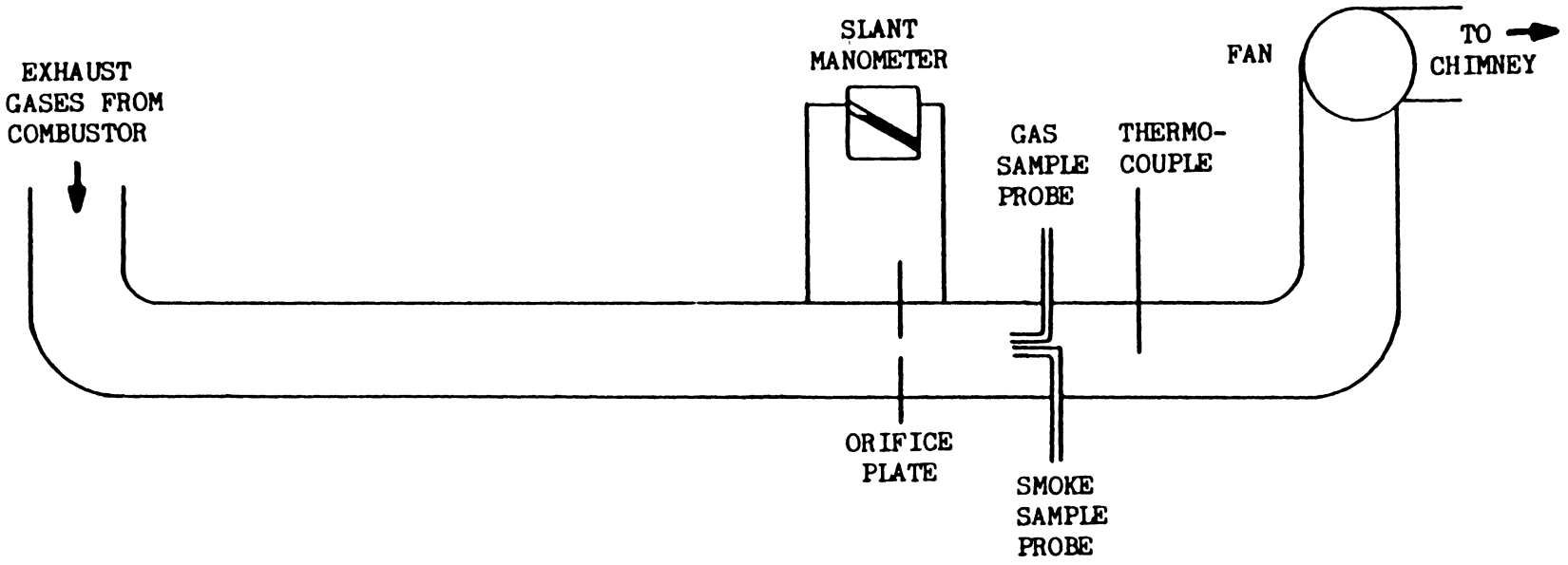

Figure 3. Exhaust Duct Schematic.

is 2.08 m downstream from the combustor exit and the pressure taps are 15 cm upstream and 7.5 cm downstream from the orifice plate. The exhaust gas sample and smoke sample probes are both near the centerline of the exhaust duct and are 24 cm downstream from the orifice plate. The thermocouple probe is 40 cm downstream from the orifice plate. A fan pulls the exhaust gases through the exhaust duct and discharges them into a chimney.

The primary and secondary air streams flow through sonic orifices before entering the combustor as shown in Figure 4. Different size orifice plates were calibrated to produce the various mass flow rates that were used. The pressures upstream of the orifice plates are regulated to maintain the desired flows. The primary air is split into two equal streams and flows down through the coal bed, while the secondary air is split into four streams which enter below the grate. The secondary air is heated before splitting into the four streams.

The nozzles through which the secondary air enters the combustor are replaceable. The nozzle design is shown in Figure 5. Different nozzle orifice sizes are used to alter the secondary air inlet velocity and tangentially directed nozzles are used to create swirl. The vertical location at which the secondary air enters the unit can be varied, although this was not done in this investigation.

The downward air flow in the combustor helps achieve steady burning conditions. The temperature and chemical content profiles through the coal bed can be kept constant and the burning coals can be kept at the grate level by using downdraft air. As the fuel burns,

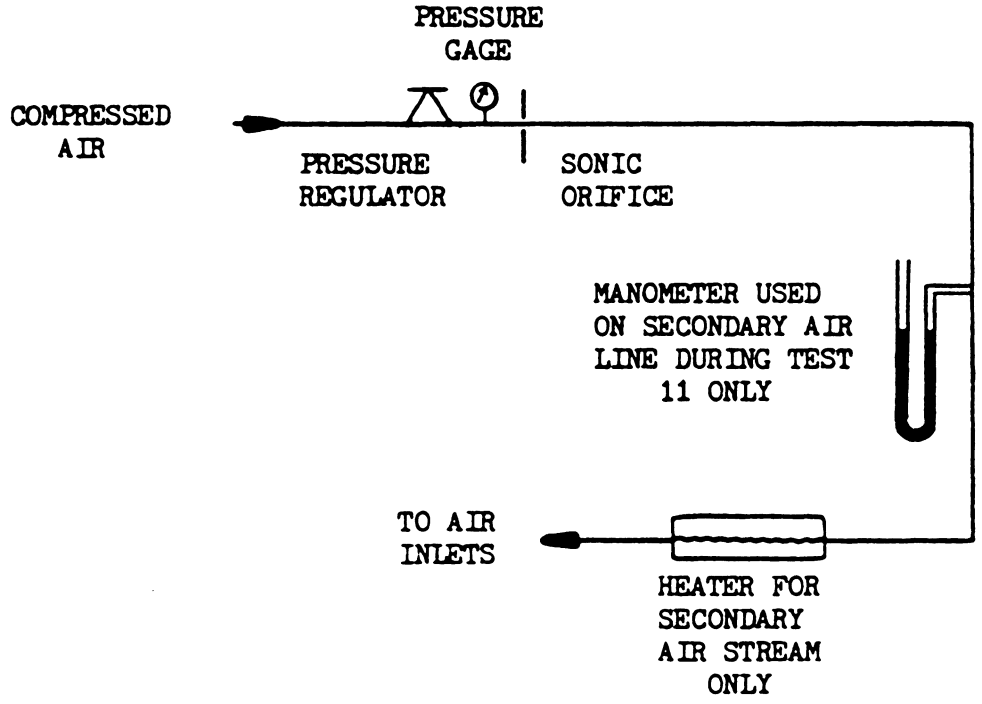

Figure 4. Schematic of Primary or Secondary Air Supplies.

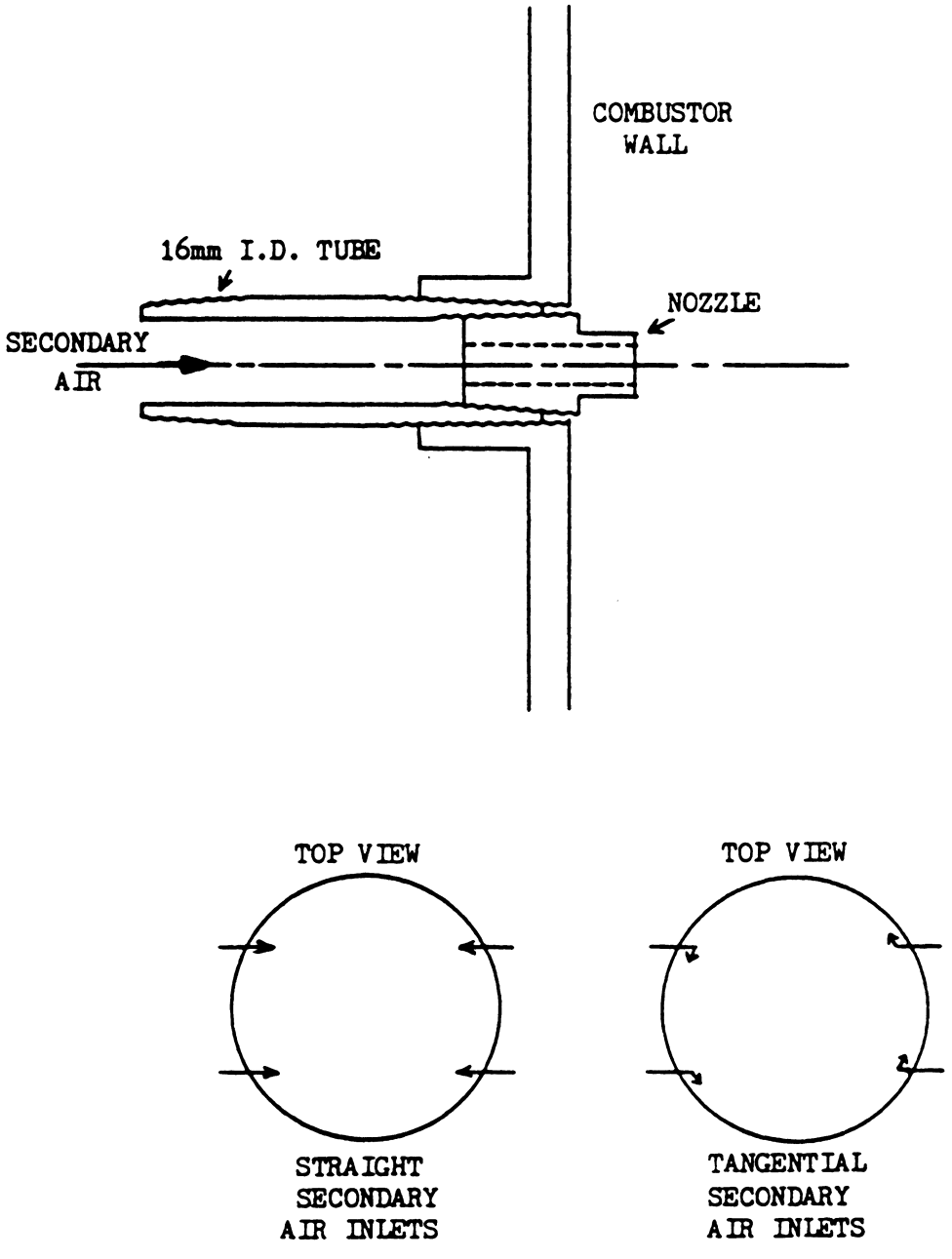

Figure 5. Secondary Air Inlet Nozzle Design and Injection Directions.

most of the ash falls through the grate and accumulates on the bottom plate of the combustor. In an updraft combustor, the ash remains on the grate and the burning coal rests on top of the ash, resulting in unsteady combustion. In addition, forced air rather than natural draft was used in the test combustor.

3.2 Test Coal

The test runs were made burning two separate samples of Wyoming bituminous coal from the same coal seam. These two samples are designated coal 1 and coal 2. Data on the coals are given in Table I. Since the heating value was not measured for coal sample 2, it was calculated using Dulong's Formula (25). Although the two coal samples have very different sulfur contents, SO_x emissions were measured for coal 1 only and comparisons were not influenced by differences in sulfur content. The coal was shipped in large chunks (roughly 25 cm in the longest dimension) and had to be broken into smaller pieces (less than 9 cm in the longest direction) before burning.

3.3 Stack Gas and Smoke Sampling Trains

The stack gas sampling train is shown in Figure 6. All tubes and fittings that come in contact with the flow are either Teflon or stainless steel to prevent reactions with the gas. The gas is sucked into the probe and is drawn through a condenser to remove the moisture in the gas stream. The condenser is a stainless steel coiled tube packed in an ice bed. The condensed water collects in a tube at the

Table I. Wyoming Bituminous Coal Properties.

	Coal 1	Coal 2
Proximate Analysis		
% Volatile	43.37	38.50
% Fixed Carbon	51.72	51.26
% Ash	4.91	10.24
Free Swelling Index	0	0
% Moisture	12.94	10.44
Dry Basis Heating Value	27,947 kJ/kg	-
Moisture and Ash Free Heating Value	29,389 kJ/kg	-
Dry Basis Heating Value (DuLong's Formula)	-	27,900 kJ/kg
Ultimate Analysis		
% Carbon	68.67	68.36
% Hydrogen	5.39	4.56
% Nitrogen	1.29	1.44
% Oxygen	19.24	12.16
% Sulfur	0.53	3.24
% Ash	4.91	10.24

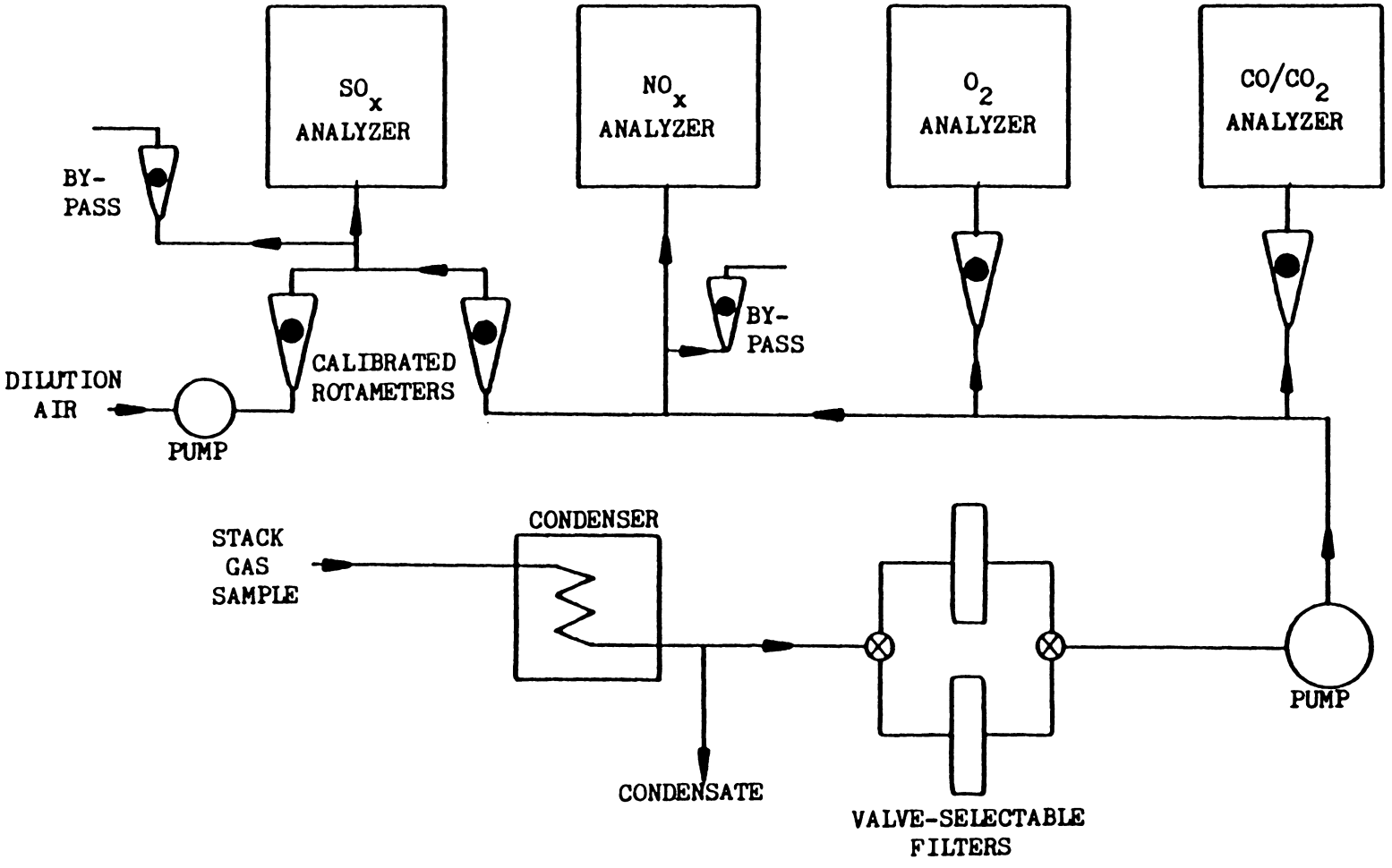

Figure 6. Stack Gas Sampling Train.

outlet of the condenser and the gas stream continues through one of the two filters before passing through the pump. Two filters in parallel are available so that when one becomes excessively loaded the other can be used. The first filter can then be changed if necessary.

After the pump the flow branches and a stream is sent to each of the gas analyzers. Rotameters are used to assure adequate flows to the CO/CO_2 and O_2 analyzers. The flow to the NO_x analyzer is regulated by a valve and a by-pass rotameter assures that the instrument inlet is not pressurized. The gas sample going to the SO_x analyzer must be diluted with an SO_x-free gas since typical exhaust duct SO_x concentrations ranged from 30 to 300 ppm and the maximum range on the analyzer is 1 ppm. Two calibrated rotameters are used -- one for the stack gas sample and one for dilution air. The two streams are mixed prior to entering the SO_x analyzer. A by-pass rotameter is also used on the SO_x analyzer to prevent pressurization of the inlet. All of the instruments' and by-pass rotameters' exhausts are vented to the chimney. The gas analyzer models and detection methods are summarized in Table II.

The smoke sampling train is shown in Figure 7. The fiberglass collection filter (Gelman A-E) has a rating of 0.3 μm and is placed as close to the probe as possible to reduce the length of line to be cleaned. The flow is sucked into the probe, through the filter, and then through a condenser similar to the one in the gas sampling train. A calibrated rotameter measures the flow before exhausting it to the chimney.

Table II. Gas Analyzer Models and Detection Methods.

Gas	Manufacturer	Model	Detection Method
CO/CO_2	Infrared Industries	IR 702 D	Nondispersive Infrared
O_2	Horiba	POA-21	Polarographic
NO_x	Bendix	8102	Chemiluminescence
SO_x	Bendix	8303	Flame Photometric

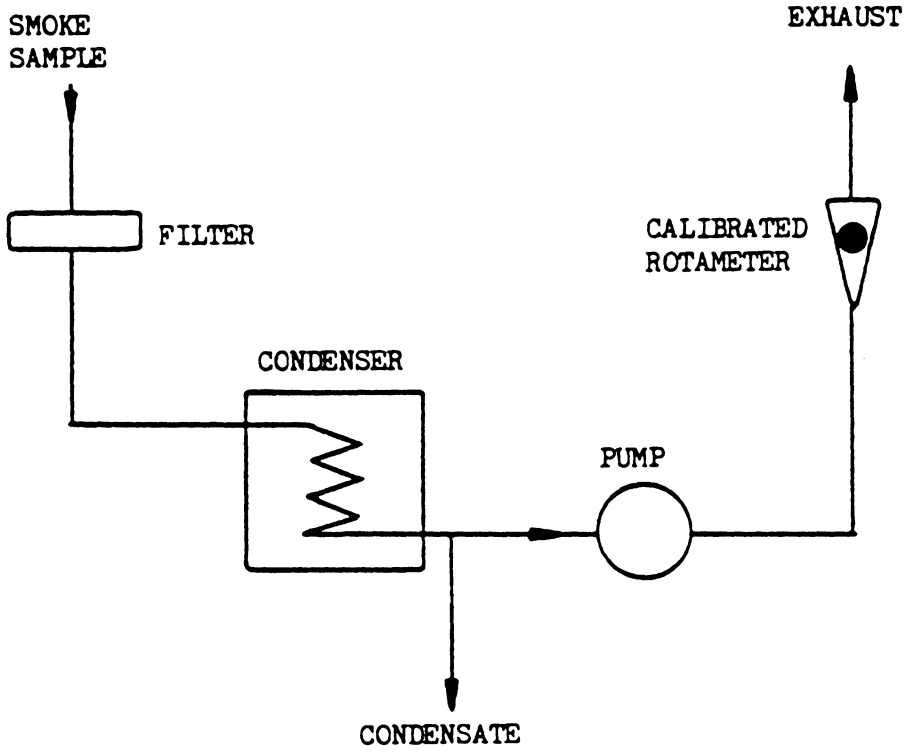

Figure 7. Smoke Sampling Train.

3.4 Gas and Temperature Probing Equipment

A water-cooled probe was used for sampling the gases in the combustor downstream of its grate. The cooled probe, which is shown in Figure 8, was needed to quench any reactions that might have occurred in the probe so that accurate species concentrations in the secondary combustion zone could be determined. Cooling was not necessary in the stack gas probe since the gases in the stack were much cooler than gases in the combustor.

The probe is made of three concentric stainless steel tubes which create separate flow paths for the gas sample and the water. A pump is used to circulate the water from a storage flask, through the probe, and back to the flask. The probe gas sample flow path is the same as the stack gas sample path except that only CO, CO_2 and O_2 are measured when using the cooled probe.

The temperature in the secondary combustion zone is determined with a suction pyrometer which is shown in Figure 9. A Platinum/Platinum-10% Rhodium thermocouple made from 0.13 mm diameter wire measures the temperature of the hot gases as they are drawn through the annular region between the thermocouple insulator and the outer stainless steel tube. The gas velocity through the probe is on the order of 40 m/s and the outside diameter of the suction pyrometer is 6.4 mm.

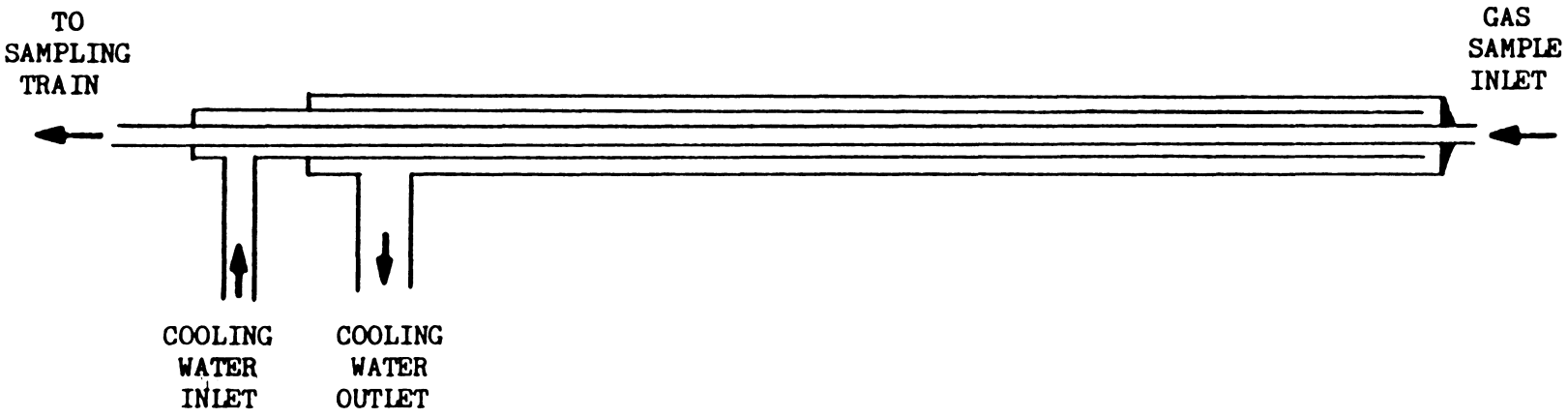

Figure 8. Water-Cooled Gas Sampling Probe.

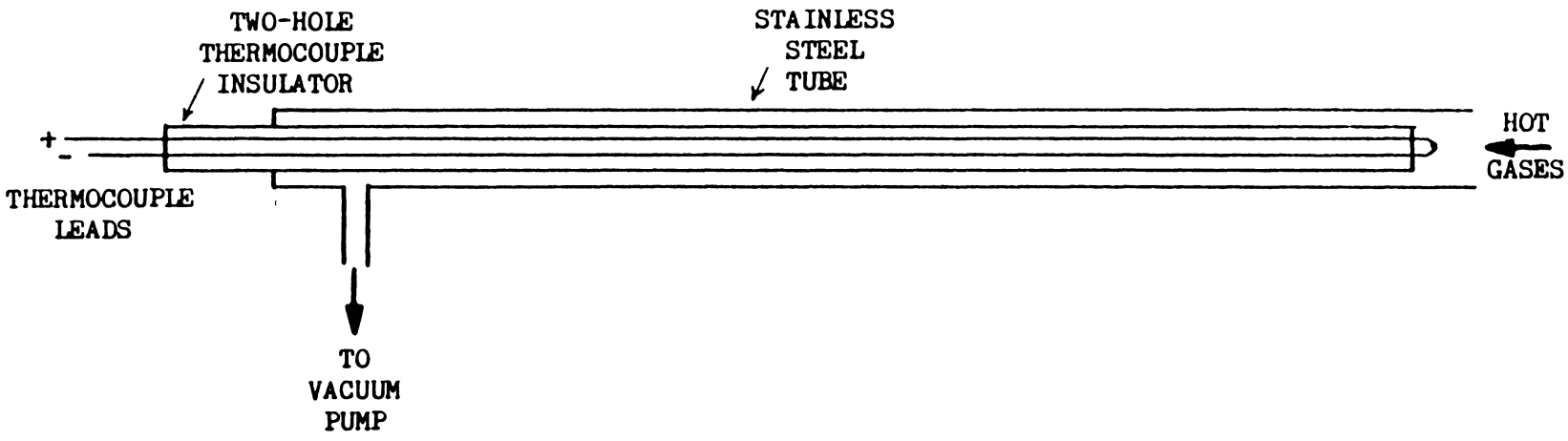

Figure 9. Suction Pyrometer.

4. EXPERIMENTAL PROCEDURES

4.1 Calibration

The sonic orifices in the air lines were calibrated by passing their flows through a Singer AL425 dry gas meter. Once the air supply system had been calibrated, a known amount of air was sent through the empty combustor. The known flow created a pressure drop across the exhaust duct orifice and allowed the orifice discharge coefficient to be determined. The pressure drop ranged from 0.01 to 0.11 kPa (0.04 to 0.43 inches of water) during calibration. The discharge coefficient, which was nominally 0.6, decreased with increasing flow. During calibration the discharge coefficient ranged from .65 to .58 while the flow rate ranged from 18.5 to 48.1 m^3/h. The exhaust fan was run when no air flow was supplied and the pressure drop across the orifice was measured to check for leaks.

The rotameters were calibrated using bubble flowmeters. Curves were fit to the calibration data for each of the rotameters used in the tests and were used in the data reduction computer program.

4.2 Emissions Testing Procedure

Prior to each test run several preliminary steps were taken. The filter for smoke collection was dessicated overnight to remove moisture and was weighed on a balance before being installed in the filter holder. The coal was broken into 9 cm pieces and 8.2 kg were set aside for the test. This amount of coal produced a 20 to 25 cm thick coal bed on the grate and left an air space of approximately 30 cm

above the bed. The wood that was used to start the coal fire was also weighed and 0.45 to 0.65 kg were set aside for the test. The slant manometer was zeroed and the gas analyzers were zeroed and spanned prior to each test.

Before starting the fire, the lid and grate were raised about 20 cm to load the wood and some newspaper on the grate. The paper was lit, and when the fire caught the exhaust fan was turned on to pull the smoke and combustion gases into the chimney. Once the wood started burning, the coal was loaded on top. The primary air was then turned on and the lid was lowered and shut tightly. The secondary air flow was turned on and the thermostat for the secondary air heater was set at the desired temperature. The SO_x sample and dilution air rotameters were set to produce SO_x readings within the analyzer range.

Twenty minutes after lighting the paper and wood, the first set of data was recorded. Recorded data included CO, CO_2, O_2, NO_x, and SO_x concentrations, rotameter settings for the SO_x gas sample, dilution air, and smoke sample flows, and wall and air temperatures. The instruments continuously displayed the above readings and the data were recorded every five minutes. The SO_x sample and dilution air rotameters were adjusted when necessary to maintain readings in the middle of the meter scale. Roughly halfway through the test the gas sample flow was switched from the first filter to the second. The smoke was collected during only a portion of the entire test. A constant flow rate of 22.2 cm^3/s was maintained on the smoke rotameter.

After recording data for three hours the test was terminated since it appeared that the fire was going out. The primary and secondary air supplies were shut off and the sample lines were disconnected. The zero and span of each analyzer were checked to ensure that the analyzer drift was within acceptable limits. The smoke filter was placed in the dessicator to prepare it for weighing at a later time.

When the combustor had completely cooled down, the leftover ash on the grate was removed. The ash that had accumulated on the bottom plate of the combustor (Figure 1) was only removed twice during all the tests. The orifice plate was removed and cleaned and the gas sample line and probe were flushed with acetone. For the first few tests the smoke sample line and probe were flushed with acetone and the dirty acetone was evaporated. The residue was weighed and indicated that the smoke collected in the probe and line was unmeasureable or negligible. The smoke sample line and probe were cleaned between all the other tests but their washings were not saved for weighing.

Twelve emissions tests were performed. The parameters that were considered include primary and secondary air mass flow rates, secondary air temperature and inlet velocity, and secondary air swirl number. Table III lists the values of each parameter for the twelve tests.

Tests one and three were duplicated to determine whether the results were repeatable. Tests one and two had intermediate conditions and were considered the baseline tests. The other test conditions differed from the baseline conditions by one parameter. Each parameter

Table III. Burning Conditions for the Twelve Emission Tests.

Test Number	Primary Air Mass Flow Rate kg/h	Secondary Air Mass Flow Rate kg/h	Secondary Air Temperature °C	Secondary Air Inlet Velocity m/s	Swirl Number	Coal
1	15.4	15.7	190	55.2	0	1
2	15.4	15.7	190	55.2	0	1
3	15.4	15.7	25	36.0	0	1
4	15.4	15.7	25	35.6	0	1
5	15.4	12.3	190	43.6	0	1
6	24.9	15.7	190	55.8	0	2
7	15.4	25.3	150	82.2	0	2
8A	12.1	15.7	190	55.8	0	2
8B	7.93	15.7	190	55.8	0	2
9	15.4	15.7	315	70.4	0	2
10	15.4	15.7	190	7.74	0	2
11	15.4	15.7	190	251.	0	2
12	15.4	15.7	190	54.4	1.56	2

was varied to the physical extremes allowed by the experimental equipment.

The secondary air inlet velocities were calculated assuming flat velocity profiles in the nozzles and neglecting vena contracta effects. The secondary air temperatures were determined from the air heater thermostat setting and readings from thermocouples in the nozzle inlets.

In tests one through five the first batch of Wyoming bituminous coal was burned, and in tests six through twelve the second batch was burned. SO_x data were recorded for the first five tests only since the SO_x analyzer became inoperative after the fifth test.

The smoke collection period ran for the entire three hour duration of tests one and two. For all of the other tests the smoke sample pump was turned on when steady state conditions were reached. The pump was turned off when it appeared that conditions were no longer steady.

Test five, the minimum secondary air test, was started with zero secondary air. After fifteen minutes of recording data, the CO reading on the CO/CO_2 analyzer went above the analyzer's full scale reading of 3.00 mole percent. The corresponding CO_2 reading was around 12.5 mole percent. To reduce CO to a measurable value, some secondary air had to be introduced. A small flow was added but was insufficient. Thirty minutes into the test a flow of 12.3 kg/s was used successfully and a CO reading of 0.31 was achieved.

Since test eight (the minimum primary air test) had some problems getting started, data were not first recorded until thirty minutes

after lighting the paper and wood fire. Because only a limited supply of coal was available, a primary air flow rate of zero was not used. (Preliminary tests on other coals had shown that a fire could not be established without primary air.) A minimum flow of 12.1 kg/h was used instead. Since this flow was successful, the flow rate was lowered to 7.93 kg/h when the conditions were no longer steady. A second steady state was then achieved for the lower flow rate. These two cases are designated as tests 8A and 8B.

As can be seen in Table III, test seven, the maximum secondary air test, had a 40°C lower-than-baseline secondary air temperature. This is due to the insufficient heat output of the air heater. A higher output heater was used for the maximum secondary air temperature test to assure a significantly higher air temperature. The minimum and maximum secondary air temperatures also affected the secondary air inlet velocities in tests three, four, and nine.

The first eleven tests had swirl numbers of zero, since the secondary air inlet nozzles were directly opposite each other and the two sets of opposing jets had approximately equal flow. The twelfth test tangentially introduced the secondary air and a swirl number was calculated based on the combustor geometry as discussed earlier.

4.3 Probe Sampling Procedure

Start up procedures for the probe tests were similar to those for the emissions tests although different data were recorded. The CO and CO_2 concentrations and the temperature in the stack were monitored so

that steady conditions could be verified. The pressure drop across the exhaust duct orifice was also recorded. Once steady conditions had been reached, probe sampling began.

Two probe sampling tests were conducted -- the first test (without swirl) burned coal 1 while the second test (with swirl) burned coal 2. Table IV lists other conditions during the two tests.

In the first test probing was conducted along the centerline of the combustor. At each axial position the water-cooled gas sampling probe was inserted and values of CO, CO_2 and O_2 concentrations were recorded. The gas probe was withdrawn and the suction pyrometer was inserted. A temperature reading was then recorded. A total of five sets of this type of axial data were recorded. Between each set stack conditions were also recorded.

To determine if the secondary combustion zone conditions were uniform at a cross section, a traverse was made across the diameter at the top probe position. A traverse across the same diameter was also done from the other side of the combustor to determine if skewing of the concentration profiles was caused by the probe's presence. In these cases gas data for five positions along the diameter were taken, and then the temperature probe was inserted and the temperatures for five positions were recorded. Figure 10 details the probe positions for both axial and radial probing.

Similar probing (axial and radial) was performed in the second probe test. In addition, due to the existence of large radial concentration and temperature gradients, radial traverses were conducted at

Table IV. Burning Conditions for the Two Probe Tests.

Test Number	Primary Air Mass Flow Rate kg/h	Secondary Air Mass Flow Rate kg/h	Secondary Air Temperature °C	Secondary Air Inlet Velocity m/s	Swirl Number	Coal
1	14.6	14.8	190	33.3	0	1
2	15.4	15.7	190	35.3	1.56	2

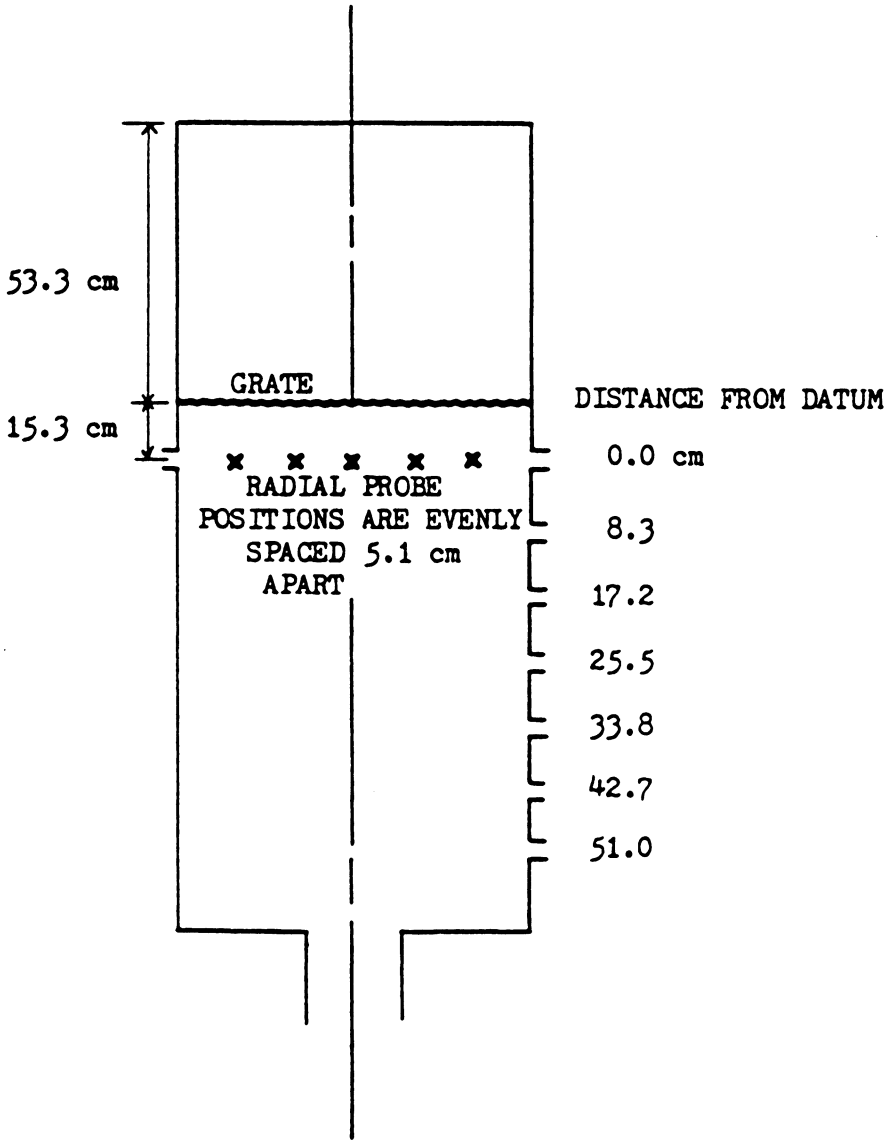

Figure 10. Axial and Radial Probe Positions.

all seven of the axial positions. These traverses were done from the right side only.

Probing continued until conditions were no longer steady in both tests. The stack conditions were still monitored until three hours of data had been collected.

5. CO OXIDATION MODEL

A simple chemical kinetic CO oxidation model was created to compare to probe data in the secondary combustion zone. The reaction mechanism used is from Dryer and Westbrook (28) and is listed in Table V. Reaction rate constants are assumed to have the Arrhenius form

$$k = \alpha T^{\beta} \exp (E/RT) \qquad (3)$$

where

k = forward reaction rate constant, units determined by reaction order.

α = pre-exponential factor, units determined by reaction order.

T = absolute temperature, K

β = temperature exponent, dimensionless

E = activation energy, J/mol

R = gas constant, J/mol K

The Arrhenius coefficients α, β, and E for each reaction are also given in Table V.

Species present in the model are CO, CO_2, O_2, H_2O, OH, H_2, OH, HO_2, H_2O_2, and N_2. The N_2 does not enter the reaction mechanism explicitly but can participate in reactions that have an unspecified reactant M.

Table V. Reaction Mechanism and Arrhenius Coefficients for CO Oxidation Model (Ref. 28).

Reactions	Arrhenius Coefficients		
	A	B	E (cal/mol k)
$CO + OH \rightarrow CO_2 + H$	0.126×10^{8}	1.3	-800.
$CO + HO_2 \rightarrow CO_2 + OH$	0.100×10^{15}	0.0	23000.
$CO + O + M \rightarrow CO_2 + M$	0.631×10^{16}	0.0	4100.
$CO_2 + O \rightarrow CO + O_2$	0.251×10^{13}	0.0	43800.
$H + O_2 \rightarrow O + OH$	0.199×10^{15}	0.0	16800.
$H_2 + O \rightarrow H + OH$	0.200×10^{11}	1.0	89000.
$H_2O + O \rightarrow OH + OH$	0.316×10^{14}	0.0	18400.
$H_2O + OH \rightarrow H_2 + OH$	0.100×10^{15}	0.0	20300.
$H_2O_2 + OH \rightarrow H_2O + HO_2$	0.100×10^{14}	0.0	18000.
$H_2O + M \rightarrow H + OH + M$	0.200×10^{17}	0.0	105100.
$H + O_2 + M \rightarrow HO_2 + M$	0.158×10^{16}	0.0	- 1000.
$HO_2 + O \rightarrow OH + O_2$	0.501×10^{14}	0.0	1000.
$HO_2 + H \rightarrow OH + OH$	0.241×10^{15}	0.0	1900.
$HO_2 + H \rightarrow H_2 + O_2$	0.251×10^{14}	0.0	700.
$HO_2 + OH \rightarrow H_2O + O_2$	0.501×10^{14}	0.0	1000.
$H_2O_2 + O_2 \rightarrow HO_2 + HO_2$	0.398×10^{14}	0.0	42600.
$H_2O_2 + M \rightarrow OH + OH + M$	0.126×10^{18}	0.0	45500.
$H_2O_2 + H \rightarrow HO_2 + H_2$	0.158×10^{13}	0.0	3800.
$O + H + M \rightarrow OH + M$	0.100×10^{17}	0.0	0.
$O_2 + M \rightarrow O + O + M$	0.501×10^{16}	0.0	115000.
$H_2 + M \rightarrow H + H + M$	0.200×10^{15}	0.0	96000.

6. DATA REDUCTION

6.1 Stack Emissions and Combustion Efficiency

The data reduction program used for the emissions tests is listed in Appendix 11.1. Equations for curves fitted to calibration data are given in Appendix 11.2. Several intermediate values must be calculated in converting from measured values to emission factors and combustion efficiency. A brief outline is given below.

Since the gas sample first passes through the condenser and the moisture is removed, the measured gas concentrations are on a dry basis and must be converted to a wet basis. The ratio of wet to dry mole fractions (RWD) is derived by Waslo (30) and is given by

$$RWD = \frac{\left(1 - \frac{\phi P_{sr} - 0.61}{P_A}\right)}{\left(1 + \left(\frac{a}{b} + \frac{1}{2b}\right) X_{CO_2,dry}\right)} \qquad (4)$$

where

ϕ = relative humidity, dimensionless

P_{sr} = saturation pressure of water vapor at room temperature, kP_a

P_A = ambient pressure, kPa

a = molar ratio of water to atomic hydrogen in the coal

b = molar ratio of carbon to atomic hydrogen in the coal

$X_{CO_2,dry}$ = mole fraction of CO_2 in the stack gas on a dry basis

The measured SO_x concentration is diluted and must be converted to the actual concentration in the stack. The flow rates of the gas sample and dilution air are calculated from equations of curves fitted to calibration data. Assuming that the gas sample and the dilution air are at the same temperature and pressure, the undiluted wet basis SO_x mole fraction (X_{SO_x}) can be determined from

$$X_{SO_x} = X_{SO_x,m} \frac{(Q_{SO_x} + Q_{air})}{Q_{SO_x}} \tag{5}$$

where

$X_{SO_x,m}$ = mole fraction of SO_x at the meter on a wet basis

Q_{SO_x} = flow rate of sample gas through rotameter, m^3/s

Q_{air} = flow rate of dilution air through rotameter, m^3/s

The stack gas volumetric flow rate (Q_s) is determined the the orifice equation and calibration data. The iterative procedure for calculating Q_s is presented in Appendix 11.3. The units of Q_s are m^3/s.

The smoke emission rate for the combustor is considered constant and is given by

$$\dot{m}_{sm} = \frac{M_{sm} \bar{Q}_s T_R}{\Delta t \, Q_{sm} \bar{T}_s} \tag{6}$$

where

$\dot{m}_{sm}$ = smoke emission rate, kg/s

M_{sm} = total mass of smoke collected on the smoke filter, kg

Δt = time interval during which smoke was collected, s

$\bar{Q}_s$ = average stack gas flow rate, m^3/s (evaluated at $\bar{T}_s$)

Q_{sm} = smoke sample flow rate, m^3/s (evaluated at T_R)

T_R = room temperature, K

$\bar{T}_s$ = average stack temperature, K

The instantaneous wet basis burning rate of coal is calculated from the measured carbon flow in the stack. It is assumed that all the carbon in the stack is in the form of CO, CO_2, or smoke.

$$\dot{m}_c = \frac{(X_{CO} + X_{CO_2})\, Q_s\, \rho_s\, MW_C + (\dot{m}_{sm}\, mf_{cs})}{mf_{cc}} \qquad (7)$$

where

$\dot{m}_c$ = instantaneous mass burning rate of coal, kg/s

X_i = mole fraction of species i

ρ_s = molar density of stack gas, $kgmol/m^3$ (evaluated at T_s)

MW_C = molecular weight of carbon, kg/kgmol

mf_{cs} = mass fraction of carbon in the smoke

mf_{cc} = mass fraction of carbon in the as-fired coal

The mass fraction of carbon in the smoke was assumed to be the same as the mass fraction of carbon in the coal since the smoke was not analyzed.

The instantaneous emission factors for the gaseous species CO, NO_x, and SO_x are calculated as shown below.

$$EF_i = \frac{X_i \, Q_s \, \rho_s \, MW_i \, 1000}{\dot{m}_c} \tag{8}$$

where

EF_i = emission factor for species i, g/kg

MW_i = molecular weight of species i, kg/kgmol

In order to calculate the combustion effiency, CO and smoke losses and the energy release rate which would occur if combustion was complete must be calculated. The instantaneous energy release rate is given by

$$\dot{E} = \dot{m}_c \, HV_c \tag{9}$$

where

$\dot{E}$ = instantaneous energy release, kW

HV_c = heating value of the coal, kJ/kg

The instantaneous loss due to CO is

$$\dot{L}_{CO} = X_{CO} \, Q_s \, \rho_s \, MW_{CO} \, HV_{CO} \tag{10}$$

where

$\dot{L}_{CO}$ = energy loss due to CO, kW

HV_{CO} = heating value of CO, kJ/kg

and the instantaneous loss due to smoke is

$$\dot{L}_{sm} = \dot{m}_{sm} \; HV_{sm} \tag{11}$$

where

$\dot{L}_{sm}$ = energy loss due to smoke, kW

HV_{sm} = heating value of smoke, kJ/kg

The heating value of the smoke is assumed to be the same as the heating value of the coal. Macumber (3) has also used this approximation. The instantaneous combustion efficiency, η, can be calculated from the above terms by

$$\eta = 1 - \frac{(\dot{L}_{CO} + \dot{L}_{sm})}{\dot{E}} \quad 100 \tag{12}$$

The coal burning rate, gaseous emission factors, and combustion efficiency given by equations 7, 8, and 12 respectively, are instantaneous values calculated from data sets recorded every five minutes.

Mass averaged gaseous emission factors are calculated from

$$\overline{EF}_j = \frac{\sum (EF_j(i) \; \dot{m}_c(i))}{\sum \dot{m}_c(I)} \tag{13}$$

where

$\overline{EF}_j$ = mass average emission factor for species j, g/kg

$EF_j(i)$ = instantaneous emission factor for species j for data set i, g/kg

$m_c(i)$ = intantaneous mass burning rate of coal for data set i, kg/s

An average smoke emission factor can be determined by

$$\overline{EF}_{sm} = \frac{M_{ss}}{\sum \dot{m}_c \Delta t} \tag{14}$$

where

$\overline{EF}_{sm}$ = average smoke emission factor, g/kg

M_{ss} = total mass of smoke passing through the stack during the smoke collection period, g

Δt = time interval for smoke collection, s

The summation for the coal burning rate is performed for the time interval during smoke collection.

6.2 Secondary Combustion Zone Conditions

The gaseous species measured in the secondary combustion zone during the probe tests are converted to a wet basis as the stack data for the emissions tests were. These are the only calculations performed for the first probe test. Further calculations are necessary for the second test in order to compare to modeling results.

The first set of data for which traverses at each axial position were made during the second test was chosen to compare to the model. Species concentrations at each cross section were averaged using weighting factors based on cross sectional areas. Figure 11 shows how the cross sectional area was divided. For regions I and II, the two probe position species concentrations were averaged to give one value for each species in each region. These average concentrations are calculated by

$$\bar{X}_i = \sum_{j=i}^{3} \bar{X}_{ij} \left(\frac{A_j}{A_{comb}} \right) \tag{15}$$

where

$\bar{X}_i$ = average mole fraction of species i over a cross section

$\bar{X}_{ij}$ = average mole fraction of species i in region j

A_j = area of region j, m^3

A_{comb} = cross sectional area of combustor, m^3

An area weighted average temperature at each cross section is calculated in a similar manner.

The position along the axis of the combustor had to be converted to a time scale. The mean axial velocity in the combustor was necessary for this conversion and is calculated from the stack data taken during the probe test.

$$\bar{V}_i = \frac{Q_s \rho_s}{\bar{\rho}_{comb,i} A_{comb}} \tag{16}$$

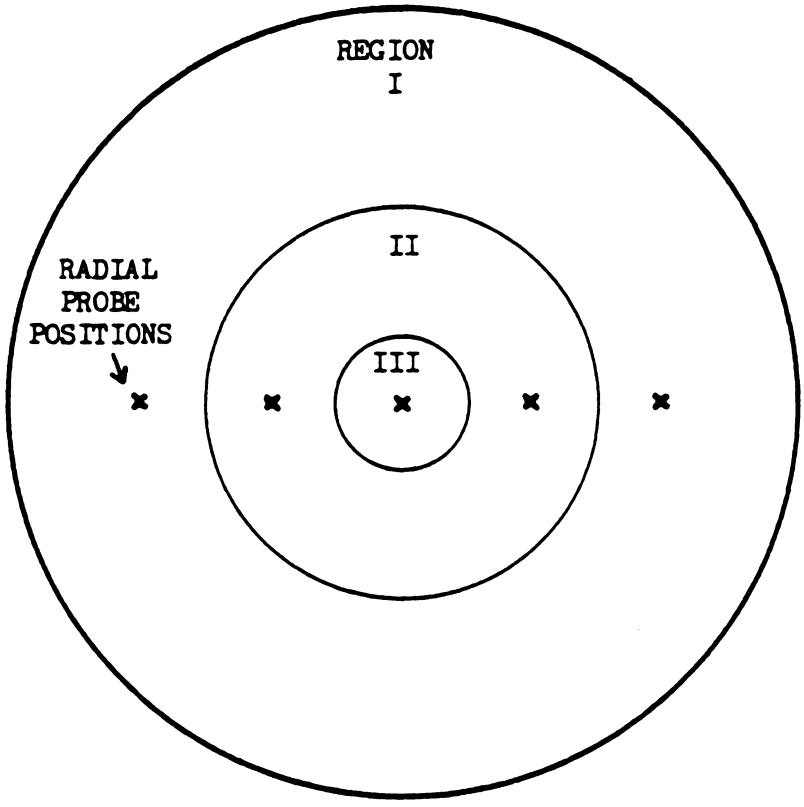

Figure 11. Division of Cross Sectional Area of Combustor for Averaging.

where

$\overline{V}_i$ = average velocity in the combustor for the cross sectional area at axial position i, m/s

$\rho_{comb,_i}$ = average molar density in the combustor for the cross sectional area at axial position i, $kgmol/m^3$ (This value is calculated using the area weighted average temperature for the cross section.)

The top axial probe position was considered the reference datum and was assigned a time of 0.0. Each successive time increment is calculated by

$$t_i - t_{i-1} = \frac{(y_i - y_{i-1})}{\left[\frac{\overline{V}_i + \overline{V}_{i-1}}{2}\right]} \qquad (17)$$

where

t_i = time corresponding to axial position i, s

y_i = distance from datum at axial position i, m

6.3 CO Oxidation Model Solution Techniques

The initial concentrations of the species which are present in the chemical kinetic reaction mechanism were needed for the model solution. Initial concentrations for CO, CO_2 and O_2 were taken from the area averaged probe data for the reference position. The initial H_2O concentration was calculated from

$$X_{H_2O} = \frac{1}{b} X_{CO_2} \left(a + \frac{1}{2}\right) + \frac{\phi P_{sr}}{P_A} \qquad (18)$$

which is derived in Appendix 11.4. Initial concentrations for OH, H_2, O, and H were calculated assuming equilibrium for the following reactions as discussed by Fenimore and Moore (17) and Caretto (23).

$$H + O_2 = O + OH$$

$$O + H_2 = H + OH$$

$$OH + CO = H + CO_2$$

$$O + H_2O = 2OH$$

Dryer (31) suggested an alternative method for calculating the initial concentrations of HO_2 and H_2O_2. First, concentrations for HO_2 and H_2O_2 that are rather high must be assumed. Using these values in the model, and taking about 500 short steps until the HO_2 and H_2O_2 concentrations seem fairly steady, the final HO_2 and H_2O_2 concentrations generated can be used as initial concentrations for the actual model.

A temperature-time history for the secondary flow was also needed for the model and was determined based on the area averaged temperatures and the time scale previously calculated. A second order curve was fit through the temperature-time data to use in the model.

Differential equations of the form (32)

$$\frac{d\,[X_k]}{d_t} = \sum_{i=1}^{I} \nu_{ki} \left(k_{fi} \prod_{k=1}^{K} [X_k]^{\nu_{ki}} - k_{ri} \prod_{k=1}^{K} [X_k]^{\nu_{ki}''} \right) \quad (19)$$

where

$[X_k]$ = concentration of species k, mol/cm^3

i = index for the I different reactions

k = index for the K different species

k_{fi} = forward reaction rate constant for reaction i, units determined by reaction order

k_{ri} = reverse reaction rate constant for reaction i, units determined by reaction order

ν'_{ki} = stoichiometric coefficient of reactant species k in reaction i

ν''_{ki} = stoichiometric coefficient of product species k in reaction i

$\nu_{ki} = \nu''_{ki} - \nu'_{ki}$

describe the changes in species concentrations.

To solve the system of differential equations, two computer programs were used. The first, by Kee, et al. (32) is a chemical kinetic program called CHEMKIN. Input to this program includes species, reactions, Arrhenius coeffients, temperature, pressure, initial concentrations, and the differential equations. CHEMKIN calls various subroutines that aid in calculating the right hand side of equation 19. The second, an International Mathematics and Statistics Library program named DGEAR, numerically integrates the system of differential equations using Gear's method. DGEAR is designed to be suitable for differential equations that may be stiff.

7. RESULTS AND DISCUSSION

Before running the emissions tests with the Wyoming bituminous coal, a locally available coal was tested in the combustor. The coal, a Clinchfield bituminous coal whose properties are listed in Table VI, did not burn properly in the combustor. This was mainly due to the high free swelling index of the coal. The Clinchfield coal tends to cake and swell while burning and needs occasional stirring to break apart the agglomerating coal. Without stirring, which was not possible in the test combustor, steady burning conditions could not be achieved.

One factor that influenced the burning conditions is the position of the burning coal. Maintaining the burning coal at the grate helps achieve steady conditions. Since the Clinchfield coal caked and swelled, the fresh coal could not drop to the grate to burn. The Wyoming coal, with a free swelling index of 0, could maintain the burning coal at the grate. The position of the burning coal could easily be determined by visual inspection of the combustor; the walls of the combustor had a reddish glow in the areas where the glowing coals were. While burning the Clinchfield coal the reddish glow gradually moved up the walls, but the glow remained near the grate level while burning the Wyoming coal. Based on the above information, the Wyoming coal was chosen for successive tests.

Because a wide range of operating conditions was tested, the energy release rate which would occur if combustion were complete (no combustible pollutants) ranged from 6.5 to 29 kW. The corresponding heat output of the combustor ranged from 5.1 to 23 kW. Although

Table VI. Clinchfield Bituminous Coal Properties.

Proximate Analysis	
% Volatile	32.76
% Fixed Carbon	59.85
% Ash	7.39
Free Swelling Index	7
% Moisture	0.54
Dry Basis Heating Value	33,375 kJ/kg
Moisture and Ash Free Heating Value	36,034 kJ/kg
Ultimate Analysis	
% Carbon	80.54
% Hydrogen	5.12
% Nitrogen	1.45
% Oxygen	4.94
% Sulfur	0.56
% Ash	7.39

overall efficiencies depend on the heat transfer characteristics of the combustor, they were calculated for the minimum and maximum heat output tests only and were found to be 78 and 79% respectively. Overall efficiencies differ from combustion efficiencies since they take into account various other flue losses such as sensible heat and latent heat of water as well as combustibles in the stack gases. The heat outputs were calculated by subtracting flue losses from the energy release rates using the flue gas temperature measured downstream of the exhaust duct orifice. The turn down capability of the combustor, which is the ratio of maximum to minimum coal burning rates, is 4.5.

7.1 Combustion Efficiency and Emission Factors

Instantaneous combustion efficiencies, emissions factors, and coal burning rates for the twelve emissions tests are shown in Figures 12 through 23. Corresponding combustor wall temperatures are tabulated in Appendix 11.5 for reference. The emission factor graphs were inspected to determine the time period for which conditions were steady for each test. Mass weighted averages were then calculated for these intervals. The averaging intervals for the smoke emission factors vary slightly from the averaging intervals for the other values since the steady state time period could not be predicted in advance. Both averaging intervals are shown for each test on the instantaneous combustion efficiency plots.

The average values of combustion efficiency, emission factors and coal burning rate are presented in Table VII. The initially specified

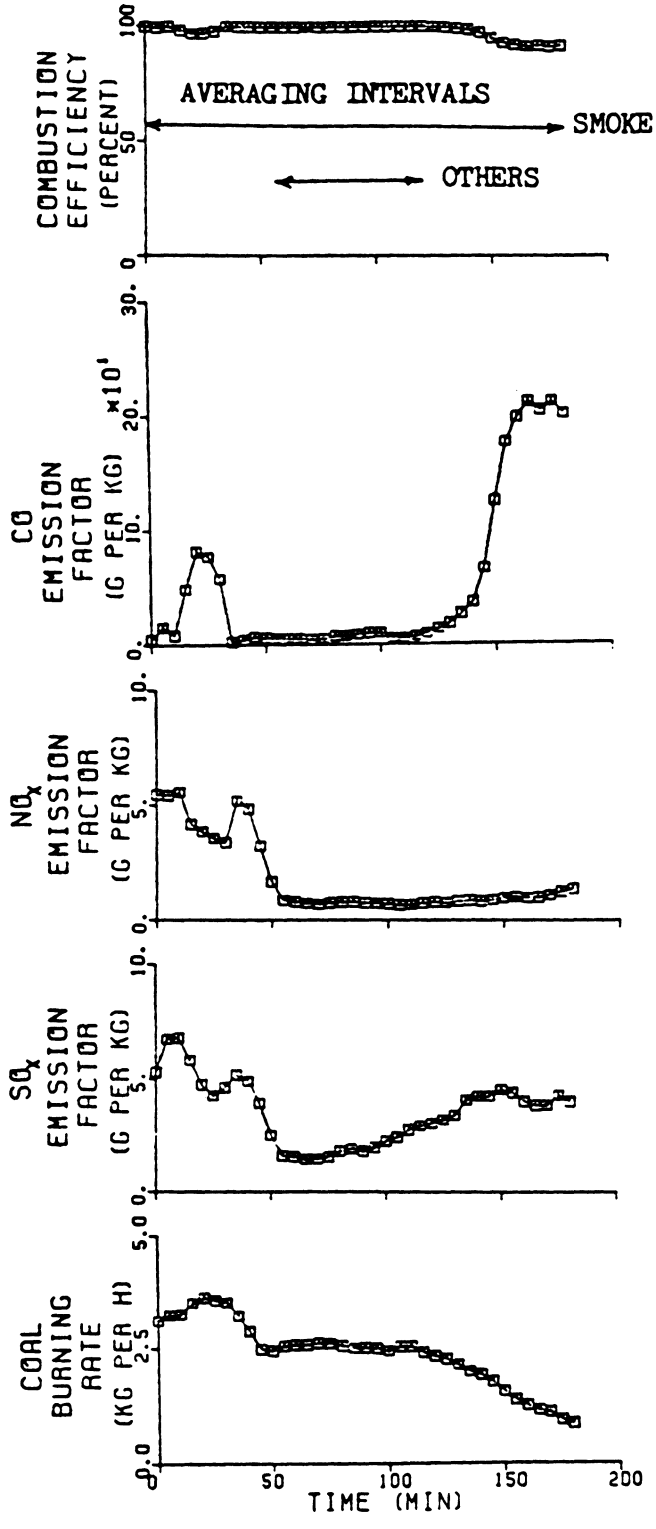

Figure 12. Instantaneous Combustion Efficiency, Emission Factors, and Coal Burning Rate for Test 1 (Baseline Conditions).

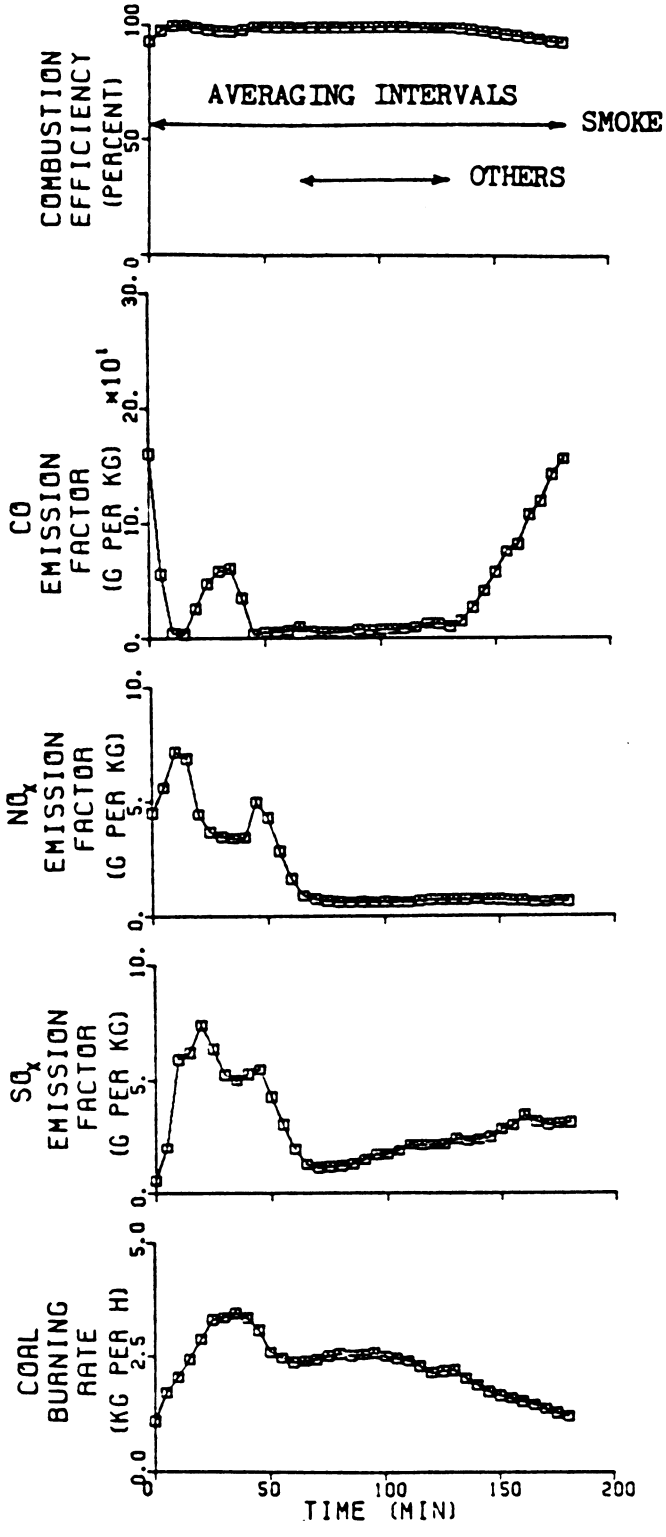

Figure 13. Instantaneous Combustion Efficiency, Emission Factors, and Coal Burning Rate for Test 2 (Baseline Conditions).

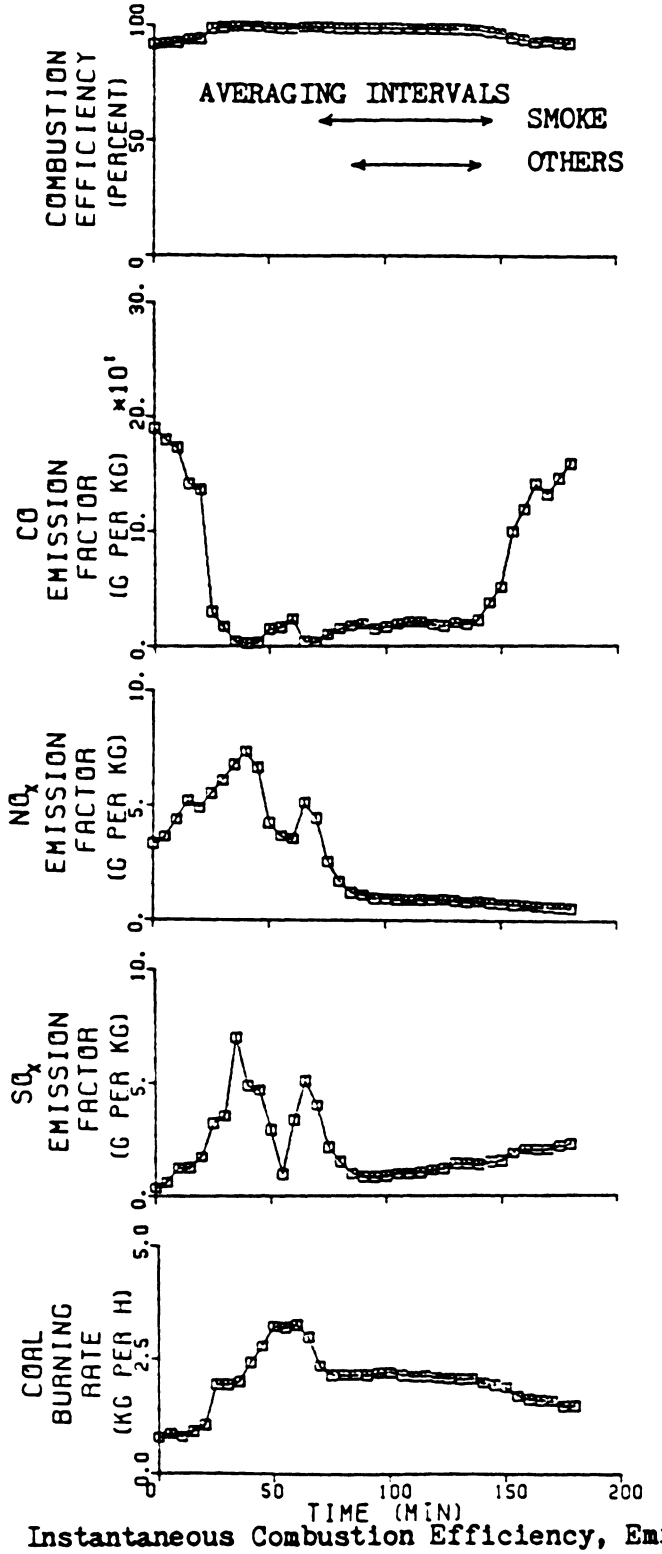

Figure 14. Instantaneous Combustion Efficiency, Emission Factors, and Coal Burning Rate foe Test 3 (Minimum Secondary Air Temperature).

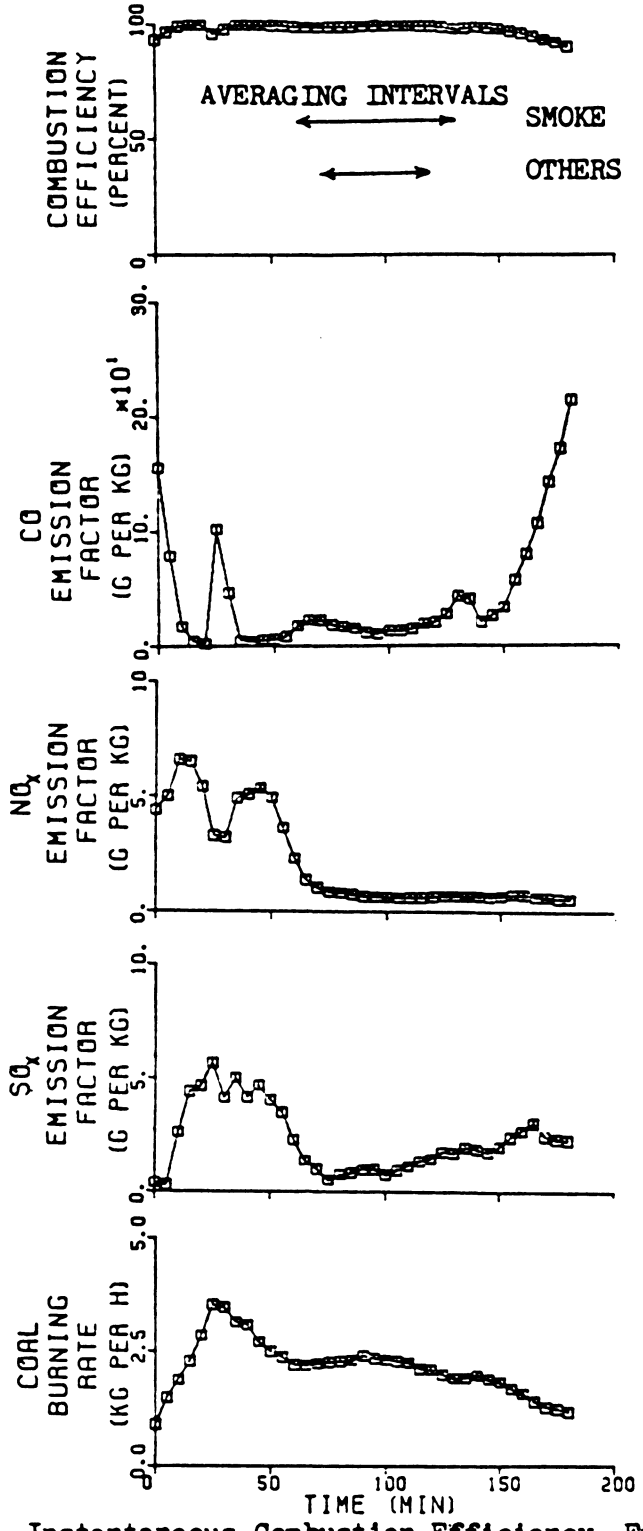

Figure 15. Instantaneous Combustion Efficiency, Emission Factors, and Coal Burning Rate for Test 4 (Minimum Secondary Air Temperature).

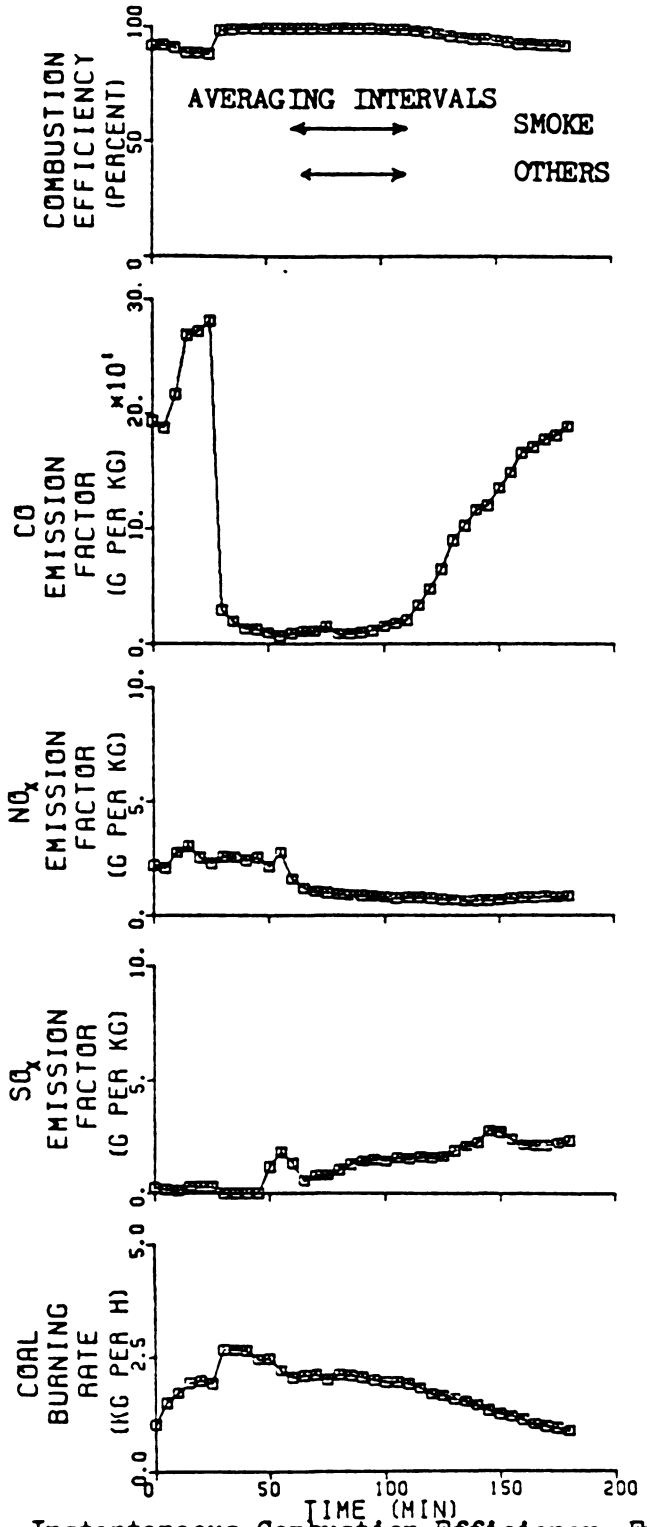

Figure 16. Instantaneous Combustion Efficiency, Emission Factors, and Coal Burning Rate for Test 5 (Minimum Secondary Air Mass Flow Rate).

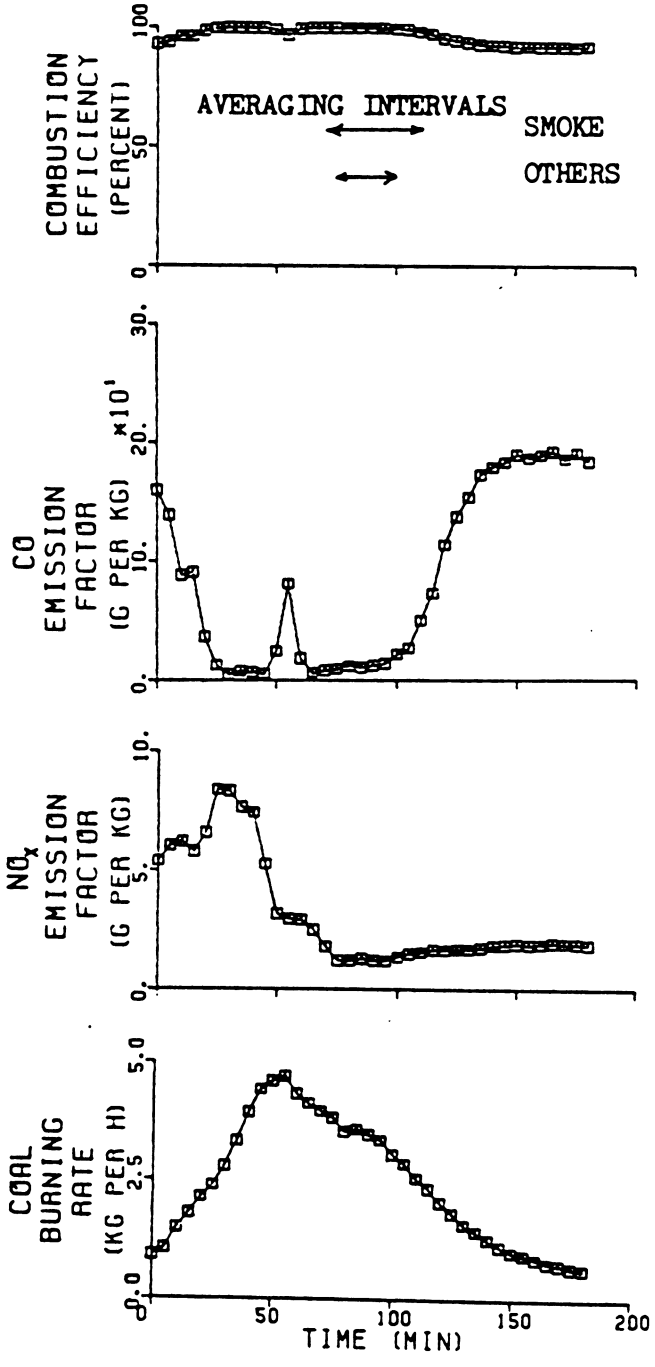

Figure 17. Instantaneous Combustion Efficiency, Emission Factors, and Coal Burning Rate for Test 6 (Maximum Primary Air Mass Flow Rate).

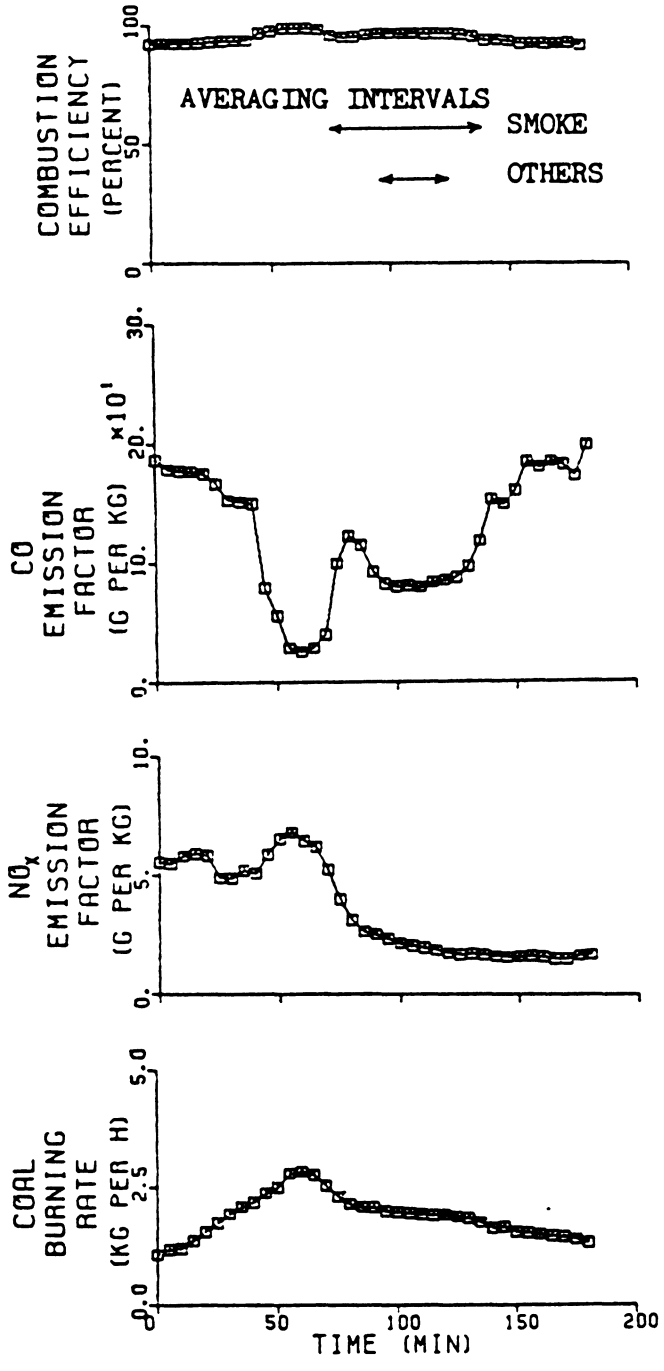

Figure 18. Instantaneous Combustion Efficiency, Emission Factors, and Coal Burning Rate for Test 7 (Maximum Secondary Air Mass Flow Rate).

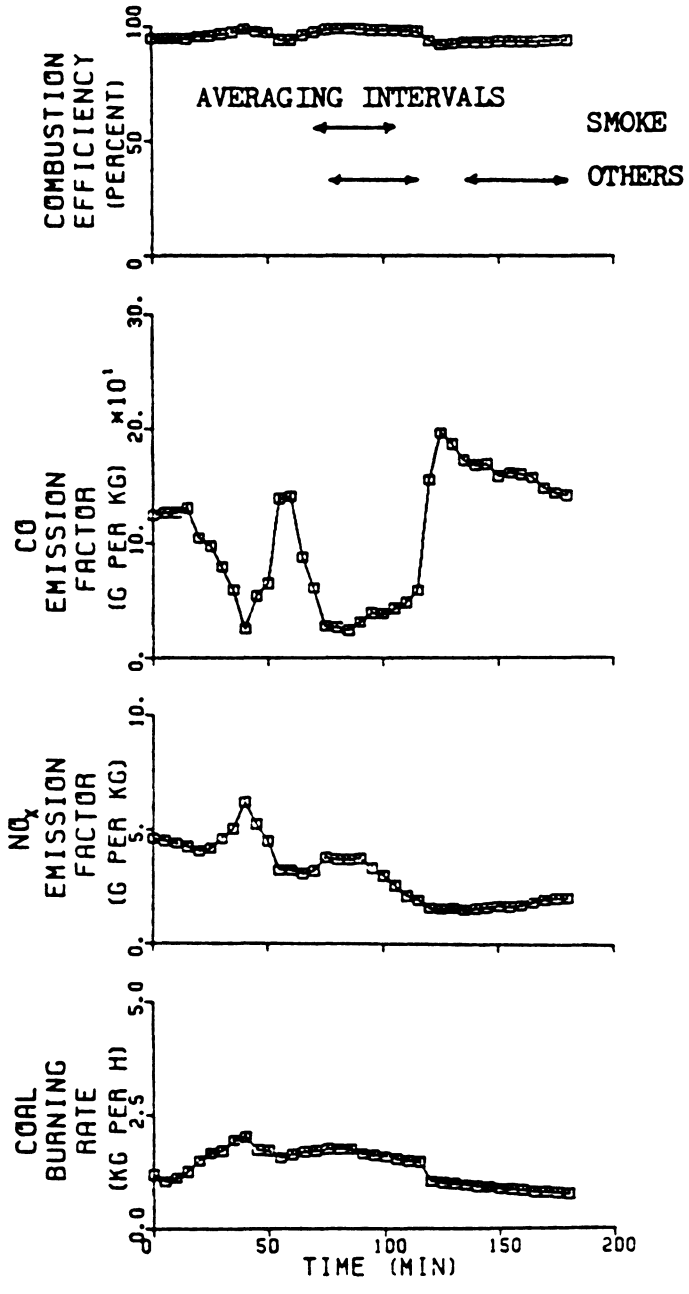

Figure 19. Instantaneous Combustion Efficiency, Emission Factors, and Coal Burning Rate for Test 8 (Minimum Primary Air Mass Flow Rate).

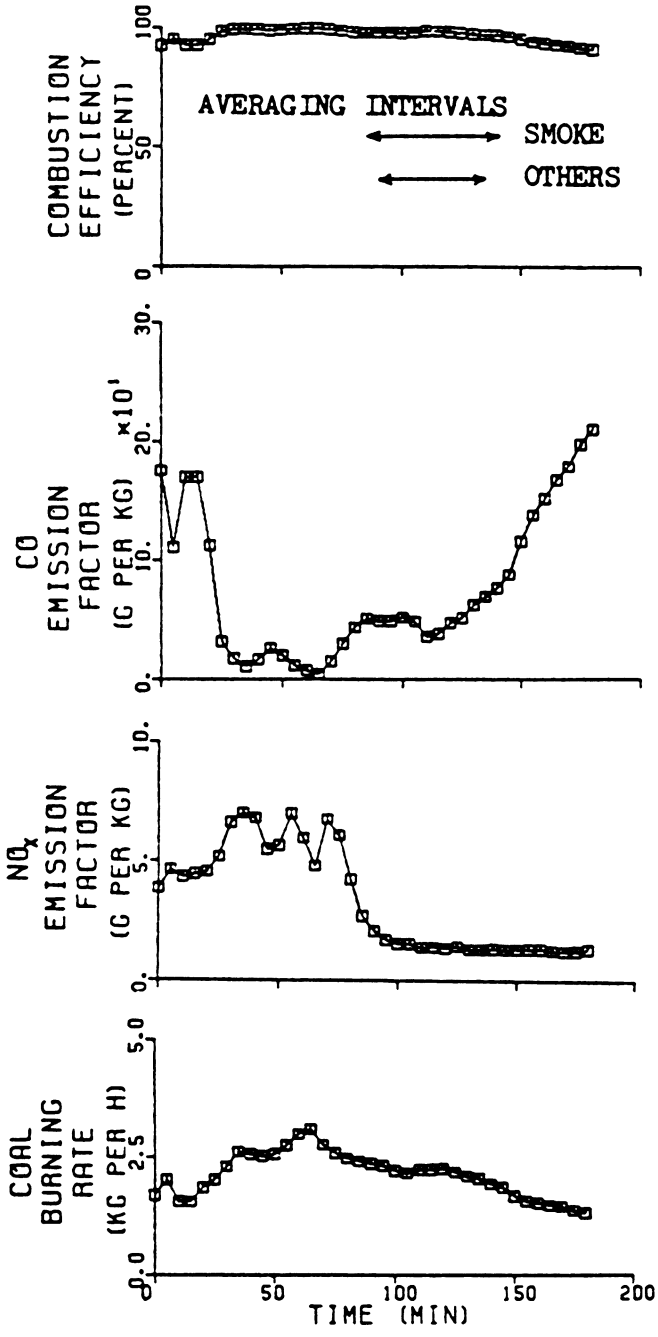

Figure 20. Instantaneous Combustion Efficiency, Emission Factors, and Coal Burning Rate for Test 9 (Maximum Secondary Air Temperature).

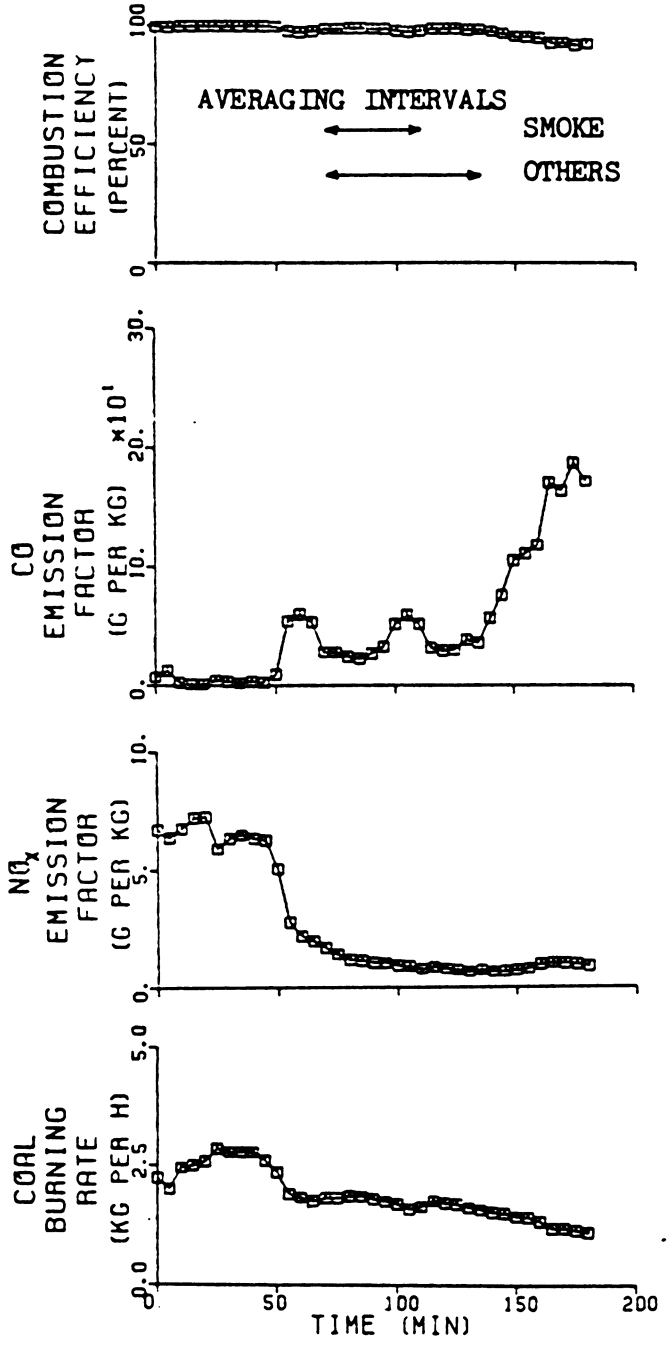

Figure 21. Instantaneous Combustion Efficiency, Emission Factors, and Coal Burning Rate for Test 10 (Minimum Secondary Air Inlet Velocity).

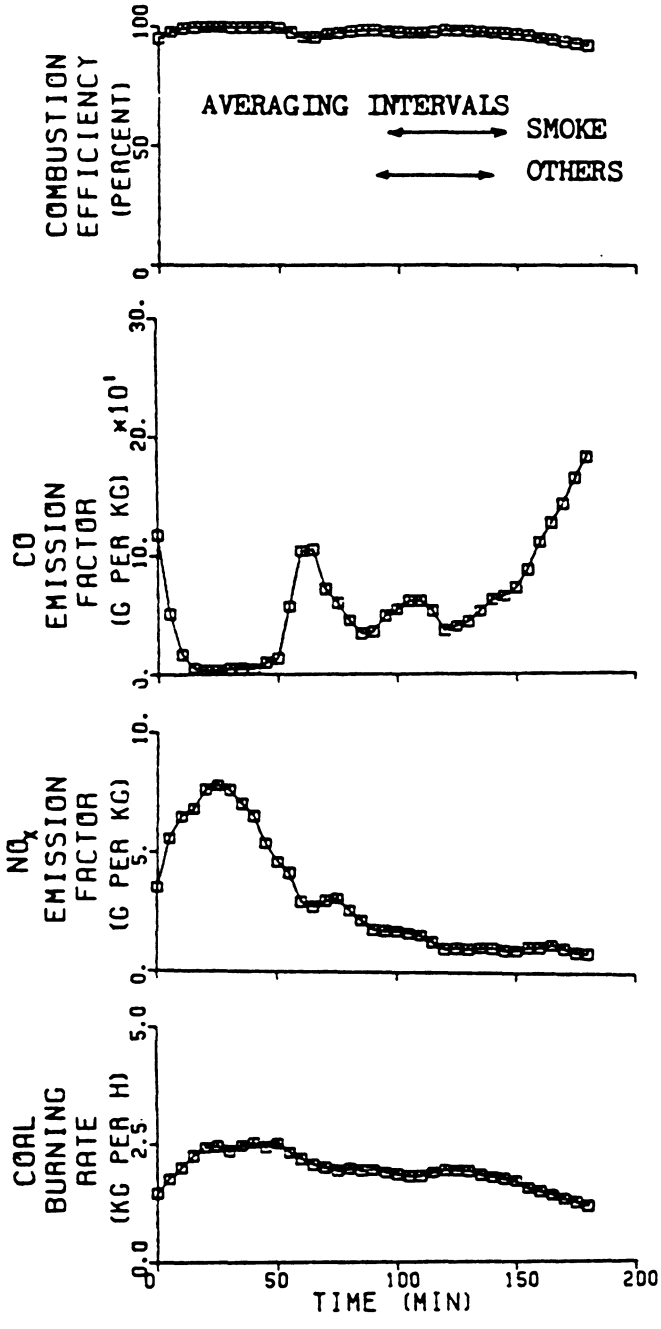

Figure 22. Instantaneous Combustion Efficiency, Emission Factors, and Coal Burning Rate for Test 11 (Maximum Secondary Air Inlet Velocity).

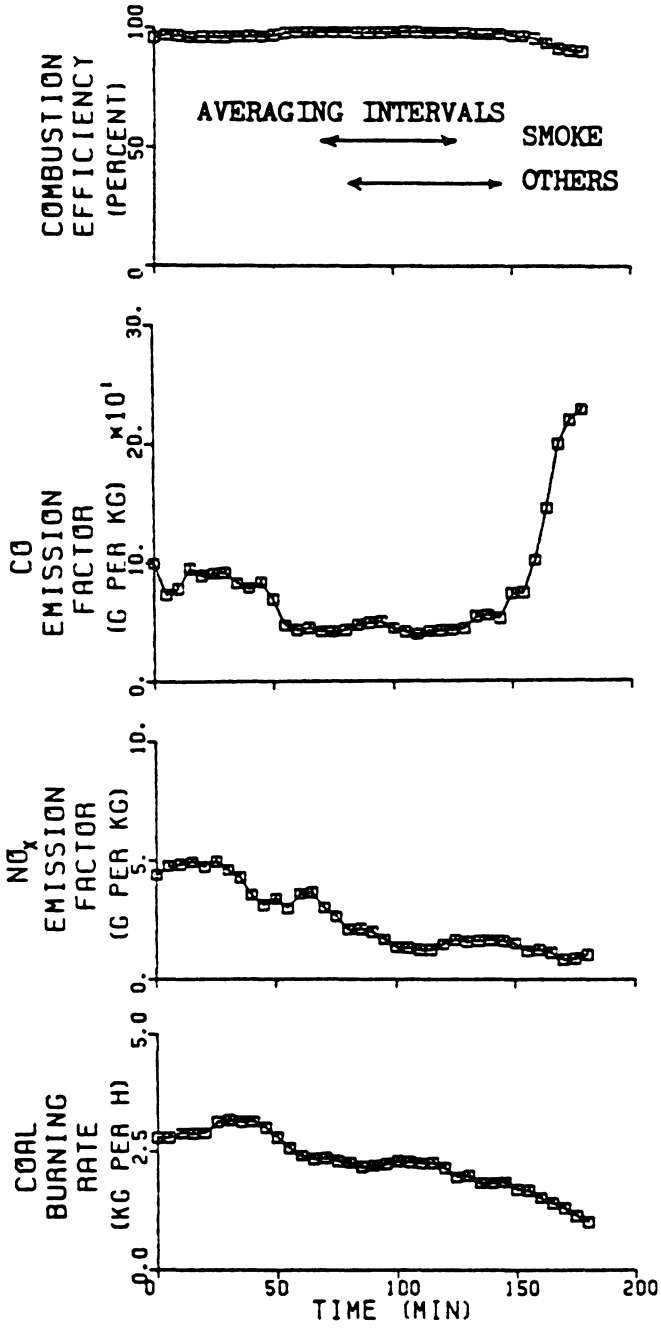

Figure 23. Instantaneous Combustion Efficiency, Emission Factors and Coal Burning Rate for Test 12 (Maximum Swirl).

Table VII. Operating Conditions, Average Combustion Efficiencies, Emission Factors, and Coal Burning Rates During the Steady State Burning Periods on the Emissions Tests.

Test Number and Burning Conditions[a]	Equivalence Ratios		Combustion Efficiency %	Emission Factors (g/kg)				Coal Burning Rate (kg/h)
	Total	Primary		CO	NO_x	SO_x	Smoke	
1.- Baseline	0.76	1.5	99.6	7.0	0.75	2.0	1.1[b]	2.7
2.- Baseline	0.73	1.5	99.5	8.0	0.67	1.7	1.5[b]	2.6
Primary Air Flow								
8B - 7.93 kg/h	0.31	0.92	93.4	160	1.8	-	-	0.94
8A - 12.1	0.53	1.2	98.5	37	3.1	-	0.16	1.8
6 - 24.9[c]	0.82	1.3	99.3	13	1.3	-	1.1	4.2
Secondary Air Flow								
5 - 12.3 kg/h	0.69	1.3	99.4	13	0.92	1.2	0.47	2.2
7 - 25.3	0.44	1.2	96.4	83	2.0	-	1.9	2.3
Secondary Air Temperature								
3 - 25°C	0.65	1.3	99.1	19	0.95	1.1	0.94	2.3
4 - 25	0.70	1.4	99.3	16	0.72	0.98	0.74	2.5
9 - 315	0.63	1.3	97.7	50	1.5	-	2.2	2.5
Secondary Air Inlet Velocity								
10 - 7.74 m/s	0.47	.95	98.2	35	1.0	-	3.7	1.9
11 - 251	0.52	1.1	97.8	50	1.4	-	1.7	2.1
Swirl Number								
12 - 1.56	0.58	1.2	98.0	46	1.6	-	0.56	2.3

a - Baseline conditions: prim. air = 15.4 kg/h, sec. air = 15.7 kg/h, 190°C, 55.2 m/s; swirl no. = 0. Other tests indicate major changes from baseline conditions.
b - Includes smoke from start-up.
c - Steady burning rate not achieved for this test.

burning conditions, as well as the total and primary equivalence ratios, are also given for comparison. The equivalence ratio, which is defined as the actual fuel/air ratio divided by the stoichiometric fuel/air ratio, indicates whether the flame is lean or rich. The variations in the equivalence ratios are due to variations in the burning rate of the coal as well as the different air flow rates.

The losses that detract from the combustion efficiencies are based only on CO and smoke, since volatile hydrocarbons were not measured and had to be neglected. The smoke emissions were considered constant throughout each test so the variations in instantaneous combustion efficiency reflects only the changes in the CO emissions. The smoke accounts for a minor portion of the losses -- typically 12% -- although for tests which have low CO emission factors, such as tests 1 or 2, the smoke accounts for up to 30% of the losses. The smoke emissions are usually higher during start-up than during steady burning conditions. Since the smoke was only collected during the steady conditions, the combustion efficiency is slightly higher for the initial portion of each test than it should be.

Figures 12 and 13, which show the instantaneous values for tests 1 and 2 at baseline conditions, indicate the repeatability of the results. The average values of the gaseous emission factors and the coal burning rate given in Table VII differ by up to 15%. The smoke emission factors differ by 36%. For tests 1 and 2 the smoke was collected during the entire three hours of each test instead of only during the steady period. Test 2 generated more smoke since the fire took longer to get

established. This can be seen on the instantaneous emission factors and burning rates in Figures 12 and 13. Test 2 follows the same patterns as test 1 but lags behind slightly. The smoke emissions from tests 1 and 2 cannot be specifically compared to those from other tests since these tests included start-up emissions. Despite the inclusion of start-up emissions, the smoke emission factors for tests 1 and 2 are not unusually high.

Tests 3 and 4, the minimum secondary air temperature tests, were also used to determine the repeatability of the results. Figures 14 and 15 also indicate fairly good repeatability although test 3 results lag behind those for test 4 due to slower starting of the fire. The average values of emission factors and burning rates for the two tests agree to within 15% for all the values except the NO_x emission factors which differ by 24%.

Figure 16 shows the instantaneous values for test 5, the minimum secondary air test. The quick drop in CO emission factor is due to the increase in secondary air flow that was previously discussed in the Emissions Testing Procedure section.

Figures 17 and 19 for the maximum and minimum primary air tests also show important information. The instantaneous coal burning rate shown for test 6 in Figure 17 indicates that for the bed depth used, steady burning conditions could not be maintained with the maximum primary air flow. Figure 19 shows the different burning conditions for the two low primary air flows for test 8.

To facilitate comparison, the average emission factors were plotted against the independent variables for the emissions tests. These plots are given in Figures 24 through 28. Before comparing these values it should be noted that there are several sources of measurement error which make comparisons difficult. One major problem involved the NO_x measurements. The NO_x emissions for tests 6 through 12 are probably 15% too high. This error, as well as others, are discussed in Appendix 11.6.

The effect of the primary air mass flow rate on emissions can be seen in Figure 24. The CO emission factors indicate that increasing the primary air flow decreases the CO emission factor. The primary air flow rate also directly affects the coal burning rate and the equivalence ratios; higher flow rates lead to higher burning rates and higher equivalence ratios. This leads to a correlation between CO emission factor and primary equivalence ratio -- as one increases, the other decreases. Fenimore and Moore (18) found a similar correlation between CO concentrations in the product gases and the primary zone equivalence ratios which ranged from 0.66 to 1.5 in their study. The smoke emissions show an opposite trend -- they generally increase with increasing primary air. If the smoke collection period for the baseline tests had been consistent with the other tests, the smoke emissions for the baseline tests may have been more compatible with the upward trend shown by the other two tests. No smoke emission factor is given for test 8B, the extremely low primary air test, because the collected smoke was unmeasurable. The correlation between increased air flow and increased

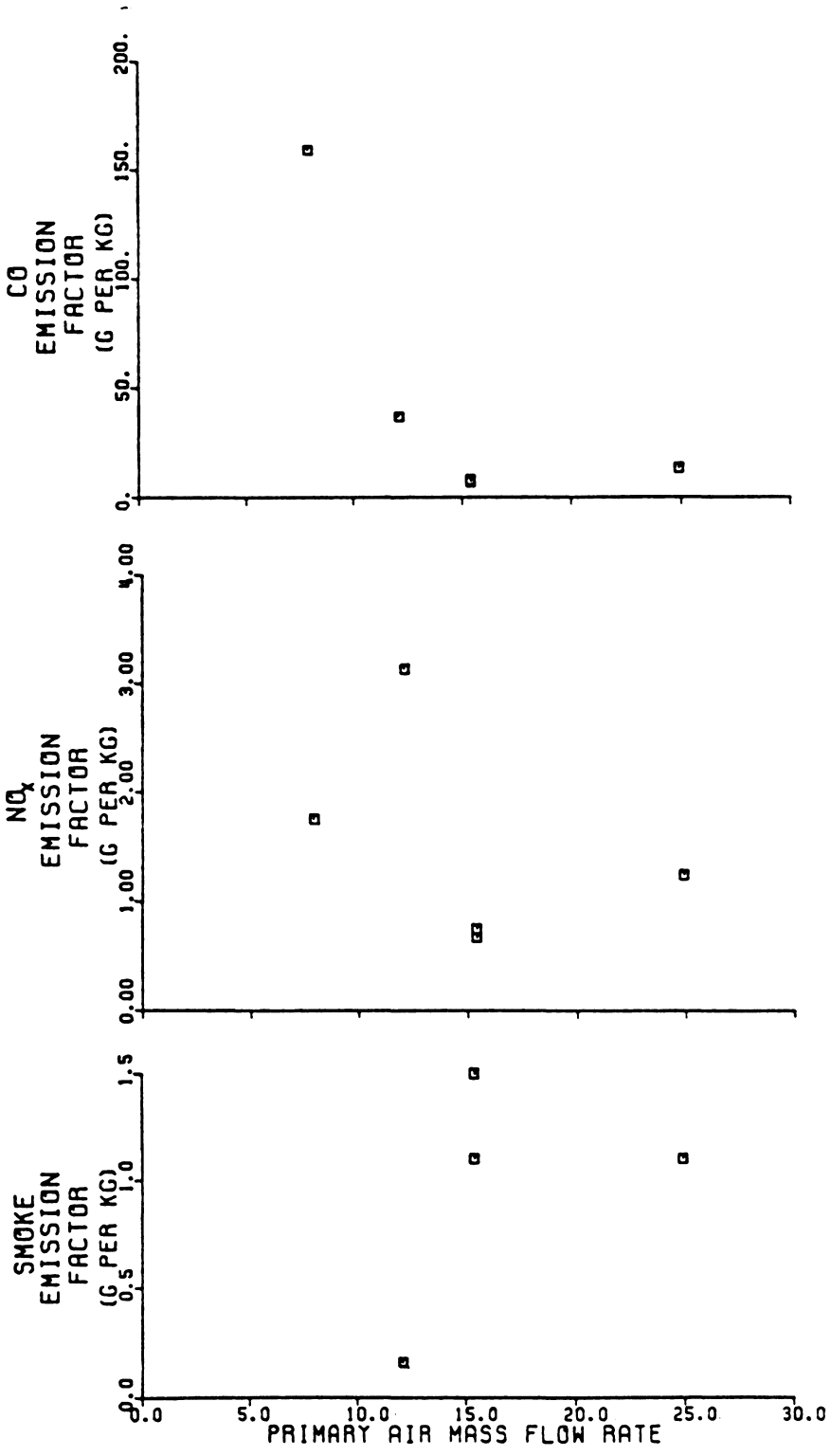

Figure 24. Effect of Primary Air Mass Flow Rate on Emissions.

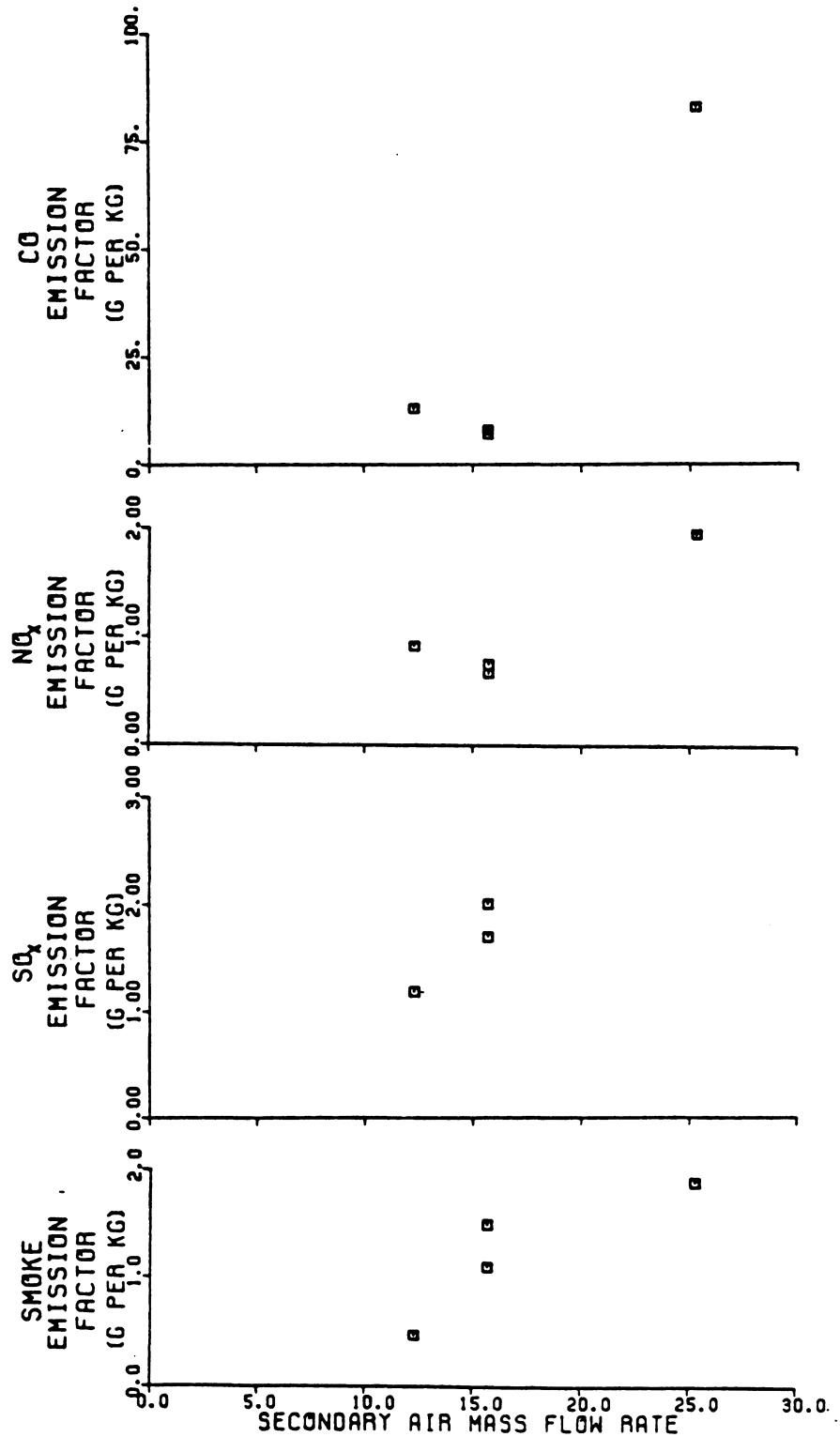

Figure 25. Effect of Secondary Air Mass Flow Rate on Emissions.

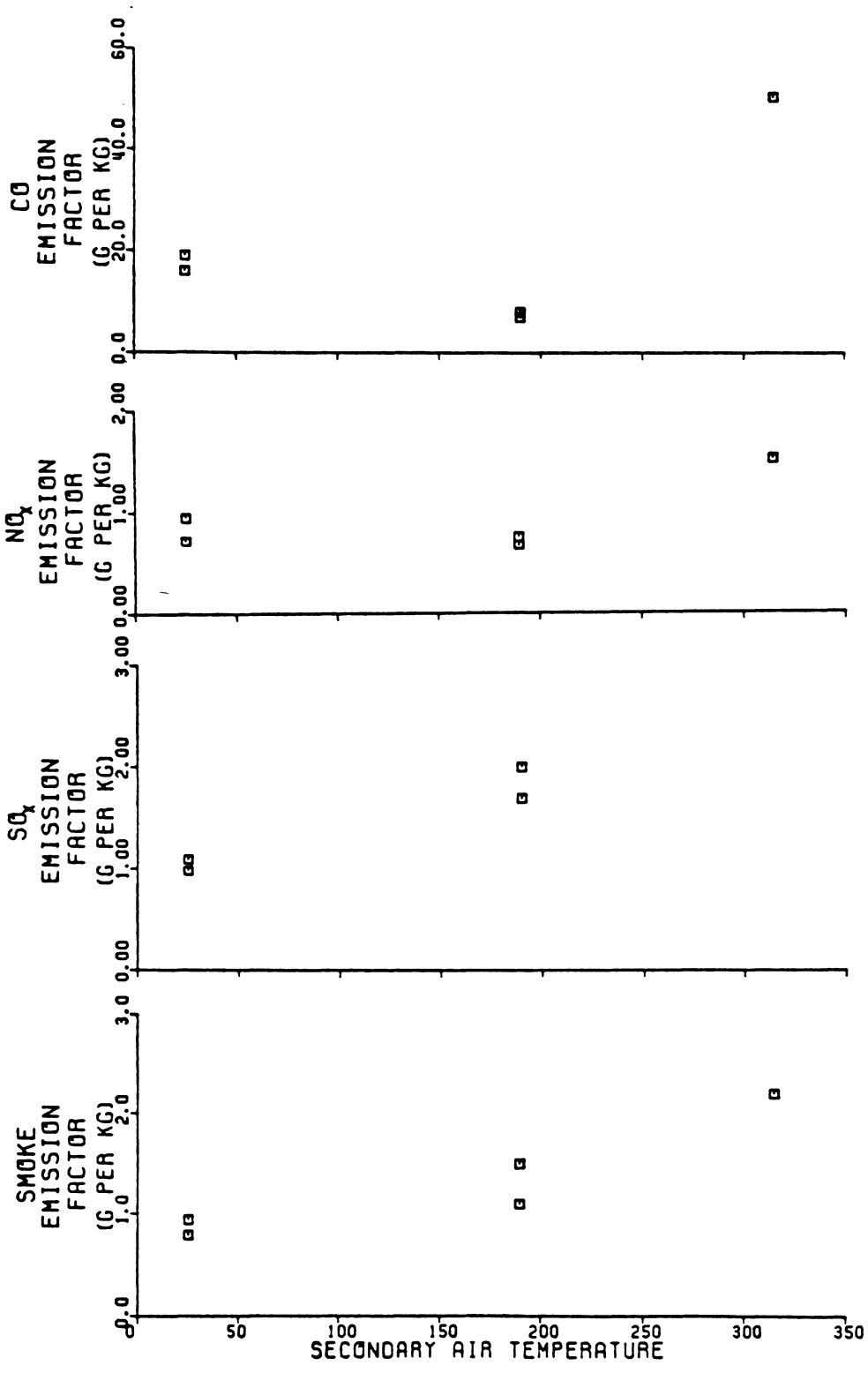

Figure 26. Effect of Secondary Air Temperature on Emissions.

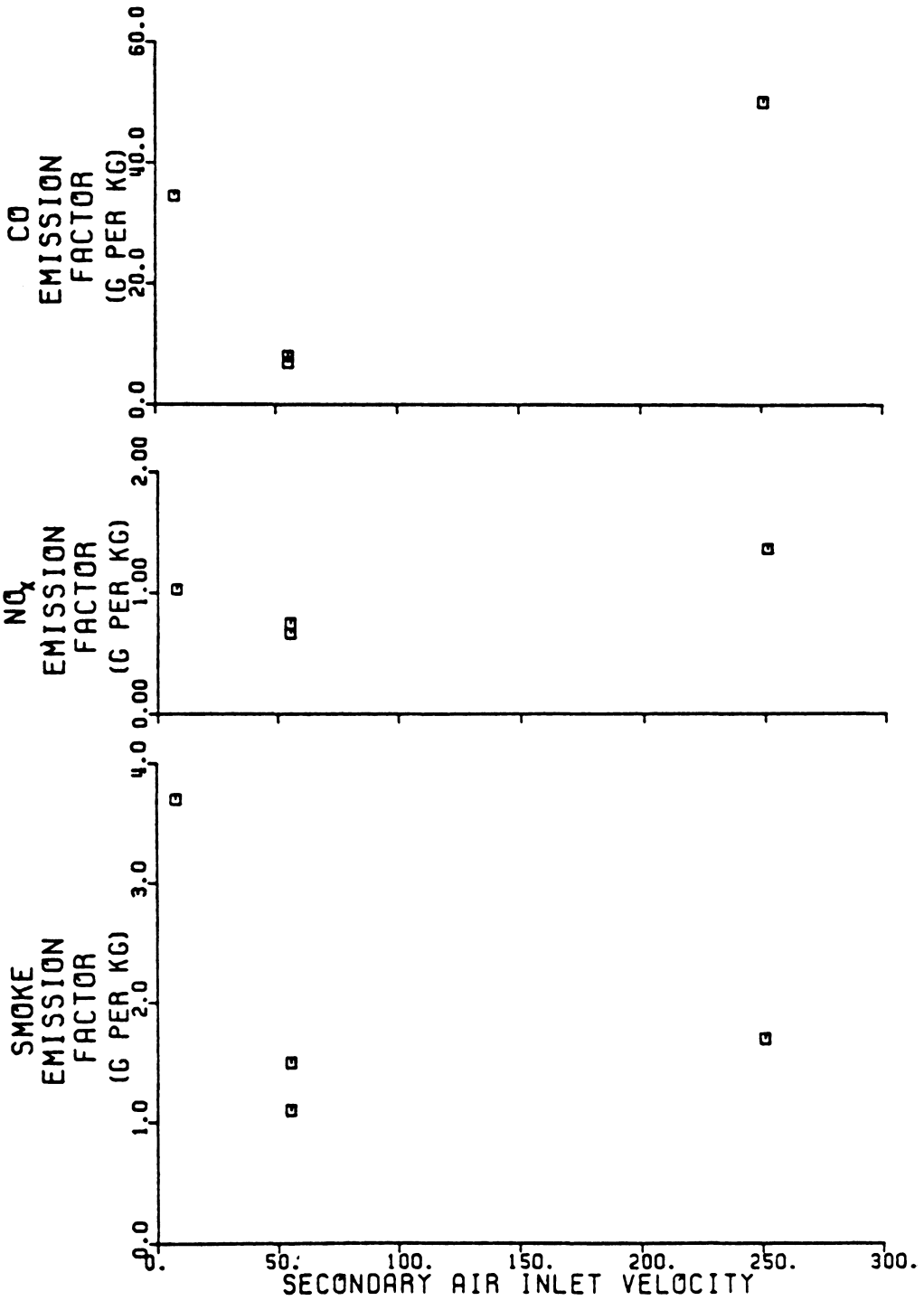

Figure 27. Effect of Secondary Air Inlet Velocity on Emissions.

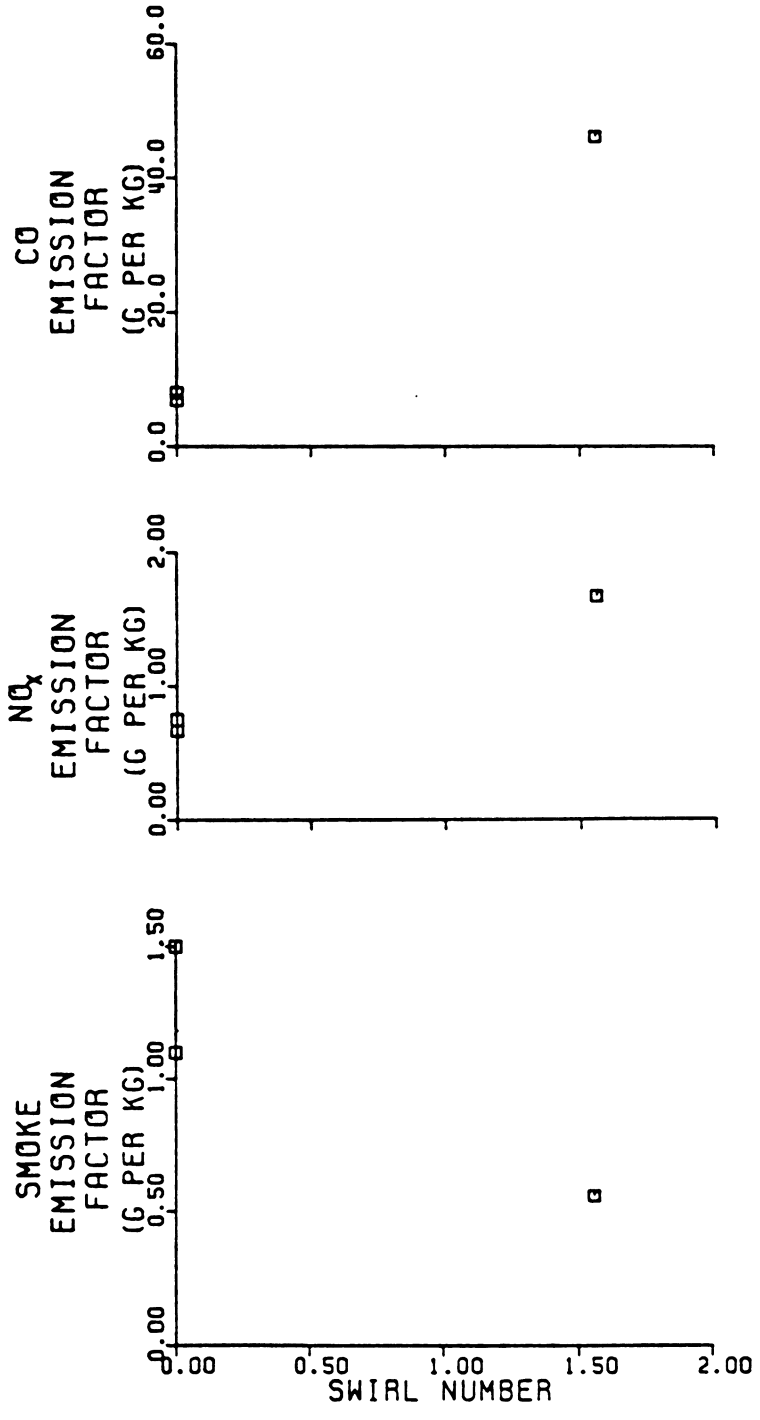

Figure 28. Effect of Swirl on Emissions.

smoke emissions may be due to increased stack velocities which entrain more particles in the gas stream. These particles may consist of fly-ash which separated from the flow at the lower velocities. Smoke particles, which are typically less than 1 μm (30), are probably too small to separate from the flow even at low velocities. The NO_x emissions show no clearly definable trends. Even if the values for tests 6 and 8 are reduced by 15%, the NO_x emissions are still scattered.

The effect of secondary air mass flow rate on emissions can be seen in Figure 25. The CO emission factors again correlate with the primary zone equivalence ratios as in the primary air flow tests. The higher CO emission factor for test 7, the maximum secondary air flow test, may also be due to quenching of the CO oxidation reactions by the large flow of relatively cool secondary air. Fenimore and Moore (20) found that a product-gas temperature of about 1250 K was needed to oxidize CO in products from lean primary flames. However, CO could oxidize in final products from rich primary flames at temperatures below 1250 K. Probe tests indicated that temperatures in the secondary combustion zone only got as high as 1100 K. Fenimore and Moore also found that CO was quenched where cooling with air was fastest. The baseline and minimum secondary air tests have fairly similar NO_x emission factors although the maximum air flow produces a much higher NO_x emission factor. This may be due to the increased availability of oxygen. The differences in the SO_x emission factors may be due to measurement errors which will be discussed later. The smoke emission factors follow a similar trend as they did for the primary air flow tests. The coal burning rates for

tests 5 and 7 are much lower than those for the baseline tests and the reason for this is uncertain.

Figure 26 shows the effect of secondary air temperature on emissions. The CO emission factor is higher for the minimum temperature tests than for the baseline tests. This may be due to quenching. The high CO emission factor for the maximum temperature test is not expected, although possible CO formation from hydrocarbons could be a contributing factor. The NO_x emissions are fairly constant for the low and medium temperatures, but the high temperature test produced high NO_x emissions. The smoke emissions also follow an increasing trend with increasing temperature.

The effect of secondary air inlet velocity on emissions is seen in Figure 27. The change in velocity affected the primary equivalence ratio and probably also affected the mixing in the secondary combustion zone. Although it is uncertain why the secondary air inlet velocity had an effect on the primary equivalence ratio, the CO emission factor again tended to increase with decreasing primary equivalence ratio. The higher-than-baseline values of CO and smoke emission factors for the minimum velocity test may also be due to poor mixing. The low velocity test may have produced kinetic energies that are similar to those from natural draft stoves. The emissions from the test combustor will be compared to those from commercial stoves later but the smoke emission factor for the low velocity test is comparable to smoke emission factors from a natural draft, downward air flow stove such as the Rayburn Prince 76. At higher velocities, the test combustor has much lower smoke

emissions than the Rayburn Prince 76. The NO_x emission factors do not vary significantly for the low velocity and baseline tests. The increased NO_x emission factor for the maximum velocity test may be due to the oxygen made available by the increased mixing. The high CO emission factor for the maximum velocity test may also be due to possible CO formation from hydrocarbons. The increased mixing may have increased the availability of oxygen for hydrocarbon oxidation.

The effect of swirl on emissions is shown in Figure 28. Both CO and NO_x emissions are higher for the high swirl number test compared to the baseline tests. While increased swirl might lead to better mixing, the probe tests discussed later indicate poorer mixing on a macroscopic scale. This poor mixing maintained high CO concentrations near the combustor walls and a high temperature zone near the center of the combustor which probably contributed to the higher NO_x emission factor. Considering the differences in smoke collection periods, the smoke emission factors are probably fairly constant for the baseline and swirl tests.

The baseline tests produced very low emissions. It may have just been coincidence that these conditions were most favorable or perhaps the extreme conditions used in some of the other tests were so far from optimum that high emissions could not have been avoided.

To determine which parameter created the largest variation in the emissions, the average emission factors given in Table VII were reviewed. Initially, it appeared that the primary air flow rate produced the greatest effect. However, the secondary air flow rate, which was

varied over a smaller range than the primary air flow rate, may also have had a considerable effect on emissions if it had been varied over a wider range. The secondary air temperature and velocity and the swirl, which were varied over a greater range than the primary air, all produced lesser effects. Based on the tests performed during this investigation, the primary air flow rate has the greatest effect on emissions.

The emission factors from the test combustor are compared to those from commercial coal stoves in Table VIII. The range of emission factors given for the test combustor encompasses the extremes of operation which were studied. The Coalmaster, Shenandoah, and Rayburn Prince 76 (as tested by Waslo (30)) stoves, which are all natural draft stoves, were tested using the same analyzers and similar experimental methods as the test combustor. The Coalmaster and Shenandoah are updraft stoves, while the Rayburn Prince 76 is a downdraft stove. Smoke emissions reported by Jaasma and Macumber (17) include start-up emissions, while the ranges of smoke emissions reported by Waslo (30) include both start-up tests and reload tests. For the tests reported by Dickinson and Payne (33), the smoke was collected on an electrostatic precipitator. The test combustor results show that low emissions can be achieved by varying the operating conditions. It is unclear whether the downdraft or forced air design of the combustor allows it to achieve lower CO and smoke emissions (compared to commercial stoves) for most burning conditions. The electrical cost of using forced air is negligible and was calculated to be $.03 per day for baseline combustor operating conditions.

Table VIII. Comparison of Emission Factors from the Test Combustor and Commercial Coal Combustors for Residential Heating.

Unit and Coal	Emission Factors g/kg			
	CO	NO_x	SO_x	Smoke
Test combustor Wyoming bituminous	7.0-160	0.67-3.1	0.98-2.0	0.16-3.7
Coalmaster, hand-fired, Clinchfield, bituminous (Ref. 17)	96	5.1	3.3	79
Coalmaster, hand-fired, Pocahontas bituminous (Ref. 17)	105	4.2	2.9	17
Shenandoah, hand-fired, Pocahontas bituminous (Ref. 17)	151	3.3	3.6	54
Shenandoah, hand-fired, Pocahontas bituminous (Ref. 17)	157	2.6	2.8	31
Rayburn Prince 76, hand-fired, Clinchfield bituminous (Ref. 30)	38-55	3.1-6.8	5.1-5.4	7.3-14
Rayburn Prince 76, hand-fired, Pocahontas bituminous (Ref. 30)	81-124	1.2-3.6	3.3	2.3-16
Rayburn Prince 76, hand-fired, bituminous - British (Ref. 33)	-	-	-	2.3-6.8
Coal stove, hand-fired, bituminous (Ref. 7,34,35)	50-120	1.6-6	7-58	10-22
Hardin furnace, stoker, Western Coal (Ref. 36)	11	5	13	16
Will-Burt, stoker, bituminous (Ref. 37)	-	-	-	1.9-9.0
Will-Burt, stoker, Western subbituminous (Ref. 37)	-	-	-	.95-2.2

7.2 Secondary Combustion Zone Conditions

The first probe test, with no swirl, indicated nonuniform conditions across the reference plane in the secondary combustion zone. Figures 29 and 30 show concentrations of CO, CO_2 and O_2 as a function of radial position for a typical set of data. Figure 29 data were probed from the right side of the combustor while Figure 30 data were probed from the left side. Due to the similarity of these results, the nonuniform conditions can not be attributed to disturbances introduced by the probe. It is also possible that nonuniform secondary air jets or nonuniform coal-bed burning contributed to the skewed concentration profiles.

Average values of species concentrations along the centerline of the combustor from five sets of data from the first probe test are shown in Figure 31. These average values are not necessarily representative of the entire cross section due to the nonuniformity discussed above. The changes in concentrations along the axis may be due to mixing patterns in the secondary combustion zone. A rough calculation for the third and fourth axial positions shows that the increase in O_2, if attributed to mixing with air, accounts for the decrease in CO_2 to within 1%. However, the CO concentration remained constant in this interval. The average stack gas concentrations during the time interval that the probe data were taken are 0.16% CO and 9.0% CO_2. No O_2 values were recorded for the stack gas. These values are close to the CO and CO_2 concentrations at the seventh axial position in the secondary

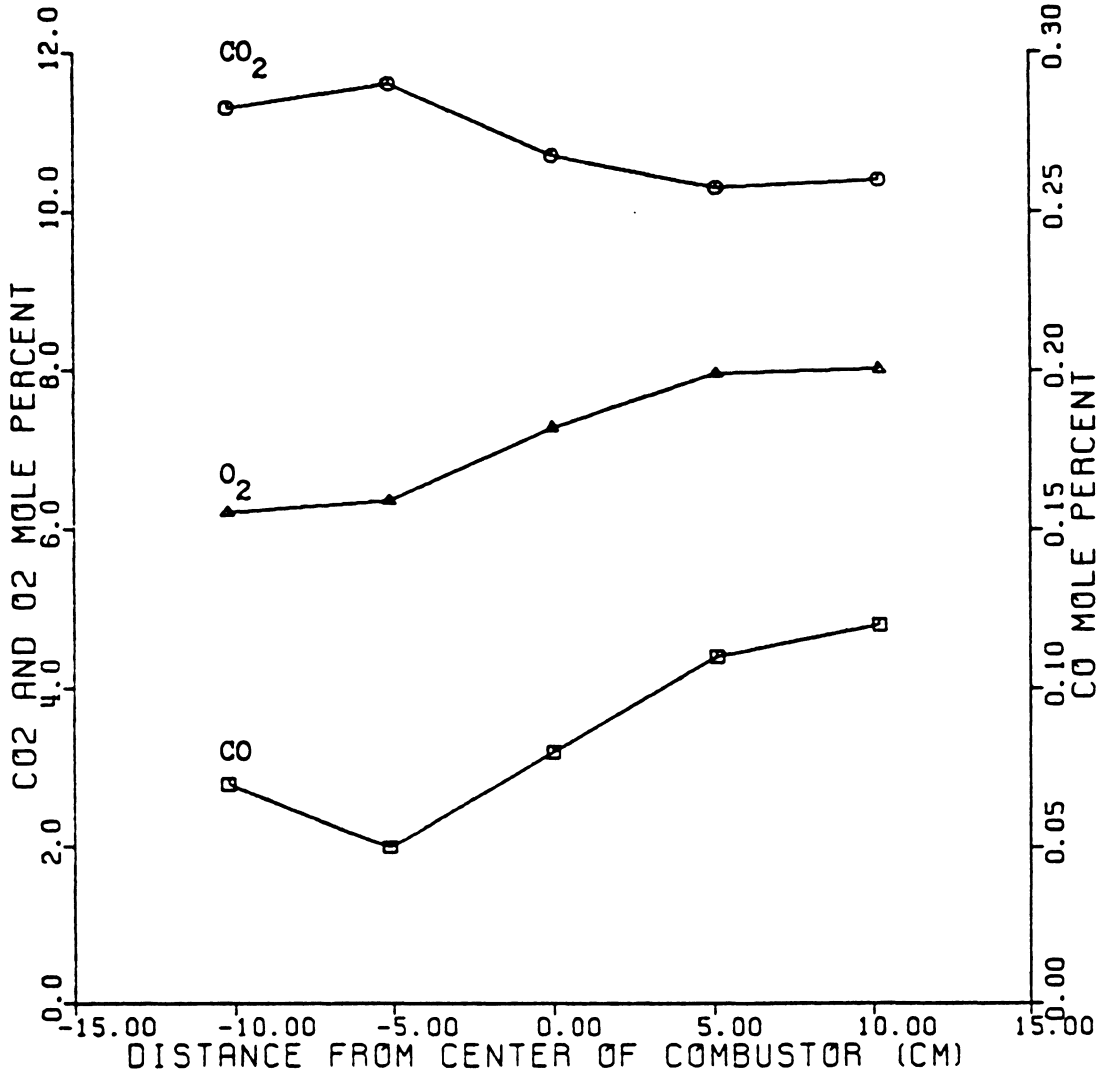

Figure 29. Species Concentrations in the Reference Plane when Probed from the Right Side of the Combustor During Probe Test 1 (No Swirl).

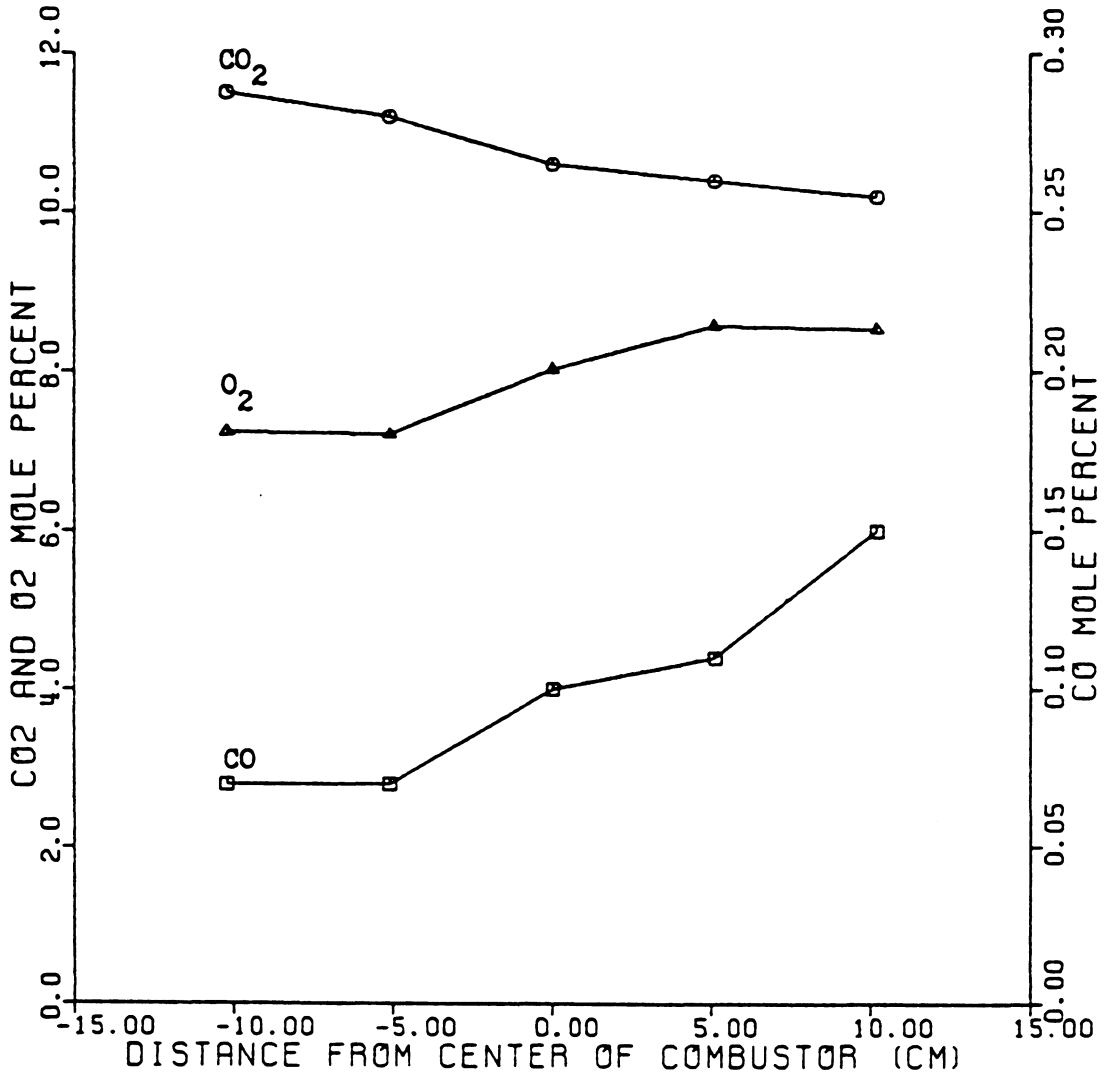

Figure 30. Species Concentrations in the Reference Plane when Probed from the Left Side of the Combustor During Probe Test 1 (No Swirl).

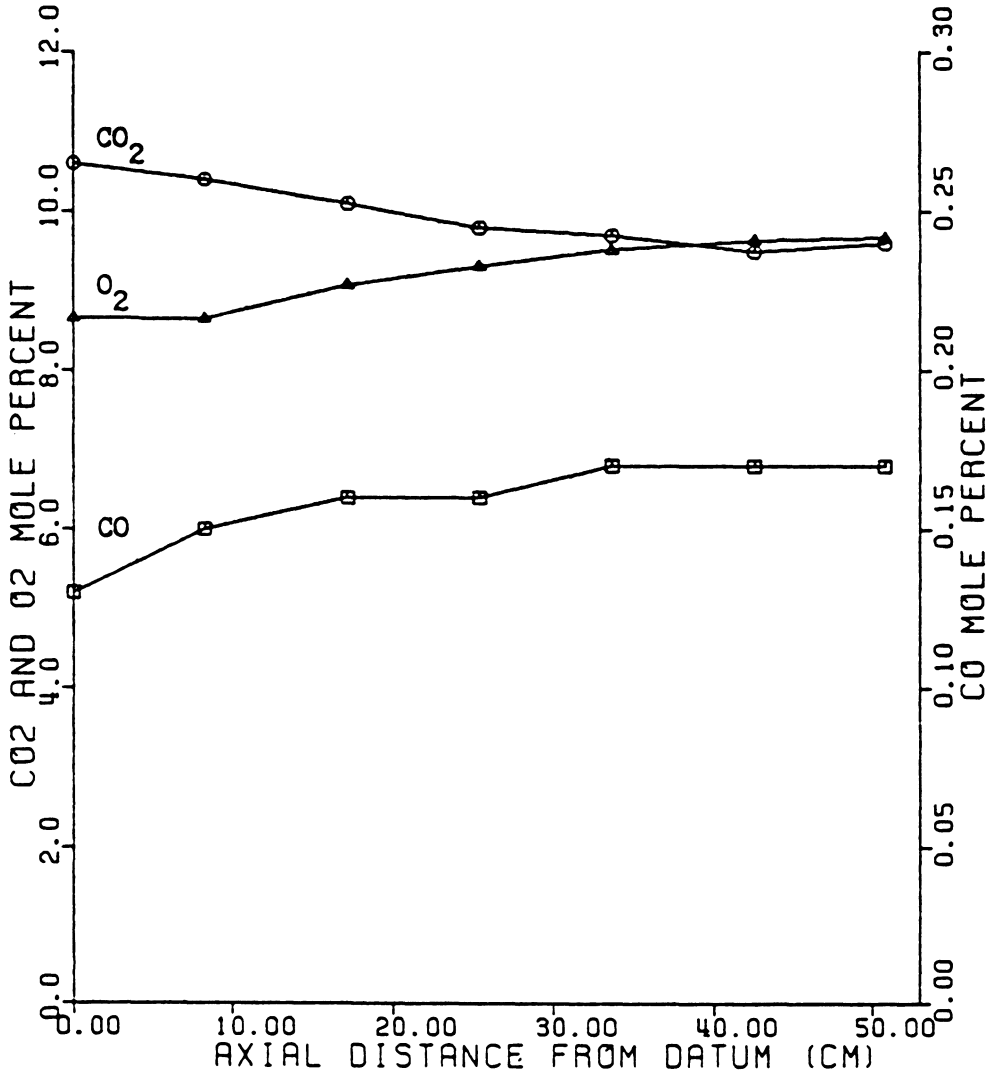

Figure 31. Species Concentrations Along the Combustor Centerline During Probe Test 1 (No Swirl).

combustion zone and may indicate that mixing was complete by the time the gases had reached the exit of the combustor.

Similar data were taken for the second probe test with swirl. The traverse across the top probe diameter showed symmetric variation. Although axial probing along the centerline of the combustor was also done, the results reflect extreme conditions at the center of the combustor. Therefore, traverses at each axial position were done. These results are much more informative. Detailed plots of species concentrations and temperatures in the secondary combustion zone are shown in Figures 32 through 35. To facilitate comparison, these plots have been reduced and are shown together in Figure 36. The plotted values are averages of two sets of data.

All of the figures show that the secondary combustion zone is not well mixed. The O_2 concentrations are very high near the wall where the secondary air stream is flowing and are low near the center of the combustor. This trend can be seen throughout the entire secondary combustion zone. The temperature profiles show lower temperatures near the walls due to the injection of the relatively cool secondary air and lower temperature profiles near the combustor exhaust due to heat transfer through the walls. Centrifugal forces may also contribute to the stratification in the secondary combustion zone since the cooler, denser gases are moved to the combustor wall. The temperature and species concentration profiles indicate that near-stoichiometric combustion may be occurring near the center of the combustor. In addition, since the CO concentration is increasing in the secondary combustion

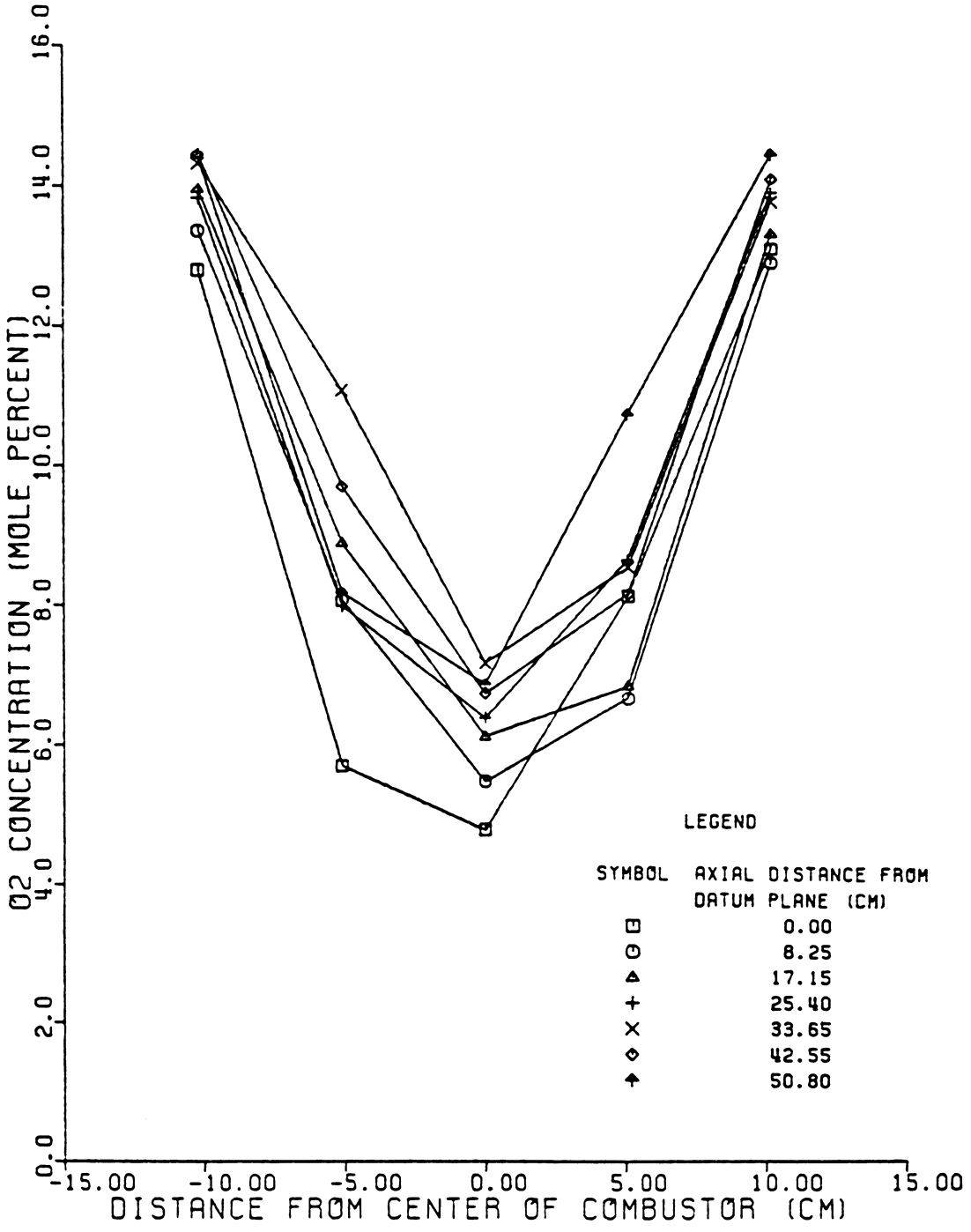

Figure 32. O_2 Concentrations in the Secondary Combustion Zone During Probe Test 2 (With Swirl).

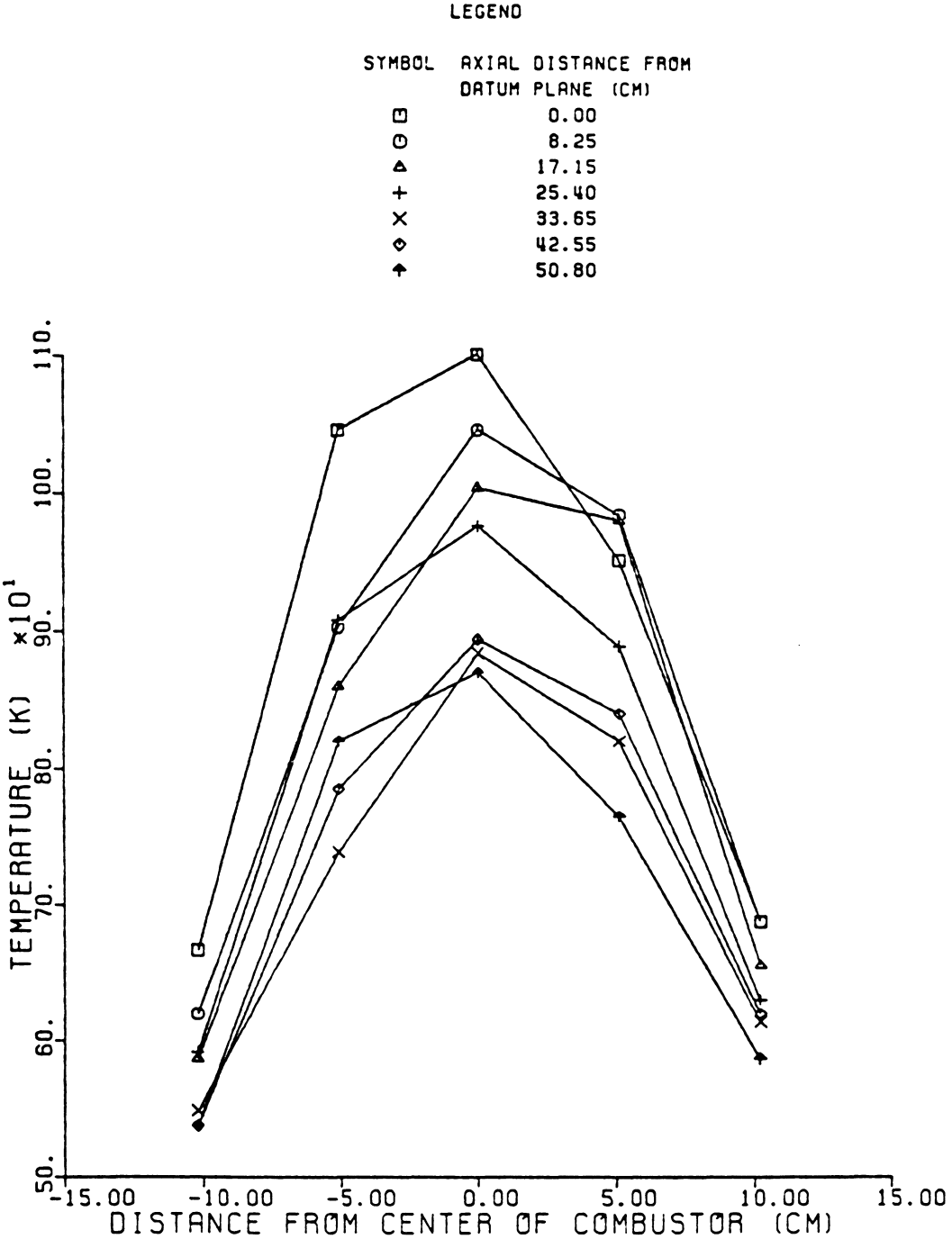

Figure 33. Temperatures in the Secondary Combustion Zone During Probe Test 2 (With Swirl).

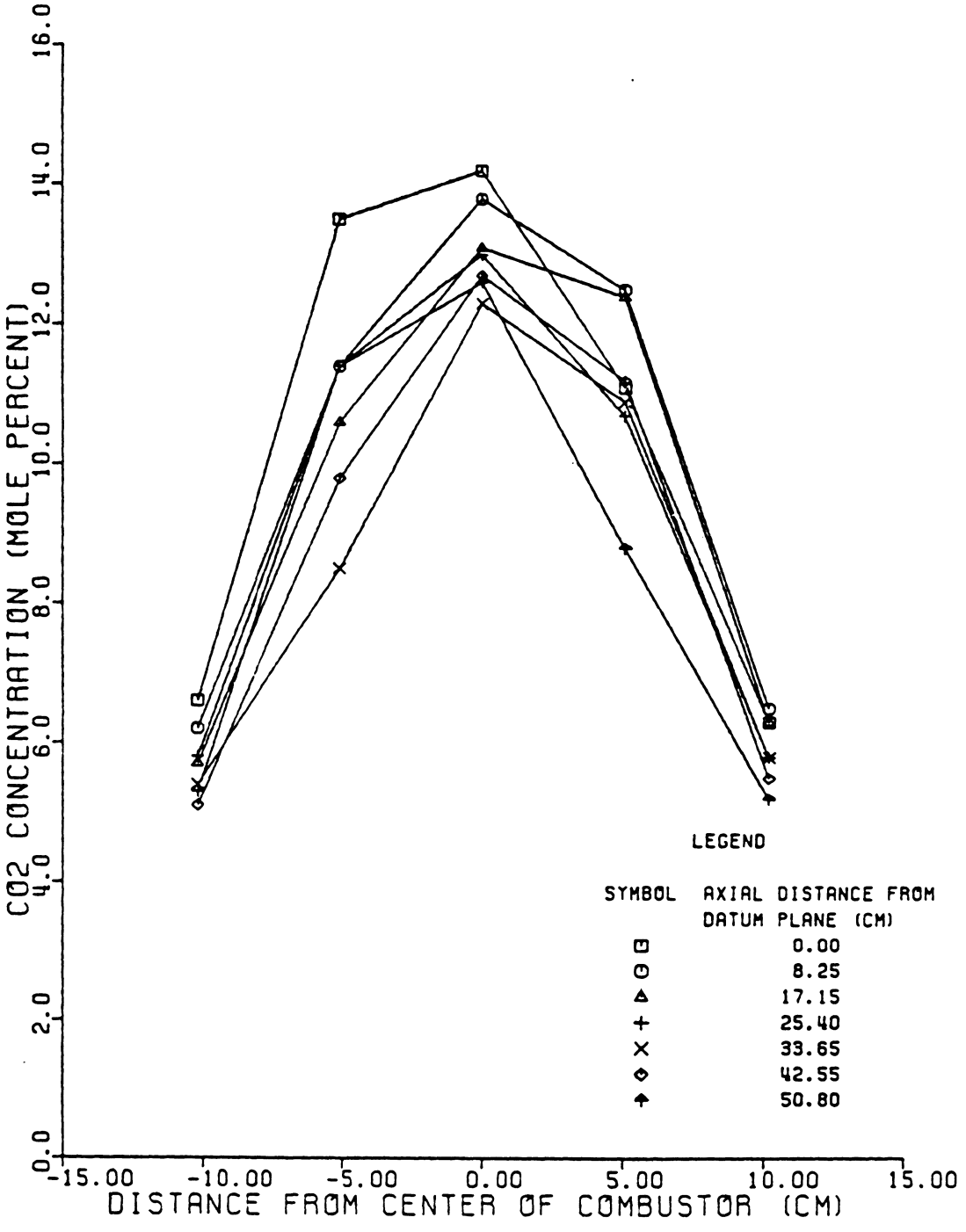

Figure 34. CO_2 Concentrations in the Secondary Combustion Zone During Probe Test 2 (With Swirl).

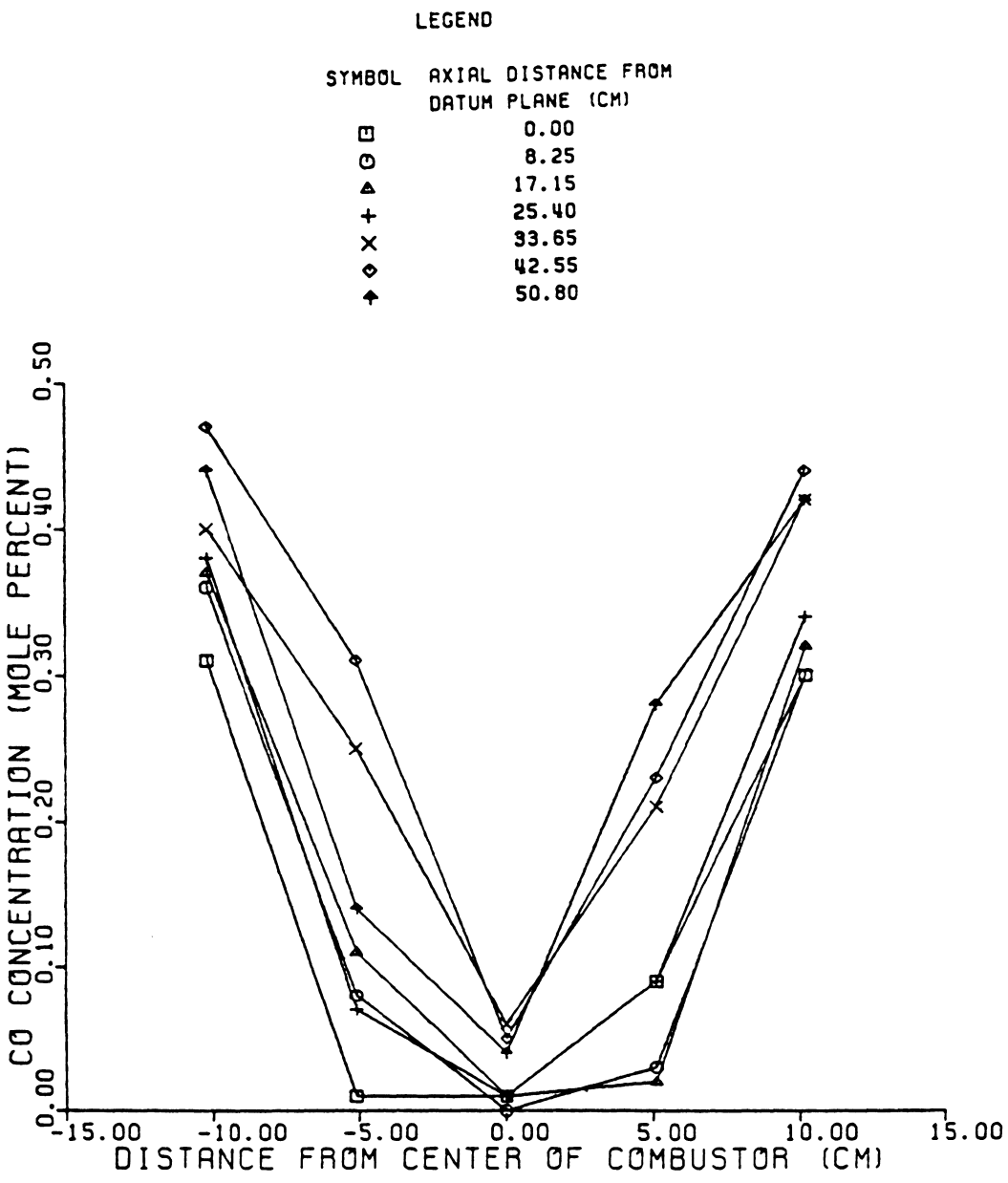

Figure 35. CO Concentrations in the Secondary Combustion Zone During Probe Test 2 (With Swirl).

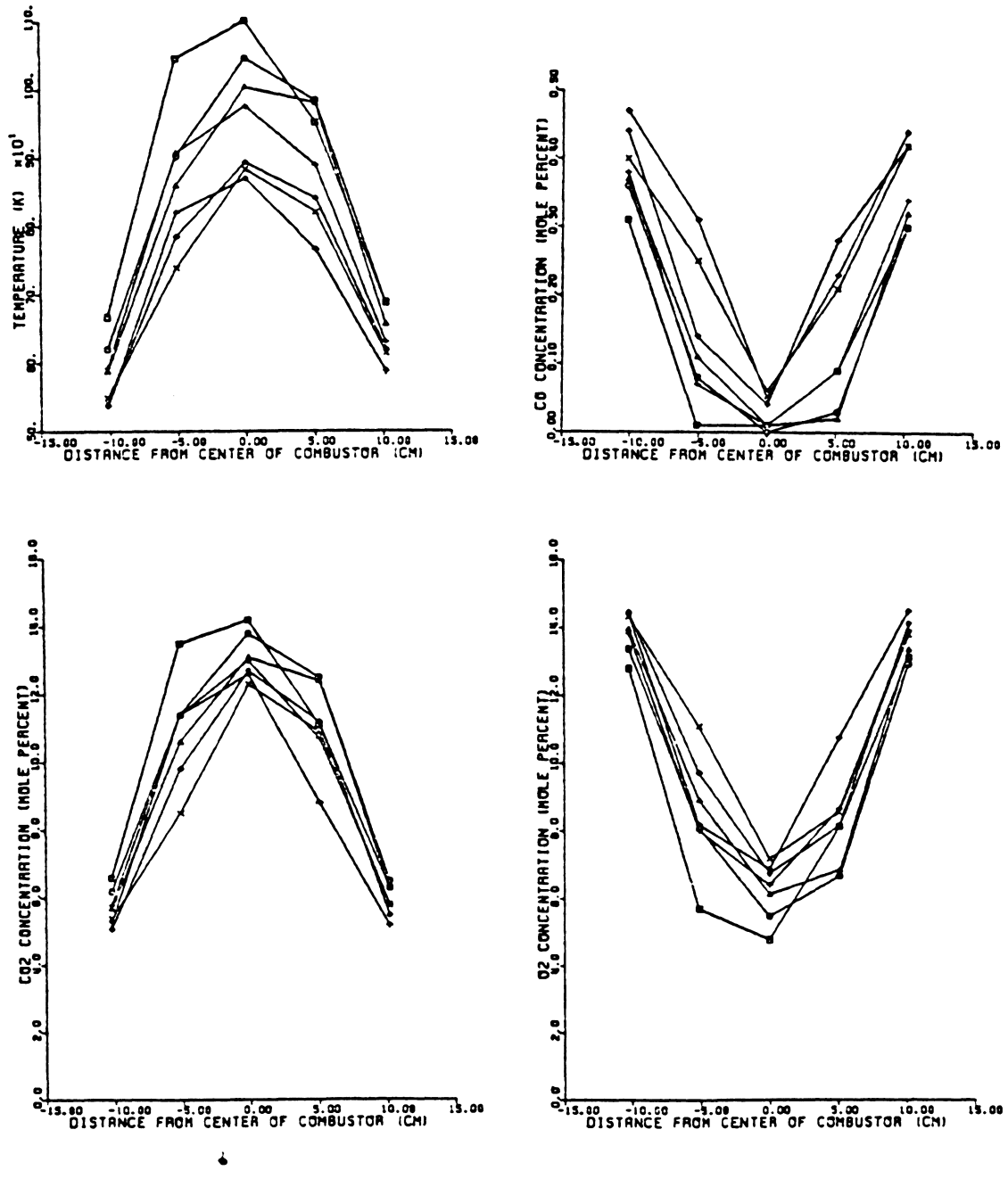

Figure 36. Temperatures and Species Concentrations in the Secondary Combustion Zone During Probe Test 2 (With Swirl).

zone, it is possible that CO is being formed from hydrocarbon oxidation. However, it is also very likely that high CO concentrations near the wall, which were not measured, allowed CO to diffuse into the secondary combustion zone and thus produce the higher CO concentration profiles. Similar phenomena may be occurring for the O_2 profiles and dilution effects may be lowering the CO_2 profiles.

7.3 CO Oxidation Model

The CO concentrations determined from the chemical kinetic CO oxidation model are compared to measured values from the first set of data taken in probe test 2 in Figure 37. The top curve represents results from the model using the temperature profile determined from area averaged temperatures in the secondary combustion zone. The average temperature was initially 810 K and dropped to 690 K near the combustor exhaust. The two other curves represent results from the model using constant temperatures of 1000 and 1500 K throughout the secondary combustion zone. These two cases were used to show the effect of the temperature on the CO oxidation model results. Other species concentrations were initially determined from measured values at the reference datum. Subsequent changes in these concentrations were due to the reactions in the CO oxidation model.

Temperature has a large effect on the kinetics of CO oxidation. All three curves in Figure 37 show an initial drop in the CO concentration, although higher temperatures cause the concentration to decrease more rapidly and produce a lower final concentration of CO. Low tem-

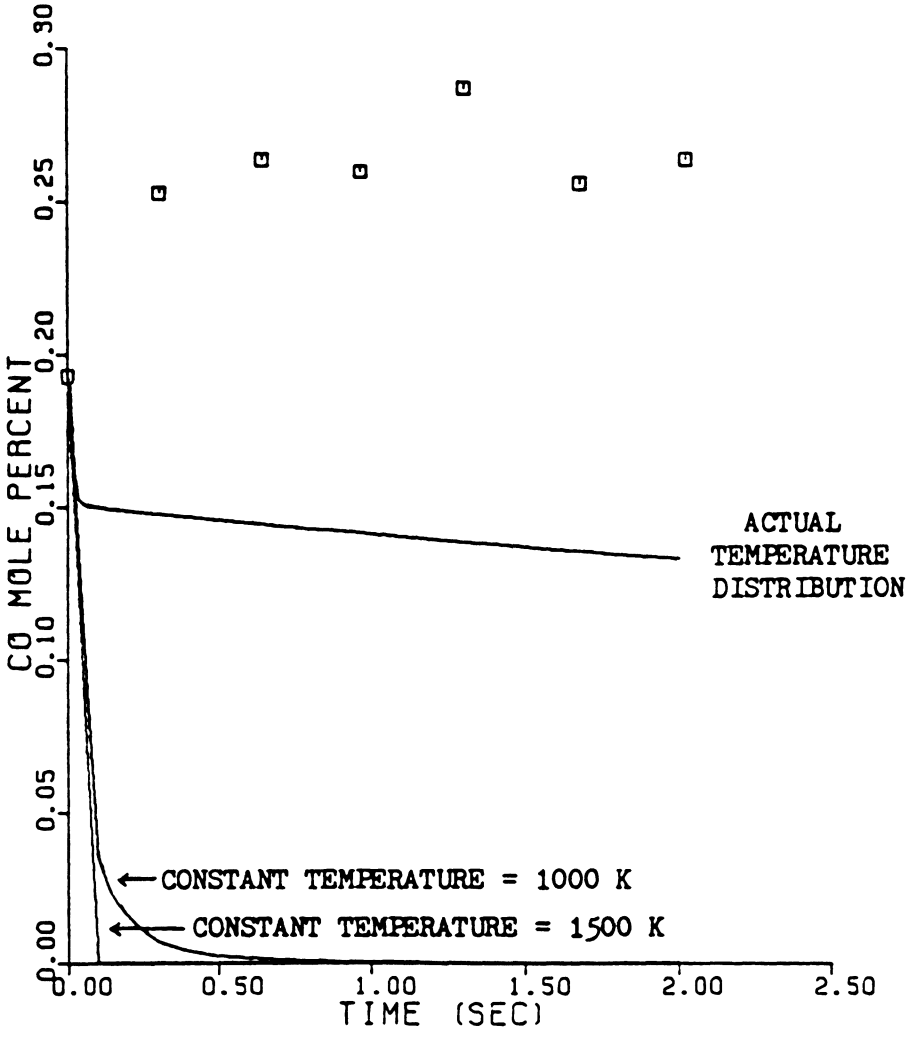

Figure 37. Measured CO Concentrations and Theoretical CO Concentrations for the Actual Temperature Distribution and Two Isothermal Secondary Combustion Zone Conditions.

peratures, which cause quenching of CO, probably contributed to the persistence of CO in the top curve. The distinct change in slope on the top curve was found to be due to the rapid depletion of OH and O, which are present in two of the CO oxidation reactions. The OH and O (as well as the H, HO_2, and O_2) concentrations decreased, since these species were consumed in other reactions that formed H_2, H_2O, and H_2O_2. It should also be noted that the Arrhenius rate constants used in the model are based on data obtained in the temperature range from 900 to 2200 K.

There are large discrepancies between the experimental and model results. While the experimental results show an increase in CO, the model depicts CO oxidation. Several oversimplifications were made in the oxidation model. No consideration was given to the radial variations in species concentrations and temperature or to the mixing in the secondary combustion zone. Possible CO formation from hydrocarbons was also neglected.

8. CONCLUSIONS

The following conclusions can be drawn from this investigation:

1. The CO emission factor and primary air equivalence ratio are inversely related.
2. The smoke emissions from the test combustor are a factor of 12 lower on average compared to other combustors even though the coal burned has a high volatile content.
3. The NO_x and SO_x emission factors are similar for the test combustor and various commercial stoves. However, the CO emission factor for the test combustor is typically lower than those for commercial stoves.
4. The downdraft, forced air design of the test combustor may help maintain low emissions. The electrical cost of supplying the air is negligible.
5. The amount of swirl in the combustor can significantly change the mixing in the secondary combustion zone. A highly stratified flow was created by the tangential secondary air inlets.
6. The low temperatures in the secondary combustion zone probably do not allow CO to oxidize.

9. RECOMMENDATIONS

To further determine the effect of operating conditions on emissions and to better quantify the secondary combustion zone conditions, the following recommendations are presented:

1. Other design and operation conditions than the ones considered here can be studied. The effects of primary temperature and coal size, which change the velocity through the bed, may be of interest.
2. Including a hydrocarbon analyzer in the sampling train would provide additional relevant information for the emissions tests, the probe tests, and the CO oxidation model. Hydrocarbon concentrations in the stack can be used to determine hydrocarbon emissions and to determine an additional chemical energy loss which affects the combustion efficiency. Measuring hydrocarbon concentrations in the secondary combustion zone can possibly provide information on CO formation which would be useful in a model of CO oxidation.
3. Since the two probe tests showed that very different temperature and species concentration profiles over a cross section could be achieved in the secondary combustion zone by changing the parameters that affect mixing, the conditions that produce the most uniform profiles over a cross section should be determined. The combustor could then be used to study the kinetics of homogeneous flows produced by coal combustion. If

sufficient uniformity cannot be obtained, a second generation combustor should be designed to achieve the needed mixing.

10. REFERENCES

1. Combustion-Generated Pollution, Science Research Council, London, 1976.

2. Breen, B. P., "Combustion in Large Boilers: Design and Operating Effects on Efficiency and Emissions, Sixteenth Symposium (International) on Combustion, The Combustion Institute, Pittsburgh, PA, 1976.

3. Macumber, D. W., Efficiency and Emissions of Hand-Fired Residential Coal Stoves, M.S. Thesis, Virginia Polytechnic Institute and State University, 1981.

4. Landry, B. A., and R. A. Sherman, "The Development of a Design of Smokeless Stove for Bituminous Coal," Paper No. 48-A-119, American Society of Mechanical Engineers, New York, 1948.

5. Engdahl, R. B., "Cross-Feed Combustion for Clean Burning of Solid Fuels for REsidences," Presented at the Air Pollution Control Association Meeting, Houston, Texas, June 1978.

6. Fenimore, C. P., "Effects of Diluents and Mixing on Nitric Oxide from Fuel-Nitrogen Species in Diffusion Flames," Sixteenth Symposium (International) on Combustion, The Combustion Institute, Pittsburgh, PA, 1976.

7. Hangebrauck, R. P., D. J. VonLehmden, and J. E. Meeker, "Emissions of Polynuclear Hydrocarbons and Other Pollutants from Heat-Generation and Incineration Processes," Journal of the Air Pollution Control Association, Vol. 14, No. 7, 1964, p. 267-278.

8. Martin, F. J., and P. K. Dederick, "NO_x from Fuel Nitrogen in Two-Stage Combustion," Sixteenth Symposium (International) on Combustion, The Combustion Institute, Pittsburgh, PA, 1976.

9. Gibbs, B. M., F. J. Pereira, and J. M. Beer, "The Influence of Air Staging on the 'NO' Emission from a Fluidised Bed Coal Combustor," Sixteenth Symposium (International) on Combustion, The Combustion Institute, Pittsburgh, PA, 1976.

10. Sadakata, M., Y. Fujioka, and D. Kunii, "Effects of Air Preheating on Emissions of NO, HCN, and NH_3 from a Two-Stage Combustion," Eighteenth Symposium (International) on Combustion, The Combustion Institute, Pittsburgh, PA, 1981.

11. Claypole, T. C., and N. Syred, "The Effect of Swirl Burner Aerodynamics on NO_x Formation," Eighteenth Symposium (International) on Combustion, The Combustion Institute, Pittsburgh, PA, 1981.

12. Beér, J. M., M. T. Jacques, W. Farmayan, and B. R. Taylor, "Fuel-Nitrogen Conversion in Staged Combustion of a High Nitrogen Petroleum Fuel," Eighteenth Symposium (International) on Combustion, The Combustion Institute, Pittsburgh, PA, 1981.

13. Baldwin, J. C. D., and C. H. Long, "Effect of Swirl on NO_x Emissions From a Gas-Fired Burner," Paper No. 74-WA/Fu-3, American Society of Mechanical Engineers, New York, 1974.

14. Wendt, J. O. I. "Fundamental Coal Combustion Mechanisms and Pollutant Formation in Furnaces," Progress in Energy and Combustion Science, Vol. 6, 1980, p. 201-222.

15. Goldstein, H. L., and C. W. Siegmund, "Particulate Emissions from Residual Fuel Boilers: Influence of Combustion Modification," Paper No. 76-WA/APC-3, American Society of Mechanical Engineers, New York, 1976.

16. Merryman, E. L., and A. Levy, "Enhanced SO_3 Emissions from Staged Combustion," Seventeenth Symposium (International) on Combustion, The Combustion Institute, Pittsburgh, PA, 1978.

17. Jaasma, D. R., and D. W. Macumber, "Measurement Techniques and Emission Factors for Hand-Fired Coalstoves," Proceedings of the Air Pollution Control Association Specialty Conference on Residential Wood and Coal Combustion, March 1-2, 1982, in press.

18. Fenimore, C. P., and J. Moore, "Quenched Carbon Monoxide in Fuel-Lean Flame Gas," Combustion and Flame, Vol. 22, 1974, p. 343-351.

19. Howard, J. B., G. C. Williams and D. H. Fine, "Kinetics of Carbon Monoxide Oxidation in Postflame Gases," Fourteenth Symposium (International) on Combustion, The Combustion Institute, Pittsburgh, PA, 1973.

20. Bowman, C. T., "Kinetics of Pollutant Formation and Destruction in Combustion," Progress in Energy and Combustion Science, Vol. 1, 1975, p. 33-45.

21. Westbrook, C. K., and F. L. Dryer, "Chemical Kinetics and Modeling of Combustion Processes," Eighteenth Symposium (International) on Combustion, The Combustion Institute, Pittsburgh, PA, 1981.

22. Westbrook, C. K., J. Creighton, C. Lund and F. L. Dryer, "A Numerical Model of Chemical Kinetics of Combustion in a Turbulent Flow Reactor," The Journal of Physical Chemistry, Vol. 81, No. 25, 1977.

23. Caretto, L. S., "Modeling Pollutant Formation in Combustion Processes," Fourteenth Symposium (International) on Combustion, The Combustion Institute, Pittsburgh, PA, 1973.

24. Cherian, M. A., "Kinetic Modeling of the Oxidation of Carbon Monoxide in Flames," Eighteenth Symposium (International) on Combustion, The Combustion Institute, Pittsburgh, PA, 1981.

25. Kondratiev, V. N., and V. V. Azatyan, "HO_2 Radicals in Combustion Reactions," Fourteenth Symposium (International) on Combustion, The Combustion Institute, Pittsburgh, PA, 1973.

26. Peeters, J., and G. Mahnen, "Reaction Mechanisms and Rate Constants of Elementary Steps in Methane-Oxygen Flames," Fourteenth Symposium (International) on Combustion, The Combustion Institute, Pittsburgh, PA, 1973.

27. Westbrook, C. K., and F. L. Dryer, "A Comprehensive Mechanism for Methanol Oxidation," Combustion Science and Technology, Vol. 20, 1979, p. 125-140.

28. Dryer, F. L., and C. K. Westbrook, "Chemical Kinetic Modeling for Combustion Application," AGARD Conference Proceedings No. 275, Combustor Modeling, AGARD, 1980.

29. Culp Jr., A. W., Principles of Energy Conversion, McGraw-Hill, New York, 1979.

30. Waslo, D. Emissions, Efficiency, and Combustion Chamber Conditions of a Smokeless Hand-Fired Coal Heater, M. S. Thesis, Virginia Polytechnic Institute and State University, 1982.

31. Personal Communication with F. L. Dryer.

32. Kee, R. J., J. A. Miller, and T. H. Jefferson, CHEMKIN: A General-Purpose, Problem-Independent, Transportable, Fortran Chemical Kinetics Code Package, Sandia Laboratories, Albuquerque, NM, 1980.

33. Dickinson, R., and R. C. Payne, "United Kingdom Efficiency Tests and Standards for Residential Solid Fuel Heating Appliances," Residential Solid Fuels, Oregon Graduate Center, Beaverton, OR, 1982.

34. Butcher, S. S., and M. J. Ellenbecker, "Particulate Emission Factors for Small Wood and Coal Stoves," Residential Solid Fuels, Oregon Graduate Center, Beaverton, OR, 1982.

35. Shaw, J. T., "Oxides of Nitrogen from a Closed Room Heater Burning a Smokeless Fuel," Journal of the Institute of Energy, Vol. LIV, March 1981.

36. DeAngelis, D. G., and R. B. Reznik, "Source Assessment: Coal-Fired Residential Combustion Equipment Field Tests," U.S. Environmental Protection Agency Report No. EPA600/2-78-004, June 1977.

37. Giammer, R. D., R. B. Engdahl, and R. E. Barrett, "Emissions from Residential and Small Commercial Stoker-Coal-Fired Boilers under Smokeless Operation," U.S. Environmental Protection Agency Report No. EPA 600/7-76-029, October, 1976.

38. Holman, J. P., Experimental Methods for Engineers, McGraw-Hill, New York, 1978.

11. APPENDIX

11.1 Emissions Data Reduction Program

```
C      NOMENCLATURE
C      A = THE MOLAR RATIO OF WATER TO HYDROGEN IN THE COAL
C      B603 = GLASS BALL READING ON 603 ROTAMETER (SMOKE)
C      CD1 = FIRST ESTIMATE OF DISCHARGE COEFFICIENT
C      CD2 = SECOND ESTIMATE OF DISCHARGE COEFFICIENT
C      ECO = CO CHEMICAL ENERGY LOSS RATE , KW
C      EFCO = INSTANTANEOUS CO EMISSION FACTOR ,
C             G OF CO PER KG OF FUEL BURNED
C      EDOT = INSTANTANEOUS ENERGY RELEASE RATE
C             IN THE STOVE , KW
C      EFFIC = INSTANTANEOUS EFFICIENCY
C      EFNOX = INSTANTANEOUS NOX EMISSION FACTOR ,
C             G OF NOX PER KG OF FUEL BURNED
C      EFSOX = INSTANTANEOUS SOX EMISSION FACTOR ,
C             G OF SOX PER KG OF FUEL BURNED
C      ESM = SMOKE CHEMICAL ENERGY LOSS RATE , KW
C      HVC = HEATING VALUE OF THE COAL , KJ PER KG
C      HVCO = HEATING VALUE OF CO , KJ PER KGMOLE
C      II=NUMBER OF DATA POINTS
C      IMAX = DATA POINT WHERE STEADY STATE ENDS
C      IMAXP = DATA POINT WHERE SMOKE COLLECTION ENDS
C      IMIN = DATA POINT WHERE STEADY STATE BEGINS
C      IMINP = DATA POINT WHERE SMOKE COLLECTION BEGINS
C      KK=NUMBER OF PIECES OF DATA IN EACH DATA SET
C      MDOT(I) = MASS BURNING RATE , KG/S
C      MFC = THE MASS FRACTION OF CARBON IN THE COAL
C      MFCSM = THE MASS FRACTION OF CARBON IN THE SMOKE
C      MSM = MASS FLOW RATE OF SMOKE IN STACK , KG PER S
C      MU = VISCOSITY , PA*SEC
C      NDOTS = STACK MOLAR FLOW RATE , KGMOLE PER SEC
C      NINT = NUMBER OF 5 MINUTE INTERVALS IN THE RUN
C      NPINT = NUMBER OF 5 MINUTE INTERVALS DURING THE
C              SMOKE TEST
C      NSSINT = NUMBER OF STEADY STATE INTERVALS
C      PA = AMBIENT PRESSURE , KPA
C      PB = BAROMETRIC PRESSURE , INCHES OF MERCURY
C      PHI = RELATIVE HUMIDITY
C      PSR = SATURATION PRESSURE AT ROOM TEMPERATURE , KPA
C      QEST = FIRST ESTIMATE OF VOLUME FLOW IN THE STACK ,
C             M**3 PER S
C      QS = VOLUME FLOWRATE IN THE STACK , M**3 PER S
```

```
C     Q600 = FLOWRATE THROUGH 600 ROTAMETER , M**3 PER S
C     Q603 = FLOWRATE THROUGH 603 ROTAMETER , M**3 PER S
C     Q604 = FLOWRATE THROUGH 604 ROTAMETER , M**3 PER S
C     R = THE MOLAR RATIO OF CARBON TO HYDROGEN IN THE COAL
C     RE = REYNOLDS NUMBER
C     RHOBAR = THE STACK GAS MOLAR DENSITY , KGMOLE PER
C              M**3
C     RWD = RATIO OF WET TO DRY MOLE FRACTIONS
C     SCALE4 = O2 METER RANGE , MOLE PERCENT
C     SCALE5 = NOX METER RANGE , PPM
C     SCALE6 = SOX METER RANGE , PPM
C     TIME = TIME OF RUN IN MINUTES STARTING AT 0.0
C     SMOKE = THE TOTAL MASS OF SMOKE COLLECTED , KG
C     TR = ROOM TEMPERATURE , K
C     TS = STACK TEMPERATURE , K
C
C     THE VARIOUS ARRAYS ARE DIMENSIONED, AND THE CONSTANTS
C     ARE INITIALIZED
C
C     IN B(I,K) , I=ITH DATA POINT AND K=KTH PIECE OF DATA
      DIMENSION B(37,11),MDOT(37),AVG(8),RWD(37),NDOTS(37)
      REAL NDOTS,MDOT,MFC,MSM,MFCSM,MDOTT,MDOTSS,MSMT,MU
C     THE VALUES OF IMIN, IMAX, IMINP, IMAXP, SMOKE, PB,
C     PHI, PSR, TR, AND B603 ARE READ IN
      READ (5,*) IMIN,IMAX,IMINP,IMAXP,SMOKE,PB,PHI,PSR,
     CTR,B603
      A=.1533
      AOR=0.001363
      DOR=0.04166
      ECOT=0.0
      EDOTT=0.0
      EFCOT=0.0
      EFFICT=0.0
      EFNOXT=0.0
      EFSOXT=0.0
      ESMT=0.0
      HV = 2500.0
      HVC=24331.
      HVCO=282993.0
      II=37
      KK=10
      MDOTSS=0.0
      MDOTT=0.0
      MFC=.5978
      MFCSM=.60
      MSMT=0.0
      NINT=II-1
```

```
      NPINT=IMAXP-IMINP
      NSSINT=IMAX-IMIN
      QST=0.
      R=1.062
      SCALE4=25.
      SCALE5=500.
      SCALE6=1.
      TST=0.
C
C     THE DATA IS READ IN TO THE PROGRAM
      READ(5,*) ((B(I,K),K=1,KK),I=1,II)
C     WHERE
C     B(I,1) = THE TIME OF THE READING IN MINUTES
C     B(I,2) = THE CO READINGS IN THE STACK (MOLE PERCENT)
C     B(I,3) = THE CO2 READINGS IN THE STACK (MOLE PERCENT)
C     B(I,4) = THE O2 READINGS IN THE STACK (DVM READING)
C     B(I,5) = THE NOX READINGS IN THE STACK (DVM READING)
C     B(I,6) = THE SOX READINGS IN THE STACK (DVM READING)
C     B(I,7) = GLASS BALL READING FOR 604 ROTAMETER
C              (DILUTION AIR)
C     B(I,8) = GLASS BALL READING FOR 600 ROTAMETER (SAMPLE)
C     B(I,9) = PRESSURE DROP OVER THE ORIFICE PLATE (INCHES
C              OF WATER)
C     B(I,10) = THE TEMPERATURE IN THE STACK (DEGREES C)
C
C     PRINT PAGE HEADING
      WRITE(6,100)
      PRINT 10
      PRINT 99
      PRINT 20
      PRINT 25
C
C     THE FLOWRATE THROUGH THE SMOKE FILTER IS Q603.
C     Q603 IS DETERMINED BY A SECOND ORDER FIT TO
C     CALIBRATION DATA.
      Q603=-9.7586E-10*B603*B603+4.5095E-07*B603-1.3729E-06
C
C     CHANGE PRESSURE UNITS
      PA=PB*3.387
C
C     THE PROGRAM IS RUN FOR THE VARIOUS DATA POINTS.
      DO 5  I=1,II
C
C     THE STACK TEMPERATURE IS CONVERTED TO DEGREES KELVIN
      TS=B(I,10)+273.
      TST=TST+TS
C
```

```
C      THE CONVERSION FACTOR FOR WET TO DRY BASIS IS
C      CALCULATED.
       RWD(I)=(1.-(PHI*PSR-.61)/PA)/(1+(A/R+1./(2.*R))*
      C(B(I,3)/100.))
C
C      THE CO AND CO2 READINGS ARE CORRECTED TO THE WET
C      BASIS AND ARE CONVERTED TO MOLE FRACTION FROM MOLE
C      PERCENT.
       B(I,2)=B(I,2)*RWD(I)/100.
       B(I,3)=B(I,3)*RWD(I)/100.
C
C      THE O2, NOX AND SOX READINGS ARE CORRECTED TO A
C      WET BASIS
C      AND ARE CONVERTED TO MOLE FRACTION FROM DVM READING.
       B(I,4)=B(I,4)*RWD(I)*SCALE4/100.
       B(I,5)=B(I,5)*RWD(I)*SCALE5*1.0E-06
       B(I,6)=B(I,6)*RWD(I)*SCALE6*1.0E-06
C
C      THE STACK GAS MOLAR DENSITY (KGMOLE PER M**3) IS
       RHOBAR=PA/(8.3143*TS)
C
C      THE FLOW RATE (M**3 PER SECOND) IN THE STACK IS
C      DETERMINED BY THE ORIFICE EQUATION AND CALIBRATION
C      DATA.
       CD1=-0.1898*B(I,9)+0.6567
       QEST=CD1*AOR*SQRT(17.18*B(I,9)/RHOBAR)
       MU=-1.72164E-11*TS*TS+5.4383E-08*TS+3.8936
       RE=(RHOBAR*29*QEST*DOR)/(AOR*MU)
       CD2=-4.9647E-06*RE+0.70182
       QS=CD2*AOR*SQRT(17.18*B(I,9)/RHOBAR)
       QST=QST+QS
C
C      THE MOLAR FLOWRATE (KGMOLE PER SECOND) IN THE STACK
C      IS
       NDOTS(I)=QS*RHOBAR
C
 5     CONTINUE
       QSA=QST/II
       TSA=TST/II
C
        DO 6 I=1,II
C
C      THE SMOKE EMISSION RATE (KG/S) IS
       MSM=(SMOKE/(NPINT*300))*(QSA/Q603)*(TR/TSA)
C
C      MDOT IS THE BURNING RATE OF COAL (KG/S)
C      AND IS CALCULATED FROM THE CARBON FLOW
C      INT THE STACK
```

```
      MDOT(I)=((B(I,2)+B(I,3))*NDOTS(I)*12.0+(MSM*MFCSM))/
     CMFC
      MDOTT=MDOTT+MDOT(I)
C
C     THE ENERGY RELEASE RATE (KW) IN THE STOVE IS
      EDOT=HVC*MDOT(I)
C
C     THE EMISSION FACTOR FOR CO IS GIVEN BY
      EFCO=(B(I,2)*NDOTS(I)*28.*1000.)/MDOT(I)
C
C     THE EMISSION FACTOR FOR NOX IS GIVEN BY
      EFNOX=(B(I,5)*NDOTS(I)*46.*1000.)/MDOT(I)
C
C     THE SAMPLE IS DILUTED BEFORE GOING TO THE SOX METER
C     SO THE ORIGINAL CONCENTRATION MUST BE DETERMINED.
C     CALIBRATION CURVE EQUATIONS ARE GIVEN FOR EACH
C     ROTAMETER SO THAT A DILUTION RATIO CAN BE DETERMINED.
C     ROTAMETER 600 IS FOR THE GAS SAMPLE.
C     ROTAMETER 604 IS FOR THE DILUTION AIR.
      Q600=3.0825E-11*B(I,8)*B(I,8)+1.8392E-09*B(I,8)
     C+5.9932E-08
      Q604=1.1176E-06*B(I,7)-4.9367E-06
C     CALCULATE THE MOLE FRACTION OF UNDILUTED SOX IN THE
C     STACK
      B(I,6)=B(I,6)*(Q600+Q604)/Q600
C
C     THE EMISSION FACTOR FOR SOX IS GIVEN BY
      EFSOX=(B(I,6)*NDOTS(I)*64.*1000.)/MDOT(I)
C
C     THE CHEMICAL ENERGY LOSS AS CO IS
      ECO=NDOTS(I)*B(I,2)*HVCO
C
C     THE ENERGY LOSS FROM THE SMOKE IS
      ESM=MSM*HVC
C
C     THE COMBUSTION EFFICIENCY IS GIVEN BY
      EFFIC=(1.-((ECO+ESM)/EDOT))*100.
C
C     SUM UP STEADY STATE VALUES
      IF(I.LT.IMIN.OR. I.GT.IMAX) GO TO 4
      EFFICT=EFFIC*MDOT(I)+EFFICT
      EFCOT=EFCO*MDOT(I)+EFCOT
      EFNOXT=EFNOX*MDOT(I)+EFNOXT
      EFSOXT=EFSOX*MDOT(I)+EFSOXT
      MDOTSS=MDOT(I)+MDOTSS
 4    TIME=B(I,1)
      MDOT(I)=MDOT(I)*3600.
```

```
C     WRITE OUT THE EMISSION FACTORS.
      WRITE (6,30) TIME,EFFIC,EFCO,EFNOX,EFSOX,MDOT(I)
 6    CONTINUE
C     CALCULATE AVERAGE VALUES AT STEADY CONDITIONS
      AVG(1)=EFFICT/MDOTSS
      AVG(2)=EFCOT/MDOTSS
      AVG(3)=EFNOXT/MDOTSS
      AVG(4)=EFSOXT/MDOTSS
      AVG(5)=(MDOTSS/NSSINT)*3600.
      AVG(6)=MSM*1000./(MDOTSS/NSSINT)
C
C     PRINT THE AVERAGE STEADY STATE VALUES
      PRINT 99
      PRINT 40
      PRINT 99
      PRINT 50
      PRINT 55
      WRITE (6,60) (AVG(J),J=1,6)
C
C     FORMAT STATEMENTS
 10   FORMAT(30X,20HINSTANTANEOUS VALUES)
 20   FORMAT(8X,4HTIME,6X,5HEFFIC,6X,4HEFCO,8X,5HEFNOX,6X,
     C5HEFSOX,5X,4HMDOT)
 25   FORMAT(9X,3HMIN,5X,7HPERCENT,3X,8HG PER KG,4X,
     C8HG PER KG,3X,8HG PER KG,3X,8HKG PER H)
 30   FORMAT (1X,F11.0,4F11.2,F11.3)
 40   FORMAT(30X,35HAVERAGE VALUES AT STEADY CONDITIONS)
 50   FORMAT(18X,5HEFFIC,6X,4HEFCO,8X,5HEFNOX,6X,5HEFSOX,
     C5X,6HMDOTSS,5X,4HEFSM)
 55   FORMAT(17X,7HPERCENT,3X,8HG PER KG,4X,8HG PER KG,
     C3X,8HG PER KG,6X,2HKG,6X,8HG PER KG)
 60   FORMAT (12X,4F11.2,2F11.3)
 99   FORMAT(3X,4H    )
 100  FORMAT(1H1)
      STOP
      END
```

11.2 Equations of Curves Fitted to Calibration Data

The flows through the SO_x sample, dilution air, and smoke sample rotameters were determined by equations fitted to calibration data. The flow through the SO_x sample rotameter is given by

$$Q_{SO_x} = 3.0825 \times 10^{-11} B_{SO}^{\ 2} + 1.8392 \times 10^{-9} B_{SO} + 5.9932 \times 10^{-8} \quad (20)$$

where

B_{SO_x} = glass ball reading on the SO_x sample rotameter

Q_{SO_x} = flow rate through the SO_x sample rotameter, m^3/s

The flow through the dilution air rotameter is given by

$$Q_{air} = 1.1176 \times 10^{-6} B_{air} - 4.9367 \times 10^{-6} \quad (21)$$

where

B_{air} = glass ball reading on the dilution air rotameter

Q_{air} = flow rate through the dilution air rotameter, m^3/s

The flow through the smoke sample rotamter is given by

$$Q_{sm} = 9.7586 \times 10^{-10} B_{sm}^{\ 2} + 4.5095 \times 10^{-7} B_{sm} - 1.3729 \times 10^{-6} \quad (22)$$

where

B_{sm} = glass ball reading on the smoke sample rotameter

Q_{sm} = flow rate through the smoke sample rotameter, m^3/s

The equations for calibration data used to calibrate the volumetric flow rate in the stack are presented in Appendix 11.3 along with the calculation method.

11.3 Determination of Volumetric Flow Rate in the Exhaust Duct

In order to calculate the volumetric flow rate in the exhaust duct, a discharge coefficient for the orifice was needed. Calibration data were used to determine a relation between Reynolds number and discharge coefficient. The discharge coefficient is given by

$$CD = -4.9647 \times 10^{-6} \, Re + .70182 \qquad (23)$$

where

Re = Reynolds number for the stack gas flow

CD = discharge coefficient for the orifice

With this discharge coefficient the volumetric flow rate in the stack can be determined by

$$Q_s = CD \, A_{or} \sqrt{\frac{2 \, \Delta P \, 1000}{\rho_s \, MW_s}} \qquad (24)$$

where

Q_s = volumetric flow rate in the stack, m^3/s

A_{or} = area of orifice, m^2

MW_s = molecular weight of the stack gas, kg/kgmol

ΔP = pressure drop across orifice, kPa

ρ_s = molar density of stack gas, $kgmol/m^3$

In order to determine the Reynolds number that was used to calculate the discharge coefficient, estimates of the flow rate, and the discharge coefficient were needed. A first estimate of the discharge coefficient was determined from calibration data. The discharge coefficient (CD_{est}) is given by

$$CD_{est} = -0.1898 \quad \Delta P \quad + 0.6567 \tag{25}$$

An estimate of the flow rate is then given by

$$Q_{est} = CD_{est} \, A_{or} \sqrt{\frac{2 \, \Delta P \, 1000}{\rho_s \, MW_s}} \tag{26}$$

where

Q_{est} = estimate of the volumetric flow rate in the stack, m^3/s

The viscosity, which is temperature dependent and is needed to calculate the Reynolds number, was determined from an equation fitted to tabular data. The viscosity is given by

$$\mu = -1.72164 \times 10^{-11} \, T_s^{\,2} + 5.4383 \times 10^{-8} \, T_s + 3.8936 \times 10^{-6} \tag{27}$$

where

μ = viscosity, Pa s

T_s = stack temperature, K

The Reynolds number can finally be determined by

$$R_e = \frac{\rho_s \, MW_s \, Q_{est} \, d_{or}}{A_{or} \, \mu} \tag{28}$$

where

d_{or} = diameter of the orifice, m

This Reynolds number is used in Eq. 23 to determine the discharge coefficient which is used to calculate the actual flow rate in the stack.

11.4 Determination of the Initial H_2O Concentration in the Secondary Combustion Zone.

The H_2O in the secondary combustion zone consists of H_2O from moisture in the coal, H_2O formed by combustion of hydrogen, and H_2O present in the combustion air. Assuming that all of the hydrogen in the coal forms H_2O and dry coal can be represented by C_bH where b is the molar ratio of carbon to hydrogen in the coal, the coal combustion can be represented by

$$C_bH + a\ H_2O + (b + \tfrac{1}{4})\ O_2 + 3.76\ (b + \tfrac{1}{4})\ N_2 \rightarrow$$
$$b\ CO_2 + a\ H_2O + \tfrac{1}{2}\ H_2O + 3.75\ (b + \tfrac{1}{4})\ N_2$$

where a is the molar ratio of water to hydrogen in the coal. The mole fraction of H_2O formed the moisture in the coal is $\frac{a}{b}\ X_{CO_2}$ and the mole fraction of H_2O formed by combustion of hydrogen is $\frac{1}{2b}\ X_{CO_2}$ where X_{CO_2} is the mole fraction of CO_2. The mole fraction of H_2O present in the combustion air is the ratio of the partial pressure of H_2O in the air at the air temperature to the total pressure, P_A. The partial pressure can be expressed as the product of the relative humidity, ϕ, and the saturation pressure of the water in the air at the air temperature, P_{sr}. The mole fraction of H_2O in the combustor can be then given by

$$X_{H_2O} = \frac{1}{b}\ X_{CO_2}\ a + \frac{1}{2} + \frac{\phi P_{sr}}{P_A} \qquad (29)$$

11.5 Combustor Wall Temperatures During the Emissions Tests

The temperatures of the inside wall of the combustor at three locations were recorded every five minutes. These values, for the twelve emissions tests, are listed in Tables IX through XIV for reference.

TABLE IX. Combustor Wall Temperatures for Emissions Tests One and Two.

Time (min)	Test 1 Temperatures (°C) Distance from Grate (cm)			Test 2 Temperatures (°C) Distance from Grate (cm)		
	6.4	32.5	58.0	6.4	32.5	58.0
0	495	356	227	224	168	121
5	577	482	334	318	243	166
10	603	521	392	488	356	226
15	612	541	431	565	437	287
20	610	545	448	596	500	359
25	607	543	453	619	522	406
30	608	540	454	627	534	432
35	597	526	442	623	538	442
40	573	483	413	621	536	447
45	529	434	376	615	528	440
50	511	404	350	583	482	407
55	510	390	330	548	443	376
60	511	389	328	516	412	350
65	510	387	324	490	385	323
70	520	390	324	504	382	316
75	522	389	323	517	388	316
80	522	385	320	529	393	319
85	520	382	317	536	396	322
90	512	380	315	538	398	323
95	511	377	313	540	400	325
100	513	377	312	538	399	325
105	523	383	315	535	399	326
110	530	388	318	531	398	324
115	527	390	320	523	393	320
120	515	385	318	510	384	313
125	509	380	315	507	380	309
130	501	374	310	514	382	309
135	491	366	302	507	378	305
140	481	360	296	494	369	299
145	466	348	286	479	354	287
150	441	329	271	465	342	279
155	411	308	256	453	331	270
160	386	288	238	443	321	261
165	366	269	224	435	312	253
170	353	257	211	429	303	245
175	338	244	200	417	293	236
180	325	232	189	405	283	227

TABLE X. Combustor Wall Temperatures for Emissions Tests Three and Four

Time (min)	Test 3 Temperatures (°C) Distance from Grate (cm)			Test 4 Temperatures (°C) Distance from Grate (cm)		
	6.4	32.5	58.0	6.4	32.5	58.0
0	185	110	82	241	163	115
5	212	128	94	348	216	151
10	240	148	107	477	320	227
15	273	168	121	514	367	262
20	312	194	139	577	459	335
25	426	270	186	595	514	408
30	500	351	246	614	538	444
35	532	382	274	610	530	447
40	562	414	309	595	506	430
45	590	444	330	578	480	410
50	611	494	408	546	445	382
55	611	498	418	504	416	360
60	600	498	427	457	375	329
65	573	478	415	433	347	304
70	517	425	373	430	334	290
75	460	371	325	436	331	282
80	441	351	305	443	331	279
85	430	331	283	449	332	278
90	425	321	269	461	336	279
95	428	316	263	470	342	282
100	430	315	260	466	343	283
105	426	312	256	464	341	281
110	422	308	253	465	340	280
115	422	306	251	466	339	280
120	430	308	249	455	332	274
125	434	309	250	453	328	270
130	436	310	252	444	322	266
135	438	311	253	441	320	263
140	437	311	252	457	325	266
145	425	305	250	462	328	266
150	416	300	245	458	328	265
155	406	293	239	444	322	259
160	394	284	232	424	312	251
165	381	274	223	406	299	242
170	377	269	218	387	285	231
175	372	262	213	370	269	219
180	369	257	209	356	256	206

TABLE XI. Combustor Wall Temperatures for Emissions Tests Five and Six.

Time (min)	Test 5 Temperatures (°C)			Test 6 Temperatures (°C)		
	Distance from Grate (cm)			Distance from Grate (cm)		
	6.4	32.5	58.0	6.4	32.5	58.0
0	304	239	176	208	162	118
5	368	321	209	220	179	131
10	450	367	241	271	218	160
15	485	374	269	325	262	196
20	507	380	288	387	316	243
25	498	378	294	445	364	288
30	573	465	353	509	423	340
35	577	487	381	573	481	394
40	562	484	392	624	517	435
45	551	477	388	638	543	470
50	550	471	385	621	539	479
55	539	446	365	605	531	476
60	511	411	342	594	525	470
65	498	385	323	588	478	424
70	490	373	312	586	465	409
75	488	364	303	568	444	392
80	496	362	299	563	431	377
85	508	367	299	561	426	370
90	501	367	300	566	421	364
95	499	365	299	-	-	-
100	495	360	295	551	404	350
105	497	356	292	537	395	341
110	492	350	287	510	380	330
115	486	344	283	480	361	313
120	473	336	278	442	336	293
125	453	330	273	414	313	274
130	436	322	265	384	291	255
135	426	314	257	360	271	238
140	412	306	250	337	253	223
145	401	297	242	313	235	208
150	393	293	238	295	221	195
155	381	285	231	279	208	183
160	369	275	223	264	195	172
165	360	268	218	250	185	162
170	349	259	211	239	176	155
175	342	253	205	229	167	147
180	333	246	199	219	160	141

TABLE XII. Combustor Wall Temperatures for Emissions Tests Seven and Eight.

Time (min)	Test 7 Temperatures (°C) Distance from Grate (cm)			Test 8 Temperatures (°C) Distance from Grate (cm)		
	6.4	32.5	58.0	6.4	32.5	58.0
0	289	207	143	363	235	160
5	302	219	154	336	244	173
10	309	223	161	338	246	178
15	311	224	165	364	256	187
20	333	235	174	-	-	-
25	364	254	184	445	306	226
30	396	280	207	460	322	241
35	432	308	230	477	345	263
40	445	326	249	509	369	282
45	472	347	268	492	372	290
50	503	377	295	473	365	288
55	537	407	322	436	344	278
60	545	420	335	412	328	267
65	531	416	341	418	326	262
70	501	399	330	425	327	260
75	463	373	314	436	332	260
80	420	339	288	442	336	263
85	397	314	266	443	337	265
90	392	300	251	435	332	262
95	395	294	243	421	322	255
100	397	291	237	409	313	248
105	397	289	233	403	305	242
110	396	288	231	395	296	234
115	395	287	229	388	289	229
120	395	286	227	323	247	196
125	394	285	226	307	232	184
130	391	283	225	297	221	173
135	382	278	221	293	214	167
140	364	268	214	-	-	-
145	356	261	208	290	210	162
150	351	257	204	288	207	158
155	342	250	200	284	205	155
160	338	245	196	281	202	152
165	337	243	192	277	199	149
170	336	241	190	275	196	146
175	335	240	189	273	194	143
180	327	235	187	271	192	142

TABLE XIII. Combustor Wall Temperatures for Emissions Tests Nine and Ten.

Time (min)	Test 1 Temperatures (°C)			Test 2 Temperatures (°C)		
	Distance from Grate (cm)			Distance from Grate (cm)		
	6.4	32.5	58.0	6.4	32.5	58.0
0	373	241	169	452	370	262
5	343	245	180	484	390	289
10	318	236	180	502	404	313
15	325	237	184	532	440	350
20	389	277	206	532	450	359
25	462	336	242	540	467	377
30	526	388	283	557	473	389
35	566	443	327	544	462	384
40	573	462	356	528	460	384
45	552	447	359	504	441	370
50	538	438	355	467	408	347
55	553	446	361	420	361	310
60	578	471	377	384	321	276
65	595	491	399	371	350	253
70	582	479	395	370	290	240
75	552	451	380	372	288	233
80	519	420	339	377	290	230
85	492	391	335	384	294	231
90	477	373	320	386	295	230
95	469	360	307	379	293	228
100	460	349	298	368	288	223
105	455	344	291	361	282	218
110	466	345	290	358	277	214
115	467	347	290	370	281	215
120	459	346	290	376	285	219
125	446	341	287	376	287	222
130	436	335	282	376	285	222
135	430	331	279	374	284	222
140	424	326	275	366	279	219
145	417	321	270	356	272	214
150	404	311	262	348	266	210
155	387	298	254	337	259	205
160	374	286	245	328	251	198
165	365	278	237	316	240	191
170	358	271	230	309	233	186
175	352	265	224	301	225	179
180	345	260	219	300	222	177

TABLE XIV. Combustor Wall Temperatures for Emissions Tests Eleven and Twelve.

Time (min)	Test 11 Temperatures (°C) Distance from Grate (cm)			Test 12 Temperatures (°C) Distance from Grate (cm)		
	6.4	32.5	58.0	6.4	32.5	58.0
0	-	312	225	573	441	315
5	-	339	254	582	470	364
10	-	373	289	588	474	388
15	-	401	315	590	475	397
20	-	429	342	585	469	397
25	-	439	356	603	479	401
30	-	437	363	603	483	404
35	-	438	364	597	481	404
40	-	434	364	590	475	400
45	-	423	355	569	461	395
50	-	413	347	532	441	385
55	-	394	334	480	406	364
60	-	367	314	466	392	352
65	-	343	295	445	373	336
70	-	326	280	435	363	324
75	-	314	269	433	358	318
80	-	305	262	421	349	310
85	-	305	258	413	343	303
90	-	303	256	401	334	296
95	-	300	252	397	328	289
100	-	295	248	407	331	290
105	-	293	245	415	338	294
110	-	292	244	420	343	298
115	-	294	245	420	343	299
120	-	301	250	415	340	296
125	-	309	255	401	330	288
130	-	312	259	396	322	280
135	-	311	260	386	313	273
140	-	309	259	373	301	264
145	-	305	256	369	295	258
150	-	303	255	361	290	253
155	-	350	253	353	284	248
160	-	295	249	339	275	240
165	-	289	245	332	268	234
170	-	281	239	317	258	226
175	-	273	233	304	248	217
180	-	267	228	292	238	208

11.6 Error Analysis

A Kline and McClintock error analysis (38) was performed for the emissions factors and coal burning rate. Uncertainties in the gas analyzer readings could have been determined from instrument specifications. The NO_x and SO_x analyzer specifications were based on percentages of the measured value, and the CO/CO_2 analyzer specifications were based on percentages of full scale readings. Using these specifications would lead to constant uncertainties of ± 0.04 mole percent CO and ± 0.3 mole percent CO_2. Since the measured CO concentrations were sometimes as low as 0.05 mole percent, a considerable error band would be associated with the value. However, because the analyzer was spanned and zeroed before each test, the uncertainty probably was lower and uncertainties of ± 1 least significant digit were used for the CO and CO_2 values. No zero drift was detected for the CO/CO_2 analyzer, although an average span drift of 0.6 percent of full scale was determined. The NO_x and SO_x analyzers both had span drifts of 6 percent of full scale.

The coal burning rate and NO_x, SO_x, and smoke emissions factors had typical uncertainties of 4, 7, 10, and 4 percent respectively. These uncertainties, which are indirectly dependent on the CO uncertainty, did not vary significantly although the uncertainty in the measured CO concentration ranged from 2 to 20 percent for various tests. The CO emission factor uncertainty ranged from 6 to 21 percent.

Some possible sources of error were not included in the above analysis. The effects of ignoring hydrocarbons in the stack were not

considered. Both NO_2 and SO_2 are soluble in water and may have dissolved in the condensate. NO can also adsorb on particulate matter (16) and sulfur can also be captured by alkalis in the coal ash (5). Therefore, lower concentrations of NO_x and SO_x could have been measured. Another factor that affects the measured NO_x concentration involves calibration gases. For tests one through five the NO_x analyzer was set on the 500 ppm scale for both spanning with 200 ppm gas and sampling. Tests six through twelve were spanned with 515 ppm gas on the 1000 ppm scale while sampling was conducted on the 500 ppm scale. Tests one through five all have lower NO_x emission factors than tests six through twelve. Later tests seem to indicate that the 515 ppm gas, which had been stored for a longer period fo time, had experienced a concentration reduction of about 15%. The average of the NO_x emission factors for tests six through twelve is double the average for tests one through five and it seems that the differences in the calibration gases would not contribute significantly to the increases in emissions factors. However, for certain tests the NO_x emission factors are close and a 15% error in the calibration gases could have a significant effect.

The vita has been removed from the scanned document

THE EFFECT OF OPERATING CONDITIONS ON EMISSIONS FROM A TWO-STAGE LUMP COAL COMBUSTOR

by

Jennifer Mackend

(ABSTRACT)

Residential coal stoves emit various pollutants such as CO, NO_x, SO_x, and smoke. The emissions can be reduced by varying the burning conditions in the stove. This investigation studied the effect of various burning conditions on the emissions from a two-stage lump coal combustor burning Wyoming bituminous coal. The parameters that were varied include primary air mass flow rate, secondary air mass flow rate, secondary air temperature, secondary air inlet velocity, and secondary air swirl. Each parameter was varied independently to attempt to isolate its effect on emissions. In addition, radial and axial probe sampling was conducted in the combustor's secondary combustion zone to determine the CO concentrations. A chemical kinetic model of CO oxidation was formulated and compared to the measured CO concentrations.

A wide range of emission factors can be achieved for the various pollutants by varying the burning conditions. The CO, NO_x, SO_x, and smoke emission factors range from 7.0 to 159, 0.67 to 3.1, 0.98 to 2.0, and 0.16 to 3.7 g/kg respectively. The emissions tests appear to be reasonably repeatable with emission factors and coal burning rates

agreeing within 15% in most cases. The various tests indicate that increasing the primary zone equivalence ratio decreases the CO emission factor. The smoke emissions from the test combustor are quite low compared to those from typical commercial coal stoves. The amount of swirl has a large effect on mixing in the secondary combustion zone, and highly stratified flows are created by certain burning conditions. The CO oxidation model does not correlate well with the experimental results since possible CO formation from hydrocarbons and stratified flow effects are not considered.